Water Quality Benefits of a MN Floodwater Storage Impoundment

A Thesis
SUBMITTED TO THE FACULTY OF
UNIVERSITY OF MINNESOTA
BY

Mariya Guzner

IN PARTIAL FULFILLMENT OF THE REQUIREMENTS
FOR THE DEGREE OF
MASTER OF SCIENCE

Joe Magner

September 2017

Acknowledgements

I acknowledge my thesis committee for their support and guidance through this work. Thank you, Bruce Wilson, for answering my many questions and being enthusiastic about the research process. Thank you, Joe Magner, for encouraging me to ask and answer my own questions. And Jeff Strock, thank you for keeping me more-or-less realistic about my undertakings.

I acknowledge the RRBC, BdSWD, LCCMR, and MPCA for creating this research opportunity. Thank you to Aaron Ostlund and Carlos Zamalloa for tremendous amounts of project support.

I acknowledge the many graduate and undergraduate students who helped me in the lab and field, and made long days completely worth it: Sierra Schadegg, Linnea Savereide, Eleanor Arpin, Travis Vieths, Alex Van Kirk, John Mueller, Bailey Rockwell, Tanner Glaza, Russell Zimmerman, Donald Hagen, and Seongjun Kim. Thank you also to the co-master's students who were always there for research and emotional support.

Huge thanks to my family and friends, who accompanied me in-spirit through every step. Special thanks to my fiancé, Matt Hoy, who reminded me to celebrate my success and laugh when it wasn't totally apparent.

Dedication

This thesis is dedicated to all the family, friends and teachers who encouraged and inspired my curiosity and wonder.

Abstract

Nutrient and sediment pollution in Lake Winnipeg and its watershed, the Red River Basin, MN, are degrading water quality and impairing aquatic health, fishability, swimmability and recreational potential. It is necessary to capture and store the pollutants phosphorus (P), nitrogen (N), and total suspended solids (TSS) on the landscape, to improve water quality and protect valuable water resources in the region. Floodwater storage impoundments have the potential to effectively capture and store nutrient pollutants and suspended sediments, and consequently improve downstream water quality. There are already several dozen similar impoundments in the state, and plans to build approximately 200 in total. The water quality benefits of a floodwater storage impoundment in the Red River Basin were tested through various methods in this study.

Nutrient budgets were built for the impoundment in 2014, 2015, and 2016. Load and concentration reductions were calculated for water entering and leaving the system, for nitrogen, phosphorus, and total suspended solids. In 2016, nitrogen and phosphorus reductions of 73% and 66%, respectively, were achieved. A hypothetical load reduction calculation was also modeled to determine the effects of impoundment water release speed on pollutant capture. The soil phosphorus storage potential of the impoundment was determined through a laboratory sorption experiment. Soils at the site were analyzed for their linear adsorption coefficient (K) and equilibrium P concentration at zero-sorption (EPC_0). Analysis compared soils under various land uses, including: cropped, planted with native vegetation, and flooded.

Results suggest that all soils within the impoundment outperform soils at the exterior of the structure regarding phosphorus storage and buffering potential. Variation

in soil-phosphorus sorption properties between sites with different vegetation types will advise cropping and planting plans to optimize water quality benefits. Results of this research are intended to advise management of the study site, similar impoundments, and constructed wetlands for water quality treatment.

Table of Contents

List of Tables

List of Figures

1. Introduction

In the past several decades the effects of natural and constructed wetlands on water quality have been investigated in numerous research efforts. Nutrient treatment capacity of wetlands is a key area on which many of these efforts focused. The nutrients nitrogen (N) and phosphorus (P) have become a research priority because they are limiters of growth in aquatic systems. When present in excess, they can result in eutrophication of water bodies, where an increase in algal growth and consequent decay of organic matter lead to increased microbial respiration and depletion of oxygen in the water. Eutrophication degrades aquatic systems by reducing habitat, altering existing aquatic food web and community structure (CENR 2003), disrupting natural biogeochemical cycling, and causing significant loss of aquatic life and biodiversity. In Minnesota, P is the primary nutrient limiting harmful algal growth. Management of P pollution is therefore of critical importance to protecting the integrity of water in the state and in the water bodies it connects to.

The mechanisms and factors controlling retention, release, and transformations of P in wetlands that have been studied extensively include: uptake by biota (Huett et al. 2005, Wang and Mitsch (n.d.)), hydrology (Gabriel et al. 2008, Dupas et al., 2015, Wang and Mitsch (n.d.)), sorption and desorption from sediments (Reddy et al. 1999, Richardson 1985, Dupas et al. 2015), and exchange reactions (Nairn and Mitsch 2000). In many cases, wetlands have been observed to serve as effective sinks for P (Nairn and Mitsch 2000; Huett et al. 2005). Research has also been conducted on the limits of P removal in wetlands (Kadlec 1999, Nairn and Mitsch 2000). In Minnesota, studies have primarily focused in the Minnesota River Basin on P-sediment dynamics (James et al. 2002, Grundtner 2013, James

and Larson 2008, Fang et al. 2002) and in lake systems on P cycling and limitation (Larsen, Schults, and Malueg 1981; Huser et al. 2016; Chapra and Canale 1991). Little is known about wetland P capture and transformations in the state of Minnesota.

This project was designed to expand the body of research on P dynamics in wetlands to include the P management benefits and limitations of flood storage impoundments. Flood storage impoundments are wetlands or ponds constructed to store water on the landscape and minimize flooding downstream. Understanding the water quality impacts of these systems is important today because there are large monetary investments and allocations of land for the construction of impoundments in Minnesota (Figure 1). Plans are in development to build approximately 200 flood storage impoundments in western part of the state in the near future. Currently, there are no data about the impact that these structures can have on P movement and storage within watersheds.

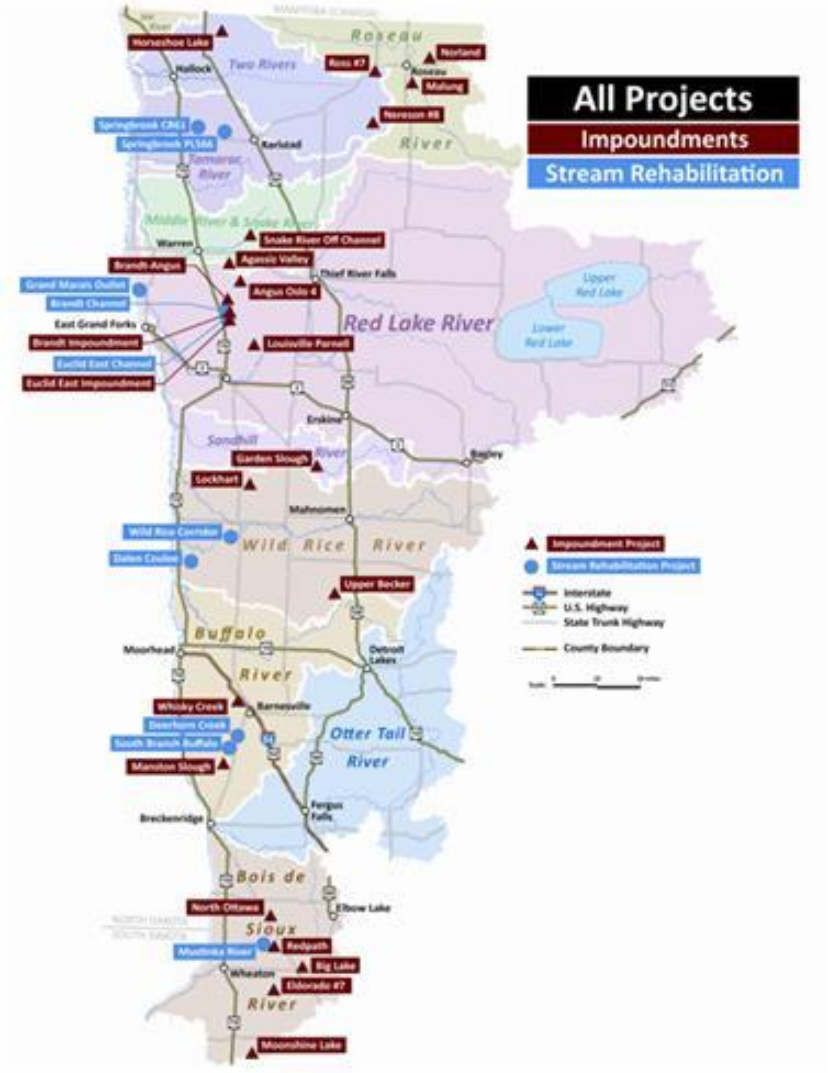

Figure 1. Map of impoundment and stream rehabilitation projects constructed in the Red River Basin, 1999-2010 (MN Center).

1.2 Research questions

This thesis research tests the capacity of an impoundment in western Minnesota to serve as a nutrient reduction and water treatment system. This thesis predicts the P sink and source function of the North Ottawa impoundment under input water conditions with a

range of P concentrations. It also quantifies the pollutant capture efficiency of the system. These research goals were met through two components: a soil-P dynamics experiment and an analysis of spatial and temporal water quality trends and pollutant loading.

The first research component is a soil-P sorption experiment that tests the concentrations of P in the water at which the impoundment soil serves as a sink or a source of the phosphorus. It will determine the equilibrium P concentration at zero-sorption, which may serve as a nutrient load limit for the management of this impoundment. The hypothesis is that soil P sorption rates in the impoundment exceed desorption rates, resulting in net P storage in the sediments.

The second component is a nutrient and sediment budget calculated for the impoundment. Water elevation data for the inlet, outlet and impoundment cells are available for 2015 and 2016. Water elevation data coupled with water quality data was used to calculate N, P, and TSS loads entering and leaving the impoundment. A percent mass capture was found for each constituent. The hypothesis is that, in 2015 and 2016, nutrient reductions of at least 30% were achieved for each pollutant: TP, TN, and TSS. For 2014, only a percent pollutant concentration reduction was calculated because impoundment construction was not yet complete.

The results of this research are intended to inform management strategies for the North Ottawa and similar impoundments, as well as designs for impoundments that will be constructed in coming years. They also contribute to the body of knowledge about P dynamics and transformations in wetland systems and at the soil-water interface.

2. Site description

2.1 Ownership and management

The North Ottawa impoundment (NOI) has an area of 8 km^2 and drains a 194. mi^2 agricultural basin in the Red River Valley in western Minnesota (Figure 2). This land accounts for 25% of the Rabbit River Watershed and 5% of the Boise De Sioux Watershed District (BdSWD) (Roeschlein 2014). It collects agricultural runoff from two large judicial ditch systems, JD #2 and JD #12. The land was purchased from agricultural land owners by the BdSWD. The total project cost was approximately $19 million, with 75% of the funding coming from the State of Minnesota Flood Damage Reduction Program, 16% from the Red River Watershed Management Board, and 9% from the BdSWD (Roeschlein 2014). The NOI management plan was written with joint advising from the BdSWD, MN Department of Natural Resources (DNR), Red River Basin Commission (RRBC), and the Magner Water Quality Lab (MMWQL) in the Department of Biosystems and Bioproducts Engineering at the University of Minnesota.

Figure 2. Map of the NOI and its watershed area (JCM Engineering, Inc. 2004).

2.2 Engineering and construction timeline

The NOI is a unique impoundment and opportune study site because of its three-square-mile size and innovative engineering, where control structures are used to move water between cells for a variety of management purposes (Figure 3). Interior dikes, built from in-situ relocated soil to a variable height of 8'-10', divide the impoundment into nine cells. The A and B cells each have an area of 0.25 mi^2. The C cell has no interior dikes and is 1.0 mi^2 in area. Exterior dikes, built around the impoundment to a variable height of 9'-14', isolate it from the neighboring agricultural land.

Water enters the impoundment over a weir in the inlet channel to the east. From this channel, it can be routed to the A cells or directly to the C cell. There are five outlets from the impoundment: four from the C cell and one from the B1 cell. Water can be moved between the A and B (A/B) cells if there is enough difference in hydraulic head. Movement of water is controlled by the opening and closing of gates between cells. There are stoplog structures at each A/B junction that allow water to be moved east-west. Running north-south along the A/B cell systems is a 30" high-density polyethylene (HDPE) culvert with a screw gate at each A/B junction. Additionally, there are screw gates between the B4/B3 cells and the B2/B1 cells that can be used to move water north in the B cell system. The C cell is isolated from the A/B cell system once water has moved over the inlet weir.

Construction of the NOI began in 2005 and took almost 11 years due to construction delays, especially in 2009 and 2010. By 2013, the impoundment had three 1 mi^2 cells, A, B and C, with no interior dikes. Interior diking of the A/B cells systems was completed in 2016.

Figure 3. Interior diking plan for impoundment cells, showing cell names and structures (Ostlund 2016).

2.3 Equipment

The NOI is equipped with a variety of instruments that allow for hydrologic and water quality monitoring. Pressure transducers (Xylem YSI brand) are grounded in each of the nine cells to measure the pressure of overlying water, corresponding to the height of water in each cell. A weather station at the site (45.99248°, -96.25634°) records cumulative precipitation, wind speed, wind direction, humidity, and temperature. Weather station and pressure transducer measurements are sent to a data logger and posted remotely on Storm Central (YSI Inc. / Xylem Inc. 2015) (https://stormcentral.waterlog.com/SiteDetails.php?a=134&site=801&pa=BdSWD) in 15

minute increments. There is an additional pressure transducer at the inlet weir for monitoring water levels in the inlet channel.

There are two automated ISCO samplers (3700 Portable Sampler Compact Model) (Teledyne ISCO, Lincoln, NE) at the NOI. The first is located 2 mi upstream of the impoundment, along the inlet channel. Because there are no significant inputs of water to the inlet between the ISCO sampler and the inlet weir, water samples collected at this location are representative of inflow water to the NOI. The second is located at the north C cell outlet channel and captures water samples representing the outflow from the impoundment.

2.4 Land use management

Because of its designation as a floodwater impoundment, storage of floodwater takes the highest priority regarding management. In the event of a large precipitation and runoff event, the C cell will be filled with water until its maximum storage capacity is reached. Once the C cell is full, water will be stored in the remaining cells of the impoundment. Maximum C cell storage is ~1.086×10^7 m^3 and total storage for the entire impoundment is ~2.919×10^7 m^3. This design provides the capacity to store 75% of a 100-year flood (BdSWD 2016), and to store all 10-year flood flows with no automatic release from the impoundment (Roeschlein 2014).

During normal flow conditions, the impoundment is designed to store water at 20% capacity and serve secondary benefits. These benefits include: downstream flow augmentation by maintaining an outflow of 0.1416 cms; water quality treatment achieved

through nutrient storage, removal by sedimentation, uptake by vegetation, and harvesting of cattails; support of waterfowl population by providing feeding and resting areas on mudflats in the impoundment; and recreational use, including bird-watching opportunities and improved hunting (Roeschlein 2014). Management of the A/B cells for these secondary benefits is shared between the DNR, RRBC, and MWQL. The cells designated for management by the DNR have land practices aimed at supporting waterfowl populations. The RRBC and MWQL manage the cells designated to maximize water quality benefits of the impoundment, specifically for storage and treatment of N, P, and TSS. Remaining cells are rented to farmers and cropped to raise revenue for the BdSWD to maintain the NOI.

Land use in the impoundment has been varied since its construction. During the construction years of the exterior and interior dikes, the impoundment area was rented to farmers and cropped. In 2014, the northern and eastern impoundment soils were planted to corn. Two of three corn parcels had fertilizer application of 125-75-30 broadcast, with no starter fertilizer. Herbicide application was post-emergent spray of Glyphosate (Roundup®) at 28 (oz acre^{-1}), and dicamba + diflufenzopyr (Status®) at 4 (oz acre^{-1}). Fertilizer and herbicide records for the third parcel were not available. The rest of the impoundment was planted to hay millet with 60-40-0 spread broadcast, and a sole herbicide application of 1.5 (pint acre^{-1}) 2,4-Dichlorophenoxyacetic acid (2,4-D).

In 2015, the eastern impoundment soils were planted to soybeans. There was no fertilizer application. Herbicide application included pre-emergent Valor® at 2 (oz acre^{-1}), followed by Roundup® at 32 (oz acre^{-1}), and post-emergent application of Flexstar® at ¾

(pint acre^{-1}). The western impoundment soils were planted to corn and had a fertilizer application of 135-75-30, impregnated with dimethenamid-p + saflufenacil (Verdict®) at 13 (oz acre^{-1}), followed by Roundup® at 32 (oz acre^{-1}), and Status® at 3 (oz acre^{-1}), post-emergence.

Land uses in the NOI cells in 2016 can be found in Table 1. Four of the eight A/B cells were rented to farmers and cropped. Two of the cells, A2 and A4, were designated for holding water. This water was released to the B2 and B4 cells, respectively, at the rates necessary to maintain the land use practices assigned to these cells. The B2 cell was managed by the DNR for supporting waterfowl populations. It was planted to native vegetation, mostly millet. The B4 cell was managed jointly by RRBC and the MWQL for water quality benefits. It was planted to cattails, and water levels were maintained to support cattail growth for eventual harvesting for biomass. The C cell was left unmanaged and had cattail growth, flooded and dry areas, and unmanaged vegetation.

Table 1. Record of land use management in the NOI cells during the growing season and fall, 2016.

Cell	Growing Season 2016	Fall 2016
A1	Corn	Harvested
A2	Water holding	Drained
A3	Wheat	Harvested; Flooded
A4	Water holding	Drained
B1	Soybeans	Harvested

Cell	Growing Season 2016	Fall 2016
B2	Native plants, mostly millet. Mudflats.	Not harvested; Flooded
B3	Corn	Harvested
B4	Growing cattails	Drained
C	Cattails and unmanaged vegetation	Cattails harvested; Drained

Land use management plans for 2017 are outlined in table 2.

Table 2. Record of land use management in the NOI cells during the growing season and fall, 2017.

Cell	Growing Season 2017	Fall 2017
A1	Cropped	Harvested
A2	Water holding	Drained
A3	Water holding	Drained
A4	Water holding	Drained
B1	Cropped	Harvested
B2	Native plants, mostly millet. Mudflats.	Not harvested; Flooded
B3	Native plants, mostly millet. Mudflats.	Not harvested; Flooded
B4	Growing cattails	Drained
C	Cattails and unmanaged vegetation	Cattails harvested; Drained

2.5 Soil, topography, hydrology, and geology

The NOI is located in the lake plain of the ancient glacial Lake Agassiz. The topography has very low relief, with only a 0.6 m gradient across the entire impoundment area. The highest elevation is the northeastern corner of the A4 cell. The lowest elevation is in the borrow pits, from which soil was taken for the construction of the exterior dikes, in the C cell. Flat topography is characteristic of the entire Red River Basin, in which the NOI is located.

The soil in the NOI is mostly silty clay loam, with some silty loam, clay loam, and loam soils (Appendix A). Average soil pH is 7.7. Underlying the soils in the Red River Basin is lake bed clay (Anderson et al. 2001). Soils rich in clay have extremely low permeability (Cummins and Grigal 1980), making the loss of water from the NOI to groundwater negligible. Components remaining in the water budget for this site are precipitation, evapotranspiration (ET), surface flow, and throughflow.

2.6 Watershed sites

Water quality monitoring sites were established at 12 locations (Figure 4) in the 2.92×10^7 m^3 basin. Their names and coordinates can be found in (Appendix B). Equipment is not installed at these sites, but they are regularly sampled and measured for water quality parameters in the field. Water quality data has been collected in the watershed since 2004 and in the impoundment since 2014. A water quality monitoring plan is in effect through 2018.

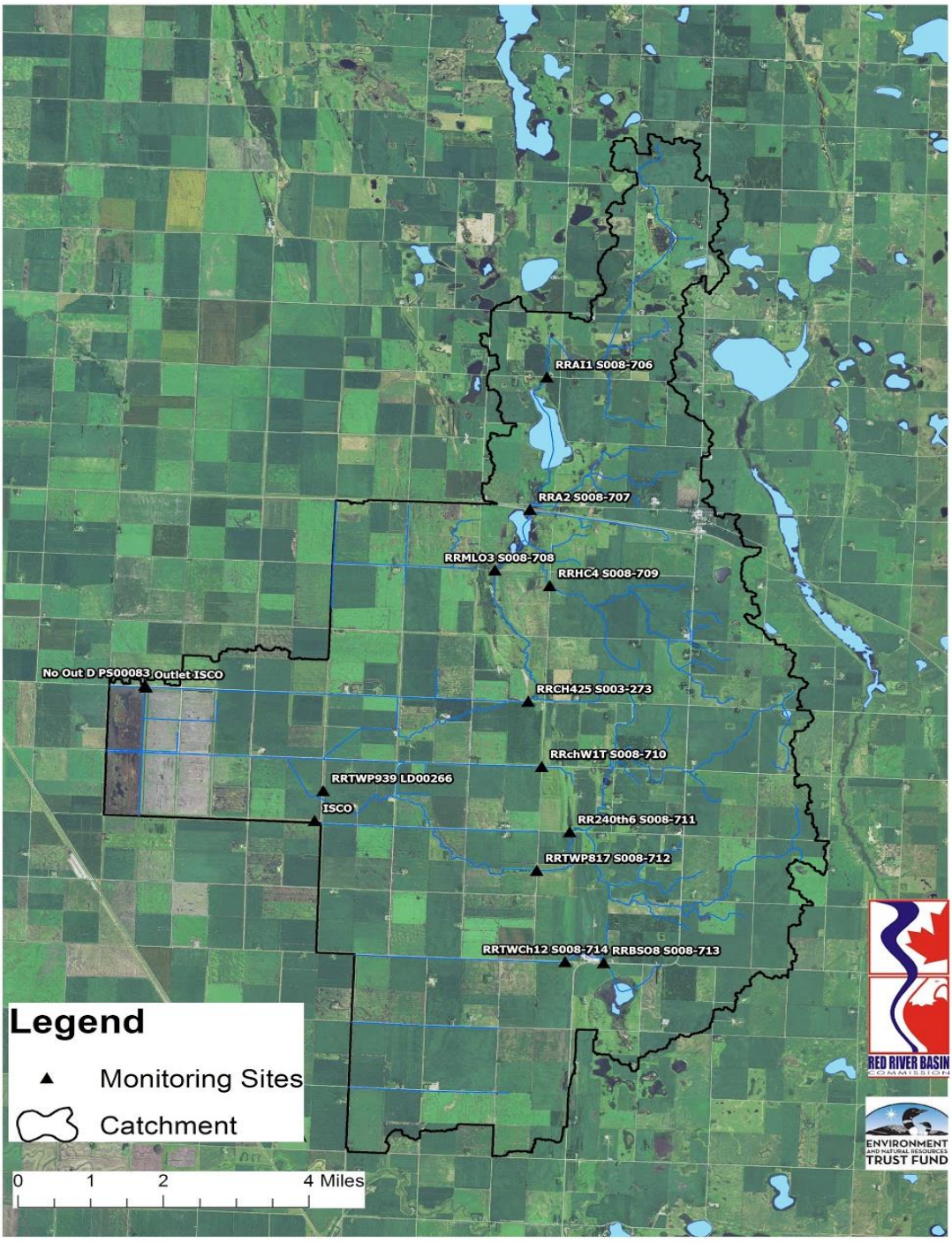

Figure 4. NOI catchment boundary and location of watershed sampling sites.

3. SOIL-P SORPTION EXPERIMENT

3.1 BACKGROUND

3.1.1 P mobility

The mobility and bioavailability of P in aqueous systems depends on exchange reactions between suspended solids and the solution (Froelich 1988). P can travel in surface water as an ion (PO_4^{3-}), as a constituent in organic matter, or bound to suspended inorganic particles. The states in which P travels are transformed by exchange reactions between the solid and aqueous phases. As organic matter decomposes, P can be released into solution. The reverse reaction occurs when plants, algae, or bacteria uptake P into their biomass. The focus of this study is the exchange of P between suspended sediments and the aqueous phase. P can sorb or bind to inorganic particles, thereby moving from solution into the solid phase. In solutions with pH 3-7, PO_4^{3-} will bind with Al, Fe, and Ca ions (Figure 4.10 in Schlesinger and Bernhardt 2013) on suspended sediments. The reduction state of the solution affects P binding dynamics. For example, P can bind to Fe^{3+} under oxic conditions. However, if the solution becomes anoxic for a long enough duration, Fe^{3+} may convert to Fe^{2+} and enter solution, re-releasing the PO_4^{3-} ion.

3.1.2. Sorption, adsorption, absorption

Sorption, adsorption, and absorption are common terms that have distinctly different definitions. Sorption combines the processes of adsorption and absorption, and refers to the process by which one substance is taken up by another. Adsorption refers the uptake of a substance by another as a film on its exterior. In absorption, the substance is

taken into the interior of another. In the context of P-soil dynamics, adsorption is the binding of PO_4^{3-} to sorption sites on the reactive exterior of the clay, silt, or other soil particles; absorption is the uptake of the PO_4^{3-} into the interior of the particle; and sorption describes the total PO_4^{3-} that is taken by the particle, by both adsorption and absorption. Sorption can simply be described as a two-step process (Bowden et al. 1977; Barrow 1983b). Rapid surface adsorption is the quick step. The slow step is the penetration of PO_4^{3-} into the subsurface of the particle by solid-state diffusion (Froelich 1988). This study does not determine the relative contributions of adsorption and absorption to the PO_4^{3-} uptake observed, therefore only the term sorption is used. It is possible that, because the experiment time was limited to 24 hrs for each sample, the slow absorption step was not fully or partially achieved. Desorption is the reverse process of sorption, in which PO_4^{3-} is released from the interior or exterior of the particle into solution.

3.1.3. Importance of studying sorption

Experimentally determining the sorption/desorption characteristics of soil–P is critical for evaluating bioavailable P in aqueous systems. Sorption reactions affect and regulate the PO_4^{3-} concentrations in surface waters and consequently the rates of algal and plant growth (Froelich 1988). Diffusive P flux from sediments is a significant source in P cycling. Determining the equilibrium P state between particulate and aqueous phases is necessary to develop an accurate nutrient budget for a system. For example, in some estuarine and lake systems, P concentrations exceed those expected based on P loads in

input waters (Froelich 1988; James and Barko 2004). In these cases, desorption of P from sediments is an important contributor to the system's total P budget.

Sorption and desorption processes in the NOI are expected to influence the P sink/source behavior of the impoundment system. Sediments in the agricultural watershed may be a significant source of P, due to application of fertilizer on crop fields. Within the impoundment, settling suspended solids and retaining water may result in sorption and storage of P in the bed sediments, allowing the impoundment to serve as a P sink. Variable land uses in impoundment cells may have pronounced effects on P-soil mechanics. This study aims to describe the sorption/desorption characteristics between the particulate and aqueous phases in the NOI, and to determine relationships between land use and (de)sorption reactions. Ultimately, it will describe the P sink and source potential (Lucci et al. 2010) of the impoundment and inform management of the NOI in order to maximize water quality benefits.

3.1.4. Buffer diagrams

Buffer diagrams (Froelich 1988) are plots of P sorption at an assumed equilibrium state between solids and solutions, with a range of starting P concentrations. They are a common method of illustrating the results of sorption/desorption experiments. These plots normally have the final, or equilibrium, concentration in the solution (C_f) on the x-axis (PO_4-P), and the amount of P sorbed (S) at equilibrium on the y-axis (mg P kg^{-1} soil) (Fig 5). Each point on a buffer diagram represents an equilibrium phosphate concentration (EPC). Several useful parameters can be determined based on these diagrams, including the

equilibrium PO_4^{3-} concentration at zero-sorption (EPC_0), and linear adsorption coefficient (K). These parameters relate to equilibrium P conditions for a given soil-solution mix and the P buffer intensity of the soil. Buffer diagrams can be used to predict P (de)sorption results for the range of solution PO_4-P concentrations tested.

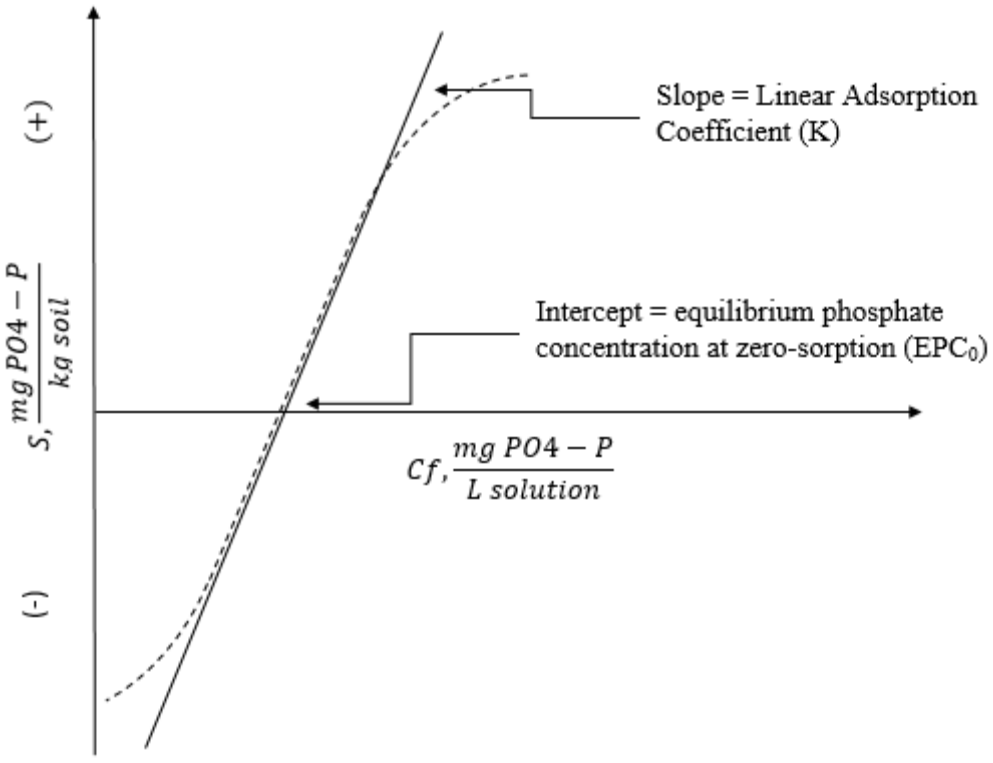

Figure 5. Schematic buffer diagram, adapted from Froelich (1988).

3.1.5. Freundlich and Langmuir models

P soil sorption data is often fit to isotherm equations to summarize and extrapolate results (Tellinghuisen and Bolster 2010). Two very commonly used isotherms are the Langmuir model (Langmuir, 1918), conventionally used to describe adsorption of gasses

(Bolster and Homberger 2007), and the Freundlich model (Freundlich 1906). P exchange reactions are complex and do not obey the physicochemical laws of adsorption, meaning that these models are not true isotherms (Froelich 1988). However, they are a convenient method of communicating P sorption/desorption mechanics of a given soil-solution complex, and the isotherm models have parameters that may be meaningful and are comparable across studies.

The Langmuir equation is useful because its parameters are related to sorption dynamics. It provides a measure of P sorption maximum (S_{max}), and a constant related to P bonding energy of the soil (K) (Hodges 2000). Whether the S_{max} term realistically represents a maximum sorption has been debated (Barrow 2008 in Hartikainen et al. 2010). The Freundlich model is an empirical equation and, therefore, its parameters are not directly connected to sorption mechanics phenomena. However, it has been suggested that, like the Langmuir S_{max} term, the adsorption constant (K) in the Freundlich equation can also be used to quantify the extent of adsorption and compare different reactors (Weber and Digiano, 1996 in Conidi and Parker 2015). A comparison of the Langmuir and Freundlich models with a proper weighting of least squares demonstrated that only the Freundlich isotherm yielded a statistically adequate χ^2 value, and that it represents the data significantly better than the Langmuir model 95% of the time (Tellinghuisen and Bolster 2010). Many studies feature modified versions of isotherm models that account for additional variables affecting P soil sorption (Zhou et al. 2005; Tian and Zhou 2008; Zhang et al. 2016; Wang et al. 2012; Koski-Vahala and Hartikainen 2001). In this study, modified

versions of the Langmuir and Freundlich models were written to force the isotherm fits through the EPC_0 determined, using buffer diagram plots of the results.

3.1.6. Research gap

Historically, P sorption dynamics research has been focused on investigating two key phenomena. The first is the role of internal loading of P from sediments in maintaining nearly constant PO_4^{3-} concentrations in surface waters. Internal loading provides a large and potentially bioavailable reservoir of P for algal growth, in excess of that dissolved in the water. The other regards the mobility of P from fertilizers in agricultural soils, and its tendency to become fixed in an unavailable form (Froelich 1988). This study aims to expand the body of knowledge about soil P sorption dynamics in Minnesota, specifically in a floodwater storage impoundment. Results of this research are applicable to similar systems in agricultural watersheds, in Minnesota and beyond.

3.2. METHODS

3.2.1. Soil sampling, processing, preservation, and storage.

Soil samples were collected from 30 sites in the impoundment on July 20th and 28th, 2016 (Figure 6). The sites were distributed evenly across the impoundment area, and represent the various land uses of the impoundment cells. Samples were collected from the upper 5 cm of soil surface and put into plastic sampling bags. Soil samples had a minimum dry weight of 150 g. All soils were transported on ice and stored in a refrigerator before processing. Soil processing involved drying at 35°C in a Model 40 Lab Oven (Quincy Lab,

Inc., Chicago, IL) for preservation, screening through a 2 mm mesh, and stirring to homogenize the sample. Dried, sieved samples were stored at room temperature in plastic sampling bags until analysis.

Figure 6. Map of soil sampling locations within the North Ottawa Impoundment (Google MyMaps ©).

3.2.2. Solution preparation

Soil-P sorption tests were conducted according to Nair et al. (1984), with some modifications. This procedure was developed as a standard method for testing P sorption for soils and sediments to resolve issues with comparing P sorption results across studies. It is highly replicable and found excellent agreement in results between the laboratories that tested it (Nair et al 1984). Solutions with initial concentrations (C_i) of 0.10, 0.25, 0.50, 0.75, 1.00, 1.50, 2.00, and 2.50 mg L^{-1} PO_4-P were prepared by dissolving KH_2PO_4 in deionized (DI) water. The range of PO_4-P concentrations represented by these solutions corresponds to the PO_4-P concentrations observed in the NOI during its years of operation. The solutions were spiked to a Ca^{2+} concentration of 201 mg L^{-1} using $CaCl_2$ to mimic average 2016 Ca^{2+} ion concentrations in the impoundment, as recommended by Lucci et al. (2010). Chloroform was added to the solution, to a concentration of 0.1% by volume, to act as a microbial inhibitor (Detenbeck and Brezonik 1991). The solutions were stored in 1-L glass amber bottles at room temperature.

3.2.3. P analysis procedure and equipment

Each soil sample was weighed into eight subsamples with a mass of 0.750 g. Each subsample was combined with 25 mL of one of the eight KH_2PO_4 solutions in an individual centrifuge tube, allowing for 50% headspace in the tube. The soil-solution slurries were shaken uniformly for 24 hours on an end over end shaker (Tube Rotator No. 60448, Scientific Equipment Products). They were then centrifuged for 30 min at 3600 g. The supernatant was filtered through a 0.45 μm pore diameter nylon filter.

Final solutions were analyzed for PO_4-P concentration using a Hach DR5000 spectrophotometer. The Ascorbic Acid method (Hach DR/800 Method 8048) (USEPA 2017) was used, with Hach PhosVer 3 10 mL powder pillows as the reagent, for low concentration subsamples (C_i of 0.10-0.75 mg L^{-1} PO_4-P). This method is adapted from *Standard Methods for the Examination of Water and Wastewater* and is equivalent to USEPA method 365.2 and Standard Method 4500-PE for wastewater (Hach 2014). For high concentration subsamples (C_i of 1.00-2.50 mg L^{-1} PO_4-P), molybdovanadate was used as the reagent, and analysis was conducted according to Hach DR/800 Method 8114, which was also adapted from *Standard Methods for the Examination of Water and Wastewater*. The ascorbic acid method is recommended for solutions with concentrations ranging from 0 to 2.50 mg L^{-1} PO_4^{3-}, and the molybdovanadate method is recommended for solutions with concentrations of 0.3 to 45.0 mg L^{-1} PO_4^{3-}. The two reagents were chosen based on the respective P concentration ranges for which they are appropriate. Subsamples were transferred to borosilicate glass cuvettes with a 12 mm diameter for analysis in the spectrophotometer.

Two programs were written for the spectrophotometer, one for each PO_4-P analysis methods. For the ascorbic acid analysis method, the program was created using a nine-point calibration curve using solutions of 0.00, 0.31, 0.77, 1.23, 1.53, 1.84, 2.30, 2.61, and 3.07 mg L^{-1} PO_4-P, and a wavelength of 880 nm. For the Molybdovanadate method, the program was created using a curve of solutions 0.00, 0.77, 1.54, 2.30, 3.07, 4.60, 6.13, 7.67, and 9.20 mg L^{-1} PO_4-P, and a wavelength of 340 nm. Absorbance read by the spectrophotometer was translated into a result in terms of PO_4-P concentration, based on

these calibration curves. The KH_2PO_4-solutions used to create the calibration curve were also sent to the University of Minnesota Research Analytical Laboratory (RAL) for external verification of PO_4-P concentration. All subsamples with C_i of ≤ 0.75 mg L^{-1} and ≥ 0.75 mg L^{-1} were analyzed using the low and high concentration range programs, respectively.

3.2.4. Quality assurance and quality control

The spectrophotometer programs written for use with the PhosVer and Molybdovanadate analysis methods were based on a calibration curve with R^2 values of 0.9961 and 0.9956, respectively. With every soil sample analysis two KH_2PO_4 solutions were analyzed on the spectrophotometer for quality assurance and control. One KH_2PO_4 solution in the low concentration range and one in the high concentration range were analyzed. Results confirmed that the initial solutions were reading at the expected PO_4-P concentrations ($\pm$ 0.10 mg L^{-1}) on both spectrophotometer programs, and the solution P concentrations were not drifting during the time that the solutions were stored between analyses. The initial solutions were externally verified at RAL, and results were also within $\pm$ 0.10 mg L^{-1} of expected PO_4-P concentrations.

All experiment materials, including centrifuge tubes, syringes, and pipettes were sterilized for P analysis by washing with 5% HCl, according to the procedure outlined in *Chapter A3: Cleaning of Equipment for Water Sampling* of the *National Field Manual for the Collection of Water-Quality Data* (Horowitz and Sandstrom 1998).

3.3. Analysis

3.3.1. Calculating sorbed P (S)

The C_f was used to determine the mass of P sorbed in each subsample. C_f is the final concentration of PO_4-P (mg L^{-1}) in the supernatant. The S for a given C_f was calculated for each subsample (eqn 1). S is the mass of P sorbed in terms of mg P kg^{-1} soil.

$$S = (C_i - C_f)\frac{mg}{L} * 25\ ml * \frac{1\ L}{1000\ mL} * \frac{1}{0.75} g * \frac{1000\ g}{kg} \qquad (1)$$

25 mL is the volume of KH_2PO_4 solution added to each subsample and 0.75 g is the mass of soil in each subsample. C_f was plotted over S to create a buffer diagram for each sample.

3.3.2. Adjustments to C_i and C_f

An adjustment of C_i and C_f was necessary for all the subsamples, due to a difference between the expected and measured Ci. All initial KH_2PO_4 solutions were sent to RAL for analysis of PO_4-P to determine whether there was a difference between the expected and measured Ci. Several of the KH_2PO_4 solutions had a slightly underestimated expected PO_4-P concentration relative to the measured PO_4-P concentration (Table 3). This is likely due to the non-zero P content of the DI water used for preparing the solution. Analysis at RAL determined that the DI water used to create the KH_2PO_4 solution had a PO_4-P concentration of 0.06 mg L^{-1}. This concentration corresponds to the higher PO_4-P concentrations in the KH_2PO_4 solutions observed by RAL, which were approximately 0.06 mg L^{-1} above the expected C_i (Figure 7).

Table 3. Comparison of expected C_i with C_i measured on the Hach DR5000 spectrophotometer used for this experiment, and C_i measured at RAL.

Expected C_i	**Hach DR5000 Measured C_i**	**RAL Measured C_i**
0.00	0.00	0.06
0.10	0.14	0.16
0.25	0.26	0.31
0.50	0.50	0.56
0.75	0.72	0.81
1.00	1.06	1.08
1.50	1.50	1.59
2.00	1.98	2.05
2.50	2.45	2.60

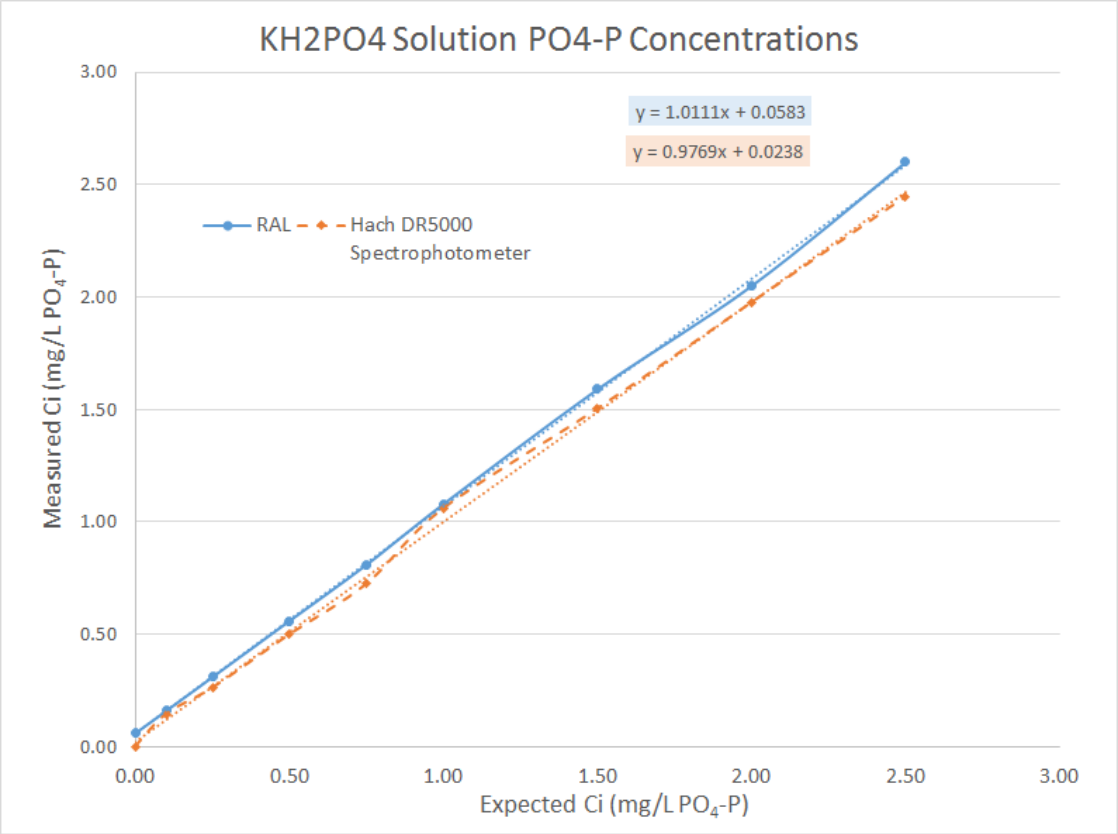

Figure 7. Plot of measured C_i over expected C_i, as determined by both the Hach DR5000 spectrophotometer and analysis at RAL.

In order to calculate the proper C_f (PO_4-P mg L^{-1}) and S (mg kg^{-1}) values the PO_4-P concentrations recorded at RAL for the KH_2PO_4 solutions were used in analysis. Because the spectrophotometer programs were created using calibration curves based on solutions with underestimated P content, an adjustment was made to the C_f values read by the instrument. The adjustment assumes that the trend of the results would be the same between the C_f recorded and C_f after the following mathematical adjustment (eqn 2).

$$Rt = Re\left(\frac{\propto(Ct)+\beta}{\propto(Ce)+\beta}\right) \qquad (2)$$

Rt is the measured C_f (PO_4-P mg L^{-1}), Re is the expected C_f (PO_4-P mg L^{-1}), Ct is the measured C_i, Ce is the expected C_i, and α and β are the slope and intercept, respectively, of a line through the data on a plot of Re over Ce. This equation has the following derivation:

$$Rt = \propto (Ct) + \beta$$

$$Re = \propto (Ce) + \beta$$

$$\frac{Rt}{Re} = \frac{\propto(Ct)+\beta}{\propto(Ce)+\beta}$$

Equation 2 relates the adjusted C_f to the original values read on the spectrophotometer using the ratio of the expected C_i to the C_i measured at RAL.

3.3.3. DOC adjustment

An additional adjustment needed to be made to the spectrophotometer reading of C_f for the subsamples analyzed using Molybdovanadate as a reagent. The adjustment was necessary because the blank used in this procedure did not account for solution color that results from dissolved organic carbon (DOC), which causes absorbance of 340 nm light. In the initial analysis procedure, a mixture of 10 mL DI water with 0.5 mL molybdovanadate was used as the blank for spectral analysis. The subsample also had 0.5 mL molybdovanadate added, to serve as the reagent. To correct the spectrophotometer readings all the soils were shaken, centrifuged, and filtered according to the original procedure, and prepared for analysis. They were analyzed using the same blank, but with no reagent in the subsample itself. This way, the spectrophotometer reading represented the absorbance that resulted solely from the color of the DOC in the filtered supernatant. The resulting value

was subtracted from the initial C_f results to account for the DOC color and correct the overestimated PO_4-P (mg L^{-1}) values. This adjustment was not necessary for the subsamples analyzed using the ascorbic acid method because the blank in this procedure is the subsample itself, with no reagent in it, and accounts for the DOC color in the solution. This method also uses a wavelength of 880 nm, which does not interact with the DOC in the subsample.

3.3.4. EPC_0 and K

Buffer diagrams (Froelich 1988) for each sample were used to determine the equilibrium P concentration at zero-sorption (EPC_0) and linear adsorption coefficient (K) values for each soil. The EPC_0 is the x-intercept on a buffer diagram, representing the C_f (mg L^{-1}) at which there is no sorption, or S=0 (mg kg^{-1}). K is the slope of a line fitted through the data at the intercept. Because the slope of the data was variable between the lower and higher concentration data, the lower four data points (C_i = 0.10 through 0.75) were isolated and fitted with the best-fit line, to determine EPC_0 and K for each sample.

3.3.5. Langmuir and Freundlich models

Sorption results were fitted using the Langmuir and Freundlich models (Bolster 2016), as well as several modified versions of the standard equations. The Langmuir (Eqn 3) and Freundlich (Eqn 4) equations are used to solve for S based on known C_f. S_{max} is the the maximum sorption capacity of the soil (mg kg^{-1}), K_l is the Langmuir linear adsorption

coefficient, K_f is the adsorption value, representing the amount of P adsorbed (mg L^{-1}), and, like n, is an empirical constant.

$$S = \frac{S_{max} K_l C_f}{1 + K_l C_f} \quad (3)$$

$$S = K_f {C_f}^n \quad (4)$$

The original Langmuir and Freundlich equations were modified to account for a non-zero C_f at zero S. By nature, isotherms have an intercept of 0,0. However, the plots of S over C_f had non-zero intercepts for all samples. To fit a curve through the data that represents the trend at near-zero S values, the Langmuir and Freundlich equations were modified to force the fit through a non-zero intercept. The modification involved adding the parameter EPC_0 to each equation. The Forced-Intercept-Langmuir (Eqn 5) and Forced-Intercept-Freundlich (Eqn 6) equations are:

$$S = \frac{S_{max} K_l C_f}{1 + K_l C_f} - \frac{S_{max} K_l EPC_0}{1 + K_l EPC_0} \quad (5)$$

$$S = K_f ({C_f}^n - {EPC_0}^n) \quad (6)$$

Because a new parameter was added to the equations, the parameters S_{max}, K_L, K_f, and n no longer represent the soil-P binding characteristics that they do in the original Langmuir and Freundlich equations. However, modeled parameters can be compared

between samples for both the Forced-Intercept-Langmuir and Forced-Intercept-Freundlich equations. The plots of modeled S over C_f are no longer true isotherms.

A spreadsheet tool created by Bolster (2016) was adapted and used to analyze results. This tool was designed to encourage the testing of nonlinear sorption models and can generate statistics related to the goodness-of-fit for each model (Bolster 2016). The sorption models that it supports are the Langmuir, Freundlich, Freundlich-Langmuir, and Two-Surface Langmuir. The latter two models were not used in this study because they are based on three and four parameters, respectively, and are unnecessarily complex for describing the relatively narrow range of P concentrations that sorption tests were conducted for. The spreadsheet tool was amended to model S by solving the Forced-Intercept-Langmuir and Forced-Intercept-Freundlich equations.

The spreadsheet tool developed by Bolster (2016) uses the Excel © Solver add-in. The solver is set to change the values of two model parameters in such a way that would result in the lowest sum of squared errors (SSE) for the model results. The parameters changed are K and S_{max} for the Langmuir model, and K and n for the Freundlich model. The solver method used is GRG Nonlinear. Constraints were added to the solver that limited both parameters in each model to positive values.

3.3.6 Soil analyses: LOI, P, pH

To better understand the characteristics of the impoundment soils, soil samples were analyzed for P content, ammonium acetate-extractable potassium (NH_4OAc-K), organic matter content, and pH. In 2014 and 2015, soils were collected from 0-5 cm depth

from the same sampling locations depicted in Figure 5. These locations correspond to the sites from which the soils were collected in 2016, for the soil-P sorption tests. Soils were dried at 35°C in a lab oven, crushed, screened using a 2 mm mesh, and analyzed at RAL for P content, NH_4OAc-K, organic matter, and pH. All soils collected and processed in July 2016 for the sorption experiment were analyzed for organic matter content. The organic matter content was determined using a loss on ignition experiment adapted from the *Loss-on-Ignition Standard Operating Procedure* (LacCore 2013) and *Direct Estimation of Organic Matter by Loss on Ignition: Methods* (SFU Soil Science lab 2011). Each soil was weighed to 5.000g ± 0.001g and heated at 550 °C for 4 hours in an Isotemp muffle furnace (Fisher Scientific). The soils were cooled in a desiccator and then reweighed. The organic matter content was calculated according to Eqn 7.

$$\%\ OM = \frac{pre.ignition\ weight\ (g) - post.ignition\ weight(g)}{pre.ignition\ weight\ (g)} \quad (7)$$

3.4 RESULTS

3.4.1. C_i, C_f, and S

Soil-P sorption results are summarized in Table 4. On average, the results for S switch from negative (desorption) to positive (sorption) between 0.25 and 0.50 (mg L^{-1} PO_4-P) as the initial concentration. However, some soil samples experienced desorption with C_i as high as 0.75 (mg L^{-1} PO_4-P), and others experienced sorption at solution concentrations as low as 0.10 (mg L^{-1} PO_4-P). Average C_f and S values show that as C_i increases, C_f and S increase, but not in a linear manner.

Table 4. Summary of soil-P sorption final concentration (C_f) and sorption (S) results for each initial concentration (C_i).

	C_f (mg L^{-1} PO_4-P)			S (mg P kg^{-1} soil)		
C_i (mg L^{-1} PO_4-P)	**Mean**	**Min**	**Max**	**Mean**	**Min**	**Max**
0.10	0.30	0.15	0.73	-10.00	-40.28	0.41
0.25	0.31	0.11	0.62	-0.40	-20.85	11.79
0.50	0.39	0.14	0.73	10.95	-11.43	26.65
0.75	0.51	0.21	1.16	19.62	-24.96	40.19
1.00	0.48	0.20	0.79	39.66	16.68	58.95
1.50	0.80	0.52	1.28	52.89	20.42	71.26
2.00	1.19	0.74	1.66	57.26	25.64	87.41
2.50	1.38	0.96	1.81	81.22	52.48	107.94

Trends between the variables C_f and S, and the constants, cell and use designation, were also analyzed. The A4 and B4 cells, which were both designated for water quality benefits, were the cells in which soils yielded the lowest average C_f, or final concentration of P in solution (Figure 8). The land use designation for these two cells is termed water quality treatment (WQT). The soil sample from the exterior of the impoundment yielded the highest average C_f. Consequently, the WQT cells, A4 and B4, had the highest average sorbed P, while the exterior soils had the lowest (Figure 9). Regarding use designation, the exterior soil still had the highest C_f and lowest S values. Flooded cells and soils cropped with soybean and wheat had the lowest C_f and highest S values (Figures 10 and 11).

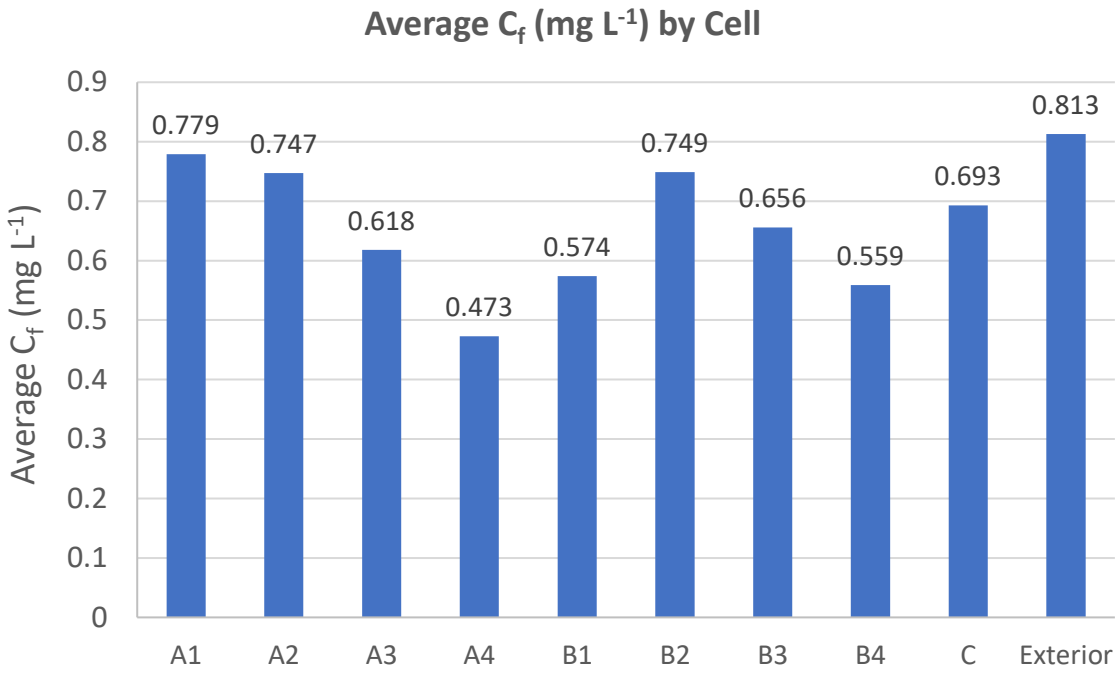

Figure 8. Average C_f by cell.

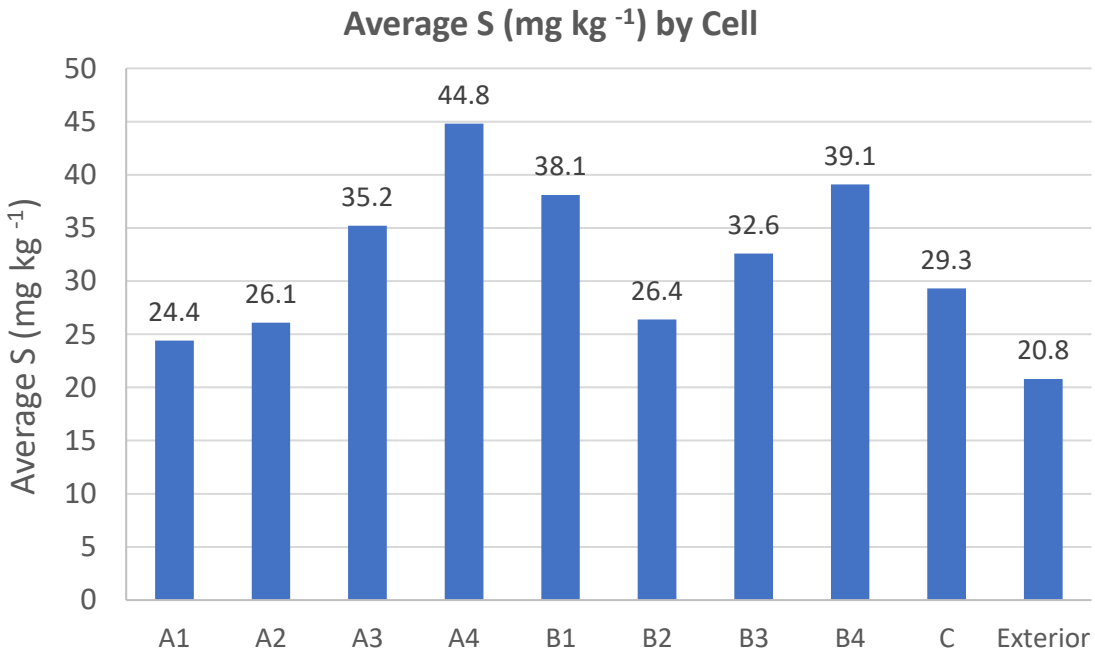

Figure 9. Average S by cell.

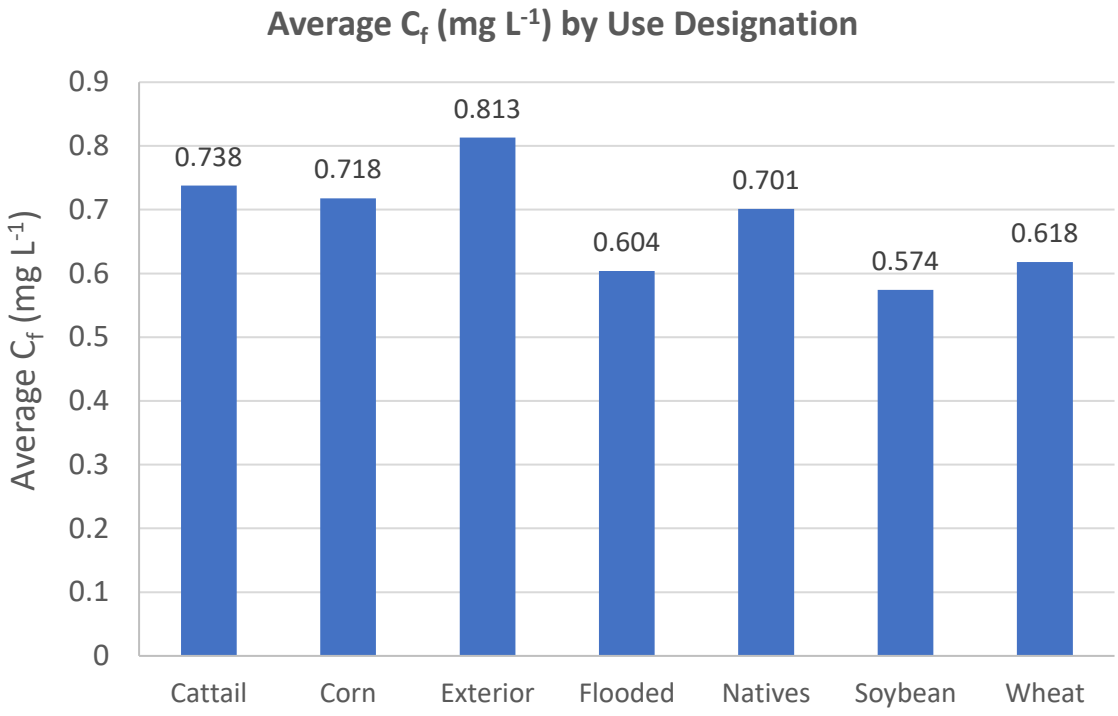

Figure 10. Average C_f by use designation.

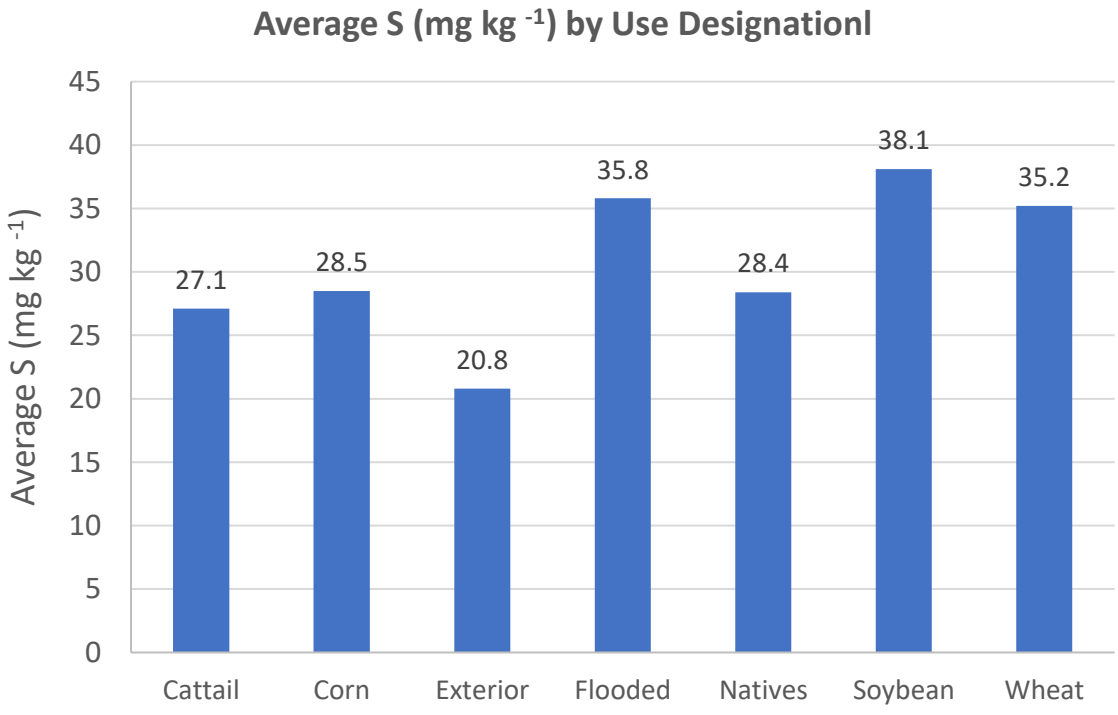

Figure 11. Average S by use designation.

The table of complete soil-P sorption results (Appendix C) features C_i, C_f, and S for each soil sample analyzed. The values in Appendix C have been adjusted to represent the most accurate C_i, based on internal and external lab verification of initial solution PO_4-P concentrations.

Adjustments have been made to the results in Appendix D to account for the influence of sample color derived from DOC. The table in Appendix D features C_i and PO_4-P concentration as read by the spectrophotometer due to DOC effects, and adjusted C_f and S values.

3.4.2. Buffer diagrams

Buffer diagrams for each sample can be found in Appendix E, grouped by cell. Each buffer diagram for the A and B cells has two trends, each trend representing a soil sample collected in the cell. One exception is the B2 cell, for which only one sample was analyzed. The C cell results are represented in three plots: all soil sites combined, sites with observed cattail growth, and sites with observed native vegetation. Each trend is fitted with a logarithmic function to highlight two important features on the diagram for each sample. The two features are the y-intercept of each trend, which corresponds to C_f when S=0, and the slope at the intercept. The y-intercept is the EPC_0 and the slope is the K, both of which will be discussed in the following section. It is important to note that for analysis of EPC_0 and K the intercepts and slopes were found by considering only the lower concentration analysis for each sample, due to the non-linear nature of the trend across the full range of concentrations analyzed.

3.4.3. EPC_0, K

EPC_0 and K were found for each sample based on the buffer diagrams (Appendix F). The averages of EPC_0 and K for each cell are as follows (Table 5, Figure 12). EPC_0 and K were also interpreted by land use classification (Table 6, Figure 13), and crop type (Table 7, Figure 14).

Table 5. Average EPC_0 and K by cell.

Cell	Average EPC_0 (mg L^{-1})	Average K (L kg^{-1})
A1	0.38	97.41
A2	0.47	100.92
A3	0.22	108.94
A4	0.15	265.24
B1	0.17	156.91
B2	0.35	98.50
B3	0.24	136.03
B4	0.14	131.22

Table 6. Average EPC_0 and K by land use designation.

Use Designation	Average EPC_0 (mg L^{-1})	Average K (L kg^{-1})
Cattail	0.71	97.23
Cropped	0.25	121.60
Exterior	0.39	49.44
Flooded	0.35	130.24
Natives	0.38	101.55
Water Quality	0.15	210.02

Table 7. Average EPC_0 and K by crop.

Vegetation Type	Average EPC_0 (mg L^{-1})	Average K (L kg^{-1})
Corn	0.31	116.72
Soybean	0.17	156.91
Wheat	0.22	108.94
Natives, Millet	0.35	98.50

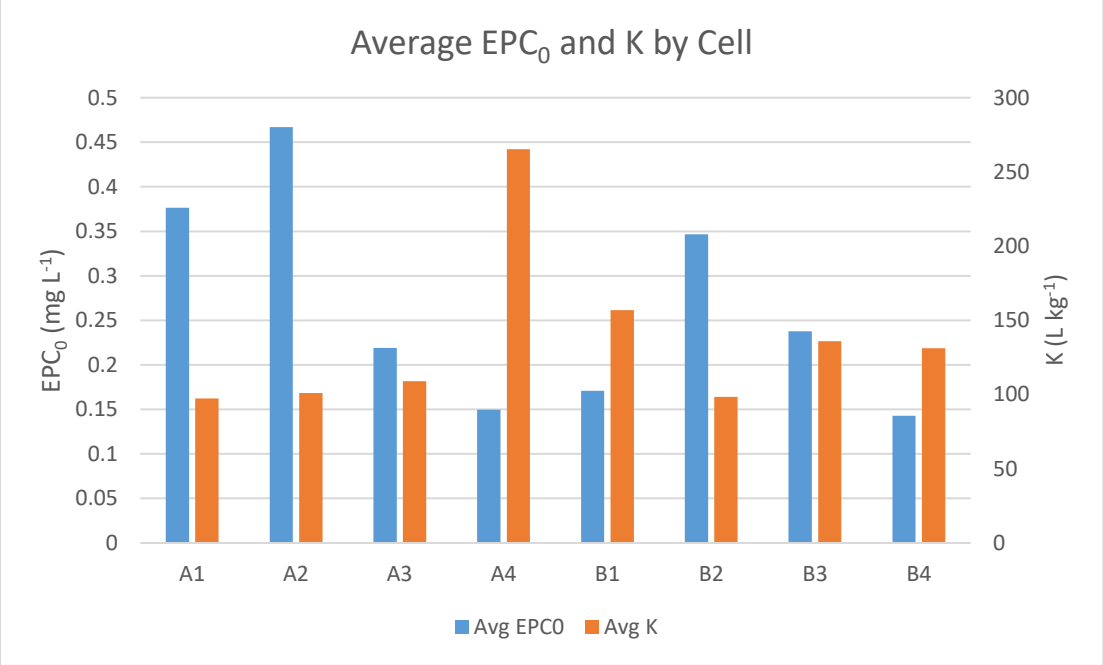

Figure 12. Graph of average EPC0 and K by cell.

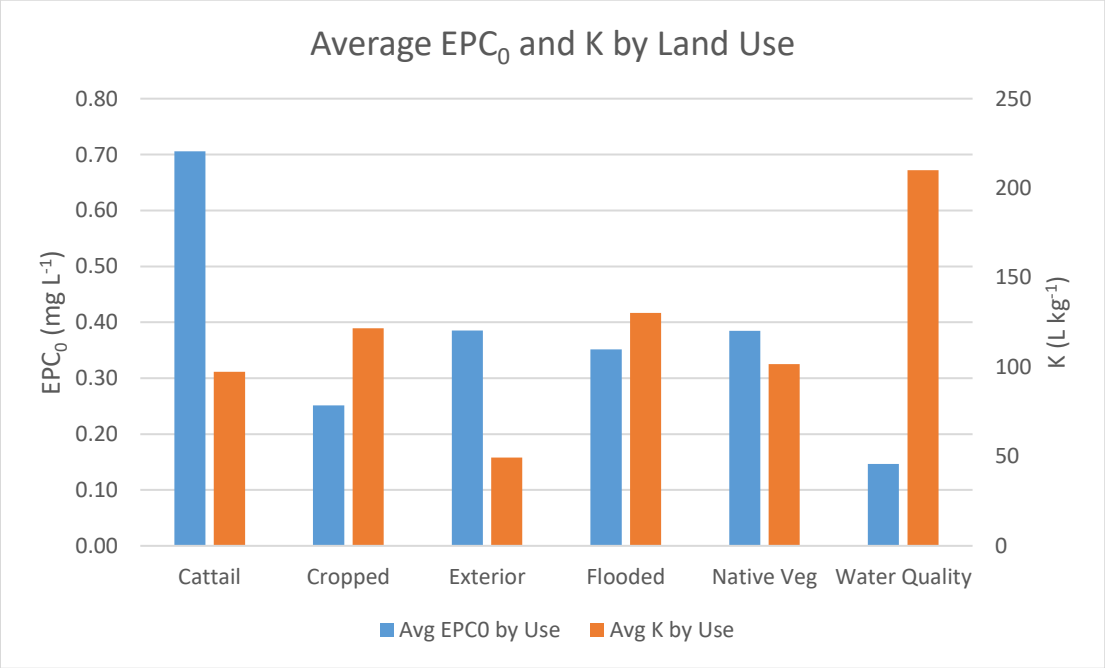

Figure 13. Graph of average EPC0 and K by land use designation.

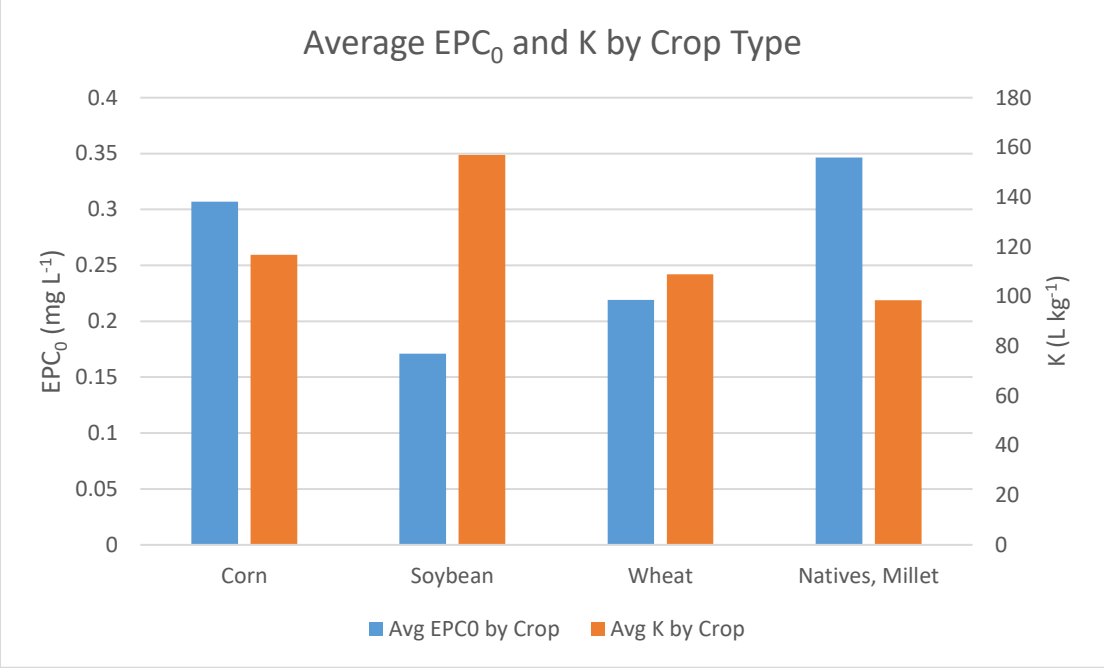

Figure 14. Graph of average EPC0 and K by crop type.

The two lowest average EPC_0 values were found for the two WQT cells, A4 and B4. The highest three average EPC_0 values correspond to the A1, A2, and B2 cells, all of which represent different land uses (corn, flooded, and millet, respectively). Regarding land use designation, samples from sites with cattails have the highest EPC_0 and WQT cell samples have the lowest. Based on Tukey-Kramer HSD analysis, the samples with WQT and cattail land use designations are statistically different at a 0.13 confidence interval. A student's t-test, at a 0.05 confidence interval, showed that the samples from cattail sites are significantly different from both the cropped and WQT sites with regard to average EPC_0. The remaining land use designations, cropped, exterior, flooded, and native vegetation all have comparable average EPC_0 results, ranging from 0.25-0.39 mg L^{-1}. Between the four different crop types, corn, soy, wheat, and millet, the soil samples from millet sites have a

slightly higher average EPC_0 of 0.35, and soil samples from soybean sites have the lowest average value of 0.17. The data collected for comparing crop types does not support the conclusion that there are statistically significant differences in EPC_0 based on crop.

The highest average K value was measured for the WQT cell, A4, and the remaining cells had comparable K values. Regarding land use designation, the sample collected at the exterior of the impoundment had the lowest average K value of 49.44, and the water quality designation had the highest, of 210.02. The WQT samples' average K is statistically different from the remaining use designations, based on a student's t-test at a 5% confidence interval and Tukey-Kramer HSD analysis at a 10% confidence interval. The remaining land use designations have comparable K values, ranging from 97-130. Of the four crop types, samples from soybean cropped soils had the highest average K result and those from millet had the lowest. The differences between crop types are not supported as statistically significant with the limited number of samples analyzed.

3.4.4. Langmuir and Freundlich: Original, Forced intercept, Model constraints

Results for the parameter values determined by each model for all soil samples can be found in Appendix H. Model statistics are summarized in Tables 8 and 9. Both the Langmuir and Forced-Intercept Langmuir models had an average model efficiency (E) value of 0.73. The Forced-Intercept Langmuir model has a higher SSE compared to the Langmuir model, with values of 2001.5 and 989.3 respectively. However, the Forced-Intercept Langmuir model had model constraints added to restrict inflation of the S_{max}

parameter. Therefore, the S_{max} and K parameters have a smaller range than the Langmuir model results.

The Freundlich and Forced-Intercept Freundlich models had similar model efficiencies, with E equaling 0.74 and 0.73, respectively. The SSE results were also comparable to the Langmuir model results, with SEE equaling 993.2 and 1898.8 for the Freundlich and Forced-Intercept Freundlich models, respectively.

Table 8. Average SSE and E, for the Langmuir, Forced-Intercept Langmuir, Freundlich and Forced-Intercept Freundlich models.

	Langmuir	Forced-Intercept Langmuir	Freundlich	Forced-Intercept Freundlich
Average SSE	989.3	2001.5	993.2	1898.8
Average E	0.73	0.73	0.74	0.73

The error and range statistics were relatively high for all model parameters, especially K_f in the Forced-Intercept Freundlich model and S_{max} in the Langmuir model (Table 9).

Table 9. Summary statistics for the Langmuir, Forced-Intercept Langmuir, Freundlich and Forced-Intercept Freundlich models.

	Langmuir			
	K	***S_{max}***	***SSE***	***E***
Mean	0.8	1.0E+04	989.3	0.7
Standard Error	0.5	3.5E+03	123.3	0.0
Median	0.1	752.9	946.6	0.8
Standard Deviation	2.8	2.0E+04	719.1	0.2
Sample Variance	7.8	4.1E+08	5.2E+05	0.0
Range	16.4	1.1E+05	2.9E+03	0.9
Minimum	0.0	72.7	49.4	0.1

Maximum	16.4	1.1E+05	2.9E+03	1.0

Forced-Intercept Langmuir

	K	S_{max}	*SSE*	*E*
Mean	3.0	217.5	2.0E+03	-0.1
Standard Error	0.4	9.0	577.4	0.5
Median	2.2	250.0	908.5	0.8
Standard Deviation	2.5	52.5	3.4E+03	3.1
Sample Variance	6.3	2.8E+03	1.1E+07	9.9
Range	8.3	250.0	1.8E+04	16.1
Minimum	0.5	0.0	3.8	-15.1
Maximum	8.8	250.0	1.8E+04	1.0

Forced-Intercept Freundlich

	K_f	*n*	*SSE*	*E*
Mean	1.0E+06	0.3	1.9E+03	0.0
Standard Error	2.2E+05	0.1	554.8	0.5
Median	3.5E+05	0.0	1.0E+03	0.7
Standard Deviation	1.3E+06	0.6	3.2E+03	3.0
Sample Variance	1.6E+12	0.4	1.0E+07	9.1
Range	3.7E+06	2.4	1.8E+04	16.1
Minimum	0.0	0.0	3.1	-15.1
Maximum	3.7E+06	2.4	1.8E+04	1.0

Freundlich

	K_f	*n*	*SSE*	*E*
Mean	58.2	1.0	993.2	0.7
Standard Error	3.8	0.1	129.7	0.0
Median	56.8	1.0	958.0	0.8
Standard Deviation	22.0	0.3	756.4	0.2
Sample Variance	483.6	0.1	5.7E+05	0.0
Range	92.2	1.8	2.9E+03	0.9
Minimum	14.8	0.1	46.8	0.1
Maximum	107.0	1.9	2.9E+03	1.0

When comparing the values determined for model parameters between the original and forced-intercept version of each model, percent errors ranged from 0% to percents in the thousands. A similar issue was encountered when comparing K values determined by the Langmuir model and buffer diagrams.

3.4.5. Soil properties: OM, Soil P, pH

Loss of ignition results (Appendix G) showed that organic matter in the impoundment soils collected in 2016 ranged from 6% to 20% by mass, with an average of 11%. Analysis at RAL for NOI soils in 2014 and 2015 showed that percent organic matter averaged 4.3%. RAL results for average Bray P, Olsen P, NH_4OAc-K and pH of the impoundment soils in 2014 and 2015 are in Table 10. Bray P and Olsen P are two measures of soil P that are used for soils with relatively low and high pH, respectively. Bray P applies to soils with a pH ≤ 7.4, while Olsen P applies to soils with a pH ≥ 7.4. Because of the pH of the impoundment soils, only Olsen P should be considered in analysis.

Table 10. Yearly averages for 2014 and 2015 impoundment soil properties, analyzed by RAL.

Year	Bray P (mg L^{-1})	Olsen P (mg L^{-1})	NH_4OAc-K (mg L^{-1})	OM (%)	pH
2014	4.5	11.0	142.4	4.3	7.6
2015	6.2	10.8	158.1	4.3	7.8

3.5. DISCUSSION

3.5.1. Analysis technique

Two spectrophotometric P analysis methods were used in the soil-P sorption experiment, creating additional steps in the experimental methods and data processing. Redesign of the methodology to use only one analysis method would reduce the number of assumptions required. It would also make the data collected more reliable and simple to work with. The two analysis methods – the ascorbic acid and molybdovanadate methods – were chosen with the intention to best represent the low and high P concentration ranges

expected in the samples, which the ascorbic acid method and Molybdovanadate method are respectively appropriate for. However, the P concentrations observed over the course of the experiment could have all been analyzed with the lower concentration range reagent, Ascorbic Acid, alone. Using only one analysis technique for all subsamples of a soil would place all measured C_f values on one calibration curve, improving the continuity and reliability of the data set. It would also remove the additional steps that were created by using two different reagents. These steps are the molybdovanadate analysis itself, adjusting for DOC, and manipulating the C_f values to account for results from RAL validation of the analysis technique accuracy. It is also likely that the Langmuir, Freundlich, and forced intercept models would have better fit results if only one reagent was used. One issue with modeling is that the data often fell into two trends when stitching the subsample results from the two different reagent analyses together: One for high P concentration samples and one for low concentration samples, with some overlap (Figure 15). This issue is most likely caused by analysis of subsamples on two different spectrophotometer programs, created using two different calibration curves.

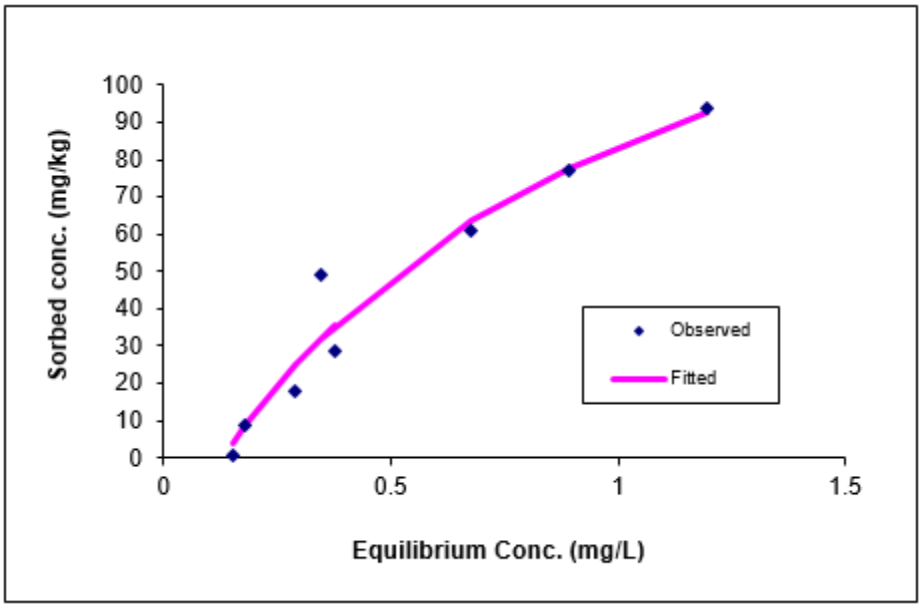

Figure 15. Example of poor Forced-Intercept Langmuir model fit, due to combining of data, measured using two different P analysis techniques. *Note the overlap of data points near the 0.35 mg/L range.*

Were this experiment to be repeated or expanded, ascorbic acid should be the only reagent used for P analysis. If the range of C_i and C_f analyzed needs to be expanded, a different analysis method with a broader range of accuracy should be selected.

3.5.2. Buffer diagrams

The buffer diagrams, in which two or more samples taken from one cell had differing trends, slopes, and intercepts, speak to the heterogeneity in soil properties that can be achieved in very little time, with small differences in hydrology and vegetation. The soils that make up the impoundment cells and dikes were formerly farmland soils that were

taken out of production and reworked, becoming homogenized in the process. The soil in this region is relatively homogenous to begin with because its pedogenic origins are lake sediments from the glacial Lake Agassiz, which covered a great portion of western Minnesota. The LOI results, RAL soil analysis, and soil pit interpretation results confirm that pH, OM, NH_4OAc-K, and P content of soils across the entire impoundment area are not highly variable. Therefore, it is noteworthy that different soils collected from one cell and processed in the same way can exhibit different (de)sorption responses in one solution. It is possible that just three years of impoundment management, during which various types of vegetation were planted, and hydrology was manipulated in such a way that water retention time varied between and within the cells across time, resulted in heterogeneous use of sorption sites and physical properties of the soils in the system. On one hand, this makes analysis of EPC_0 and K more complex, requiring a greater sample size for meaningful statistical analysis. On the other, it speaks to the power of intentional land management aimed at capturing and storing phosphorus in the impoundment for water quality benefits.

Regarding experimental design, the heterogeneity within the cells, especially in the C cell, may inform a redesign with a narrow scope and greater sample size. The C cell is the size of all four A or B cells combined, and therefore has more heterogeneous vegetation types, hydrology, and consequently soil properties than the A or B cells individually. There is a greater land gradient in the C cell than in the A or B cells, resulting in areas with standing water and a range of moist to dry areas in which vegetation varies. The C cell also has more TSS inputs from the watershed than the A or B cells. Following large inflows,

water moves freely within the C cell, blurring the effects of land management on soil sorption properties. If this experiment were to be continued or used as a model, focusing efforts on more isolated and homogenous systems like the smaller A and B cells may be advantageous. Though less representative of natural systems without constructed dikes and engineered control structures, these cells can help to constrain what the expected effects of land management on soil-P sorption properties may be.

3.5.3. EPC_0 and K

EPC_0 and K are useful parameters in that they relate to sorption properties of the soils analyzed. The EPC_0 represents the concentration of P in solution at which soils have the maximum capacity for buffering added P. If the system is perturbed by an influx of P from senescence of vegetation or from sediments following a storm event, equilibrium will be re-attained quickly near the EPC_0 concentration (Froelich 1988). Conversely, if P is lost from the system by rapid uptake by vegetation during the spring or other means, equilibrium will be established to the EPC_0 by desorption from the soils.

The average EPC_0 results for the impoundment, by cell, ranged from 0.14-0.47 (mg L^{-1}), which is relatively high compared to lake EPC_0 values reported by Wang and Li (2010) for lake sediments, and even higher compared to EPC_0 reported for other aquatic systems: estuary, marine, wetland, river, and canal. River systems, in general, have much lower average EPC_0 values than those observed for the impoundment soils. Comparison of EPC_0 results from 12 different stream and river studies showed an average EPC_0 range from 0.005-0.155 (mg L^{-1}) (James and Barko 2004, James et al. 2002, James and Barko

2005, Mayer and Gloss 1980, Carignan and Vaithiyanathan 1999, Meyer 1979, Klotz 1985, Wauchope and McDowell 1984, and Chang-Ying et al. 2006 in James and Larson 2008). Few soil-P sorption studies have been conducted in systems resembling the NOI.

Comparing EPC_0 values determined in laboratory soil-P sorption experiments with natural P concentrations observed in the NOI (Table 11) can help to predict the expected soil-P behavior under a variety of inflow chemistries. Inlet water chemistry monitoring shows that average TP concentrations in inflows to the NOI were 0.46, 0.43, and 0.27 (mg L^{-1}) for 2014, 2015 and 2016, respectively. For OP, the average inflow concentrations for these three years were 0.34, 0.23, and 0.16 (mg L^{-1}), respectively. Because the EPC_0 represents the natural equilibrium state of a system, and OP concentrations are very close to the average EPC_0 results (EPC_0=0.14-0.47 mg L^{-1}), sorption and desorption rates of P from soils in the impoundment should be approximately balanced. If P concentrations in the inflows to the NOI increase significantly, P sorption rates will exceed desorption rates to re-attain the equilibrium state, EPC_0. However, sorption sites on soil surfaces are finite and can become saturated. If inflow P concentrations continue to be higher than the EPC_0, outlet water P concentrations may begin to exceed inflow P concentrations.

Table 11. Comparison of monitored NOI inlet TP and OP concentration averages and ranges for 2014-2016 with the experimentally determined average and range of average EPC_0 values.

	Average (mg L^{-1})			
Year	**TP**	**OP**	**TP Range**	**OP Range**
2014	0.46	0.34	0.31-0.64	0.28-0.40
2015	0.43	0.23	0.21-0.74	0.004-0.35

	Average (mg L^{-1})			
Year	**TP**	**OP**	**TP Range**	**OP Range**
2016	0.27	0.16	0.05-0.51	<0.003-0.36
* Considering averages, by cell.			**EPC_0 ***	**EPC_0 Range***
			0.14-0.47	0.14-0.47

While EPC_0 averages by cell were comparable to the inlet OP concentrations, analysis of EPC_0 by land use designation demonstrated that equilibrium states depend on the hydrologic and vegetation status of the soil. For example, the average EPC_0 for soils that have cattail growth is 0.71 (mg L^{-1}). This means that the average inflow water has a lower P concentration than the EPC_0 and could be expected to cause desorption of P from the soils into solution, to reach the equilibrium state. Conversely, the average EPC_0 for the WQT soils was 0.15 (mg L^{-1}). Inflow waters with average P concentrations, based on monitoring from 2014-2016, have a higher P concentration than the equilibrium state and can be expected to cause sorption of P from the solution to soil surfaces. Consequently, cells managed for water quality benefits have the potential to capture and store P, reducing outflow concentrations. In comparison, cells managed for cattails can release P into solution, which increases P concentrations in the outflows of the NOI. These predictions, however, are based solely on EPC_0 results, and do not yet consider the effect of the P-buffer strength property, K.

The slope parameter, K, represents the P-buffer intensity of the soil. Samples with steep slopes, meaning high K values, have high buffer intensity; samples with shallow slopes and low K values have low buffer intensity (Froelich 1988). The average K results, by cell, ranged from 98.5 to 265.2 (L kg^{-1}). By use designation and vegetation type, the ranges were 49.4-210.0 and 98.5-156.9 (L kg^{-1}), respectively. These averages are lower

than K values determined for a variety of land uses by James, Eakin, and Barko (2004). The K values in their study for barnyards, cornfields, and woodlots, are 451, 633, and 950 (L kg^{-1}), respectively. The NOI impoundment averages are also lower than K values determined for river systems. Examples of reported K values averages are 400 (L kg^{-1}) for the Lower Mississippi River floodplain sediments (Wauchope and McDowell 1984), 600 (L kg^{-1}) for TSS in the Colorado River, and between 250-1380 (L kg^{-1}) in South American Rivers (Carignan and Vaithiyana 1999) (James and Larson 2008). The range of K values identified for the NOI soils is relatively narrow, suggesting a degree of homogeneity in the soil properties, as previously discussed.

Though the range of K values for the NOI is not broad, there are some differences between soils corresponding to different cells and land use designations that warrant mention. The K value for soils at the exterior of the impoundment (49.4 L kg^{-1}) is lower than the K value for all the soils in the impoundment. Within the impoundment, the soils in the cells designated for water quality treatment have the highest K value of 210.1 (L kg^{-1}). The A4 cell, designated for WQT, has the highest recorded average K value of 265.2 (L kg^{-1}). These results suggest that all the impoundment soils have a higher P-buffer potential than the soils just outside of the impoundment system, despite the exterior soils having the same pedogenic origin and historic land use. The results also suggest that soils that have been managed for water quality benefits do, in fact, have the strongest potential to buffer P added to the system.

Each cell of the impoundment has varied in terms of land management since the start of operation for the NOI, but there is one difference that sets all the impoundment

soils apart from the exterior of the system. All the impoundment cells have been flooded or saturated with water at some point each year, for the past three years, regardless of vegetation. The exterior sample was taken from a corn field, just across the road from the impoundment and has similar soil properties, climate, and management, compared to the cropped cells in the impoundment. However, the corn field outside of the impoundment did not experience the water volume or retention time that the impoundment cells received. It is possible to interpret that periodic saturation or flooding of the soils may contribute to the higher P-buffer capacity of the soils in the NOI. Based on the results, it may be worth further investigating the effects of residence time and frequency of ponding water on soil-P dynamics in the NOI and similar systems.

Vegetation may also play a significant role in soil P-buffering potential. Between the different vegetation types, soybeans have the best performance and millet has the worst, regarding soil P-buffering. Not enough samples were collected and analyzed to identify statistically significant relationships between vegetation type and K, but this may be a valuable area to research in the future, in order to identify the optimal plant communities and rotation schedules for P capture and water quality benefits.

Interpretation of EPC_0 results suggests that the highest P sorption would be achieved in the WQT cells, and soils managed for cattails would have the poorest P capture performance. Interpretation of K results supports the prediction that the WQT cells would achieve the best water quality benefits, and suggests that soils inside of the impoundment outperform the exterior soil with regard to P capture. Analyses of average C_f and S by cell supports the predictions, made based on EPC_0 and K, about the WQT cells. These two cells

(A4 and B4) yielded the lowest average C_f, or final concentration of P in solution and the highest S, or mass of sorbed P. The interpretation of K values suggesting that the exterior would yield the least water quality benefits is also supported by the analysis of C_f and S values. The soil sample from the exterior of the impoundment yielded the highest average C_f and lowest S values. However, conclusions drawn about the applicability of these predictions are limited by the small sample size; for the exterior site, n=1.

3.5.4. Models

Four different models were compared in analysis of the soil-P sorption results, because each has advantages and disadvantages over the others. However, the model results have approximate equal model efficiencies, when averaged for all the samples. The range of SSE is 993 to 2002, and all models performed relatively poorly compared with similar studies. Each model parameter, especially K_f in the Forced-Intercept Freundlich model and S_{max} in the Langmuir model, yielded a great range and standard deviation between values for different samples. Because of the way in which the relatively small and homogenous system is expected to behave, a large range of parameter values is not appropriate. The parameter values yielded by the model runs are therefore unlikely to be representative of true soil-P adsorption phenomena and are not considered in interpretation of the experiment results. Focusing on observed EPC_0, K, C_f, and S for interpretation is more consistent with understanding of the physical and mathematical significance of these parameters. Modeling soil-P adsorption isotherms using the Langmuir, Freundlich, and Forced-Intercept models may be more appropriate for studies with higher P-concentration

samples and a greater number of samples and subsamples. The advantages and disadvantages of using one versus another are discussed briefly in the methods section, but suggestions on model selection are outside of the scope of this paper.

3.5.5. Limitations

The soil-P sorption experiment was designed and controlled to simulate measured soil and water properties at the NOI site, but there are still limitations to laboratory (de)sorption experiments that warrant mention. Firstly, this experiment tested soil-P responses based on (de)sorption only – it did not measure the results of the absorption step, which is an important process in total P sorption. If the contact time between the soil and solution was longer than the 24 hours required in the methodology used, there would be potential for a significant amount of absorption to occur, affecting the C_f measured for each subsample. Secondly, soil-P dynamics depend on the redox state and pH of the solution. In this experiment, the solution was kept aerated and oxic for the entire sample analysis, and the pH of the P-solutions was approximately 8. Although it is likely that the impoundment water will remain oxic during most or all of the wet season, due to the shallow depth of water and wind activity, there is no control on the redox state of the impoundment soils. Inflow pH is also not controlled and will depend on upstream sources. Redox state, pH, and other environmental and chemical factors will affect the soil-P processes occurring. Results based on laboratory experiments are useful for predicting behavior at the research site, but do not necessarily define the rate of soil-P reactions and equilibrium concentrations that will be achieved on-site.

4. CONCENTRATION AND LOAD REDUCTIONS

4.1. BACKGROUND

Wetlands have been observed to capture nutrients and reduce downstream loads across the world, and the use of wetlands for pollutant storage in agricultural watersheds has been a growing research interest in recent years (Nairn and Mitsch 2000). However, less is known about the performance of created wetlands, like the NOI, in water quality treatment (Mitsch et al. 1995).

In order to best understand and characterize nutrient storage and movement on the landscape, both nutrient concentrations and loads need to be analyzed. The concentration of a pollutant, expressed as a mass per volume water (i.e. mg L^{-1}), relates to its abundance in an aquatic system and availability to affect aquatic life and water quality. The load of a pollutant is expressed in terms of a mass (i.e. kg, lbs), and derived from a known concentration and volume of water. Calculating loads entering and leaving an aquatic system is important for identifying pollutant storage and transport rates. For the NOI, these calculations are used to describe the system's ability to capture pollutants and reduce downstream loads.

Load and concentration are related by volume of water. For example, the load of TP in a waterbody is the product of the concentration of TP and the volume of water. The load of TP in a liter of water is 1 mg, if the TP concentration is 1 mg L^{-1}. Because load calculations are based on water volumes, a nutrient budget is always based on a water budget. Once a water budget is developed, observed or modeled concentrations of a

pollutant can be multiplied by the corresponding water volume on each day to find a pollutant or nutrient budget.

A water budget is essentially a model that accounts for water movement into and out of a defined system (Healy and Scanlon 2010). In this case, the system is the impoundment cells. Water budgets are built based on the principle of conservation of mass. In hydrologic systems, water can enter and exit a system through a variety of pathways. In the NOI, inputs are precipitation and surface runoff. Outputs are evapotranspiration (ET) and outflows when the impoundment outlets are opened. Losses by interflow and to groundwater recharge are normally considered in water budgets, but because of the dense, clay-rich soils in the region, these components are approximated to be zero. Theoretically, when the change in storage of the impoundment system is zero, the volume of water inputs and outputs sum to zero (Eqn 8). Water balance calculations can also be derived from energy balance equations, but they are outside of the scope of this paper.

$$S = 0 = Ri + P - ET - Ro \qquad (8)$$

Where
S = storage
Ri = runoff into the system
P = precipitation
ET = evapotranspiration
Ro = runoff out of the system.

Unlike precipitation and runoff, which are monitored at the impoundment, ET needs to be calculated from several other parameters measured and approximated for the site. ET calculation requires information about factors including radiation, temperature, humidity,

and wind. There are many equations with which ET rates can be calculated, but one of the most popularly used is the Penman-Monteith equation (Eqn 9), adapted from FAO (2016). Articles or chapters focusing on this method should be referenced for the derivation of this equation and some of its parameters.

$$ET_o = \frac{0.408\Delta(R_n - G) + \gamma \frac{900}{T+273} u_2 (e_s - e_a)}{\Delta + \gamma(1 + 0.34u_2)} \quad (9)$$

where

ET_o = reference evapotranspiration (mm day^{-1})
R_n = net radiation at the crop surface (MJ m^{-2} day^{-1})
G = soil heat flux density (MJ m^{-2} day^{-1})
T = mean daily air temperature at 2 m height (°C)
u_2 = wind speed at 2 m height (m s^{-1})
e_s = saturation vapor pressure (kPa)
e_a = actual vapor pressure (kPa)
$e_s - e_a$ = saturation vapor pressure deficit (kPa)
Δ = slope vapor pressure curve (kPa $°C^{-1}$)
γ = psychrometric constant (kPa $°C^{-1}$)

4.2 METHODS

4.2.1 Data collection

Water chemistry data were collected at the impoundment in 2014, 2015, and 2016. For inlet and outlet water, samples were collected from the two automated ISCO samplers (3700 Portable Sampler Compact Model) (Teledyne ISCO, Lincoln, NE) located at the inlet and outlet of the impoundment. As reported in Vieths et al. (2017), the data collection design was adjusted over time, “in terms of sampling timing and frequency, to achieve a

comprehensive and representative water chemistry record. In 2014, the ISCO samplers were not yet programmed and sampling was conducted by field technicians and other staff manually running the ISCO when they were on-site. Sampling did not necessarily correspond to runoff events. Therefore, the record collected in 2014 did not fully represent the range of water chemistries associated with storm and baseflow events at the site. In 2015, the ISCO was programmed to collect a sample every 24 hours, so that each day's water chemistry would be captured. Not every sample was sent to RMB Environmental Laboratories for analysis. ISCO bottles were selected for analysis based on their proximity in time to runoff events, and water monitoring needs.

In 2016, a more sophisticated ISCO program was written and launched. The ISCO sampler was connected to a pressure transducer and set to trigger sampling any time the stage increased by 1.6" in 2 hours, or 2.4" in 1 hour. Under this scheme, samples collected were representative of water chemistry on the rising and falling limbs of the hydrograph, following runoff events at the site. Baseflow samples were collected intermittently. Each time a field technician collected samples from ISCO bottles on-site, data was downloaded from the ISCO and pressure transducer in order to create a hydrograph and determine which bottles were most important to have analyzed, based on the timing of their collection. The intent is to use this sampling design going forward, and increase sampling frequency in order to build a complete and reliable water chemistry record."

The volume of water in the impoundment and its movement between the impoundment cells were tracked using two different methods. The first method involved gate and weir equations, written for the impoundment structures based on mathematical and

hydrological principles. The second method determined volume of water in each Cell based on pressure transducer data and stage-to-storage relationships for the site. The readout from the pressure transducers, located throughout the impoundment, indicates the height of water in each cell. The stage-to-storage curves, provided by the engineering firm that completed this project (Widseth Smith Nolting) relate height of water to volume of water, in each cell. The stage-to-storage curves were made accessible to UMN and the RRBC in 2016 and used for the 2016 water budget and load reduction calculations. Water budget calculations for 2014 and 2015 relied on the gate and weir equations.

The weather data used in the 2016 water budget calculation was collected in 15 minute increments for the entire sampling season. It included wind speed, temperature, relative humidity, and cumulative rainfall, and was collected by the weather station installed on-site. These parameters, along with solar radiation data for the region, found at (http://www.nrel.gov/gis/solar.html), were used to calculate the ET rate at the site on a daily time-increment. A spreadsheet tool called the Penman-Monteith Calculator (academic.uprm.edu/abe/backup2/.../PENMAN-MONTEITH%20CALCULATION.xls) (Harmsen 2001/2002) was used for these calculations. Daily ET results were compared with regional estimates on (http://agwx.soils.wisc.edu/uwex_agwx/sun_water/et_wimn) (UW Extension 2010), to ensure that rates calculated using weather-station data corresponded with estimations made for this region. This site allows for an entry of latitude and longitude to find regional ET estimates.

The number of water chemistry samples collected each year varied based on staff availability for monitoring, the lab analysis budget, and timing and frequency of runoff

events. The 2014 pollutant concentration reduction analysis was conducted based on 23 total water chemistry samples, collected in June and July of 2015. Samples were collected from the inlet and outlet of the impoundment, two judicial ditches connected to the impoundment system, and in-Cell grab samples for the A, B, and C cells. In 2015, the load reduction calculation was based on 37 total samples, comprised of 17 inlet samples, and 20 outlet samples. Sampling dates ranged from May to October, 2015. The 2016 load reduction calculation was based on 33 total samples, 19 for the inlet water and 14 for the outlet. Sampling dates ranged from March to November, 2016. The sampling seasons for 2015 and 2016 were bracketed by the date of the first snowmelt or runoff event, and the date of final draw-down of impoundment water before freeze-up.

4.2.2 Analysis

There was no water or nutrient budget calculation performed for the 2014 impoundment operational year. Pollutant reduction data for 2014 is limited to concentration reductions between water at the inlet and outlet of the impoundment. Reduction percentages were calculated for TN, TP, and TSS, and expressed in terms of percent (mg/L).

For the 2015 operational season, a water budget was calculated for the impoundment based on the mathematically derived weir and gate equations (Table 12). The weir equation (Eqn 10) was written by Bruce Wilson and is a modified version of the general weir equation (LMNO 2014) for a simple rectangular or v-notch weir, because of the unusual shape of the weir at the NOI (Figure 16) The weir is winding both in the

positioning and bending of the metal sheets, and in the corrugation of the weir material. The principle behind the weir equation written is that with low water height above the weir (i.e. low flows into the impoundment), the entire winding length of the weir affects water flow. When the stage of water is high above the weir, (under high flow conditions), the winding length affects the flow to a smaller degree and the weir behaves more like a simple, rectangular weir. The equation has a weighting factor, which depends on the height of the water, and determines whether the length of the weir used to calculate flow is the long, winding weir length or the rectangular weir length.

Figure 16. Photograph of the weir at the NOI inlet.

$$CwLw = Cw * L + Cw * (W - L) * \frac{S}{H2 - H1} \qquad (10)$$

$$Qw = CwLw * S^{2/3}$$

Where L= 209.46, curvy length of the weir (ft)

W= 108.64, rectangular length of the weir (ft)

H1=0.1, low flow height (ft)

H2= 3.0, high flow height (ft)

Cw= 3.09, $\sqrt{g}$ * 〚2/3〛 ^ (3/2) ((ft $(s^2)^{-1}$)

G = 32.2, gravity (ft $(s^2)^{-1}$)

S= observed stage above the weir (ft)

Qw= flow over the weir (cfs)

Table 12. Table of NOI gate rating curve equations, relating gate opening and hydraulic head to flow. Developed by Brad Hansen, 2014.

Gate Rating Curve Equations (Hansen, 2014)												
Gate Opening (feet)	Head (feet)											
	1	2	3	4	5	6	7	8	9	10	11	12
	Flow (cfs)											
0.125		0.7	0.8	1.1	1.2	1.4	1.5	1.7	1.8	2.0	2.0	2.0
0.25		2.0	2.5	3.2	3.7	4.1	4.5	5.0	5.5	6.0	6.1	6.2
0.375		4.0	5.0	6.4	7.4	8.2	9.0	10.0	11.0	12.0	12.2	12.4
0.5	4.5	7.5	9.0	10.2	11.8	12.8	14.0	15.0	16.0	16.8	17.9	18.0
0.625	6.3	10.3	12.5	14.4	16.5	17.9	19.5	20.8	22.0	23.4	24.9	25.3
0.75	8.0	13.0	16.0	18.5	21.2	23.0	25.0	26.5	28.0	30.0	31.8	32.5
1	14.0	22.0	27.0	32.0	35.0	38.0	42.0	45.0	47.0	50.0	52.0	54.0
1.25	20.0	31.0	38.0	44.5	49.8	54.0	58.0	62.0	66.0	70.0	73.0	76.0
1.5	28.0	42.0	52.0	58.0	66.0	73.0	78.0	84.0	88.0	94.0	98.0	102.0
1.75	34.0	52.0	64.0	75.0	83.0	91.0	97.5	104.0	110.0	116.0	122.0	126.0
2	42.0	62.0	77.0	88.0	97.0	107.0	115.0	123.0	130.0	136.0	143.0	148.0
2.25	48.0	72.0	86.0	100.0	112.0	122.0	130.0	139.0	147.0	155.0	162.0	168.0

To build the 2014 water budget, pressure transducer data at the impoundment inlet, where the weir is located, were used to determine the height of water above the weir. Gate operation logs maintained by all staff at the site were referenced for the timing and amount

of gate opening, both for the stop-log walls and the screw-gates. Combined, these data were used to determine the volume of water moved into and out of the impoundment on a daily time-step. The 2015 water budget did not account for precipitation or ET. The 2015 water and nutrient budgets are exclusively for the C cell of the impoundment because, during the 2015 operational season, all water reaching the impoundment was routed into and out of the C cell, only. The A and B cells were not used for water storage or movement.

Once a water budget was completed for the 2015-year, water chemistry measured at the inlet and outlet of the C cell was applied, on a daily increment, to build a nutrient budget. For the water chemistry data gaps on the days between sampling events, average baseflow, peak flow, and normal-flow concentrations of each pollutant were interpolated. Averages were based on the year's water chemistry data and matched to the precipitation record for the days with chemistry data gaps. The load reduction results were calculated separately for each pollutant, TP, TN, and TSS, but based on the one water budget for the year. In order to calculate 2015 pollutant load reduction, the loads in and loads out for each pollutant, on each day of the NOI operation season, were summed. The load reduction is calculated as in Eqn 11. Dividing the result by 100% yields the load captured, in lbs. Load capture data is calculated in lbs because the unit is more convenient to report and visualize than mg, the original measure of mass in the concentrations measured (mg L^{-1}). Nutrient mass captured can be reported in any unit, as long as the unit of concentration measured for pollutants in the water sample is properly converted.

$$\%\ Nutrient\ Reduction = \frac{Load\ In\ (lbs) - Load\ Out\ (lbs)}{Load\ In\ (Lbs)} * 100\% \qquad (11)$$

A more detailed water and nutrient budget was completed for 2016. Load reductions in 2016 were calculated for TP, TN, and TSS. The water budget was built using the engineer-provided stage-to-storage curves, which relate water height in each cell to water volume. In 2016, water was routed into the A, B, and C cells, and a budget was therefore calculated for the A/B cell system as well as the C cell. The reason that the A and B cells were combined for this analysis is that water was moved between the A and B cells during the course of the season, and the C cell remained isolated. To build this water budget, daily water height data for each cell, derived from the pressure transducer readouts, was matched to the corresponding cell water volume, according to the stage-to-storage curves. Changes in water volume were related to water movement, such that negative changes were considered outflows and positive changes were considered inflows. Cumulative rain and cumulative ET for each day were subtracted and added, respectively, to remove the impacts of these two sources on the water and nutrient budget. If they had not been removed, the budget would include positive and negative changes in water height measured by the pressure transducer, caused by precipitation and ET, even though they do not represent inflows and outflows from a given cell.

Once a water budget with a daily time-step was completed for the C cell and the A/B cell system, water chemistry data was applied to build a nutrient budget. Inflow and outflow data relating to the C cell, only, were used for the C cell load reduction calculations. The same is true for the A/B cell load reduction calculations. Gaps in water chemistry data were filled with interpolations of pollutant concentration using positive and negative growth functions (Excel), and estimations of whether baseflow, peak-flow, and

normal-flow chemistries would have been observed, based on careful examination of the regional precipitation record for the year. Like in 2015, load reduction was calculated for 2016 according to Eqn 11.

4.2.3. Slow drawdown scenario (modeled)

In addition to the measured water and nutrient budget built for 2016, a modeled water and nutrient budget was created to determine the effect of drawdown speed on pollutant capture. In fall 2016, water was held in the impoundment too close to freezing temperatures and had to be drained in a matter of only several days. The quick draw-down caused resuspension of sediments and consequently P, lowering the pollutant reductions achieved for the year (Vieths et al. 2017). A nutrient budget with slower end-of-season drawdown was modeled for TP, TN, and TSS. In this nutrient budget, the final week of the season was adjusted in the original 2016 water and nutrient budget, with a negative growth function used to interpolate water volume under a hypothetical slow-drawdown scenario. The gradual decrease in water volume decreased the load out on each day of the final week of operation, in turn.

4.3. RESULTS

4.3.1. Pollutant concentrations

Water quality monitoring results for 2014 in-cell grab samples are summarized in Table 13. All concentration and load reduction results in this paper have been reported

previously in Vieths et al. (2017), a project report prepared for the Legislate-Citizen Commission on Minnesota Resources (LCCMR). In 2014, the interior diking system for the A and B cells was not yet built, and grab samples represent water chemistry from the entire A, B, and C cells. Regarding average TP concentration, Cell C had the highest monitored values and Cell B had the lowest, but the averages only had a difference of 0.7 mg L^{-1}. Cell C had the highest average OP concentration and Cell A had the lowest. The average NH_3 concentration in Cell A was lower than that in Cells B and C. Average TKN concentrations were comparable across all impoundment cells. There was greater variation between the cells regarding average TN and TP concentrations. The A cell had the highest concentrations of these two parameters while the B cell had the lowest.

Table 13. 2014 pollutant concentration averages and ranges in the A, B, and C cells.

2014 In Cell Water Chemistry			
ID	**Parameter**	**Average Concentration**	**Range**
Cell A	TP (mg L^{-1})	0.24	0.17-0.31
	OP (mg/L)	0.06	0.004-0.15
	NH_3 (mg/L)	0.06	<0.04-0.15
	Kjeldahl N (mg/L)	1.52	0.98-2.28
	N + N (mg/L)	3.05	0.65-6.72
	TN (mg/L)	4.56	1.64-8.54
	TSS (mg/L)	22.00	8.00-38.00
	Turbidity (NTU)	19.30	5.80-40.10
Cell B	TP (mg/L)	0.23	0.12-0.31
	OP (mg/L)	0.11	0.004-0.17
	NH_3 (mg/L)	0.24	0.08-0.41
	Kjeldahl N (mg/L)	1.63	1.42-1.76
	N + N (mg/L)	0.593	0.23-1.23
	TN (mg/L)	2.22	1.74-2.94
	TSS (mg/L)	29.33	8.00-64.00
	Turbidity (NTU)	31.30	8.60-74.20

2014 In Cell Water Chemistry			
Cell C	TP (mg/L)	0.30	0.19-0.39
	OP (mg/L)	0.18	0.01-0.26
	NH_3 (mg/L)	0.22	0.14-0.37
	Kjeldahl N (mg/L)	1.93	1.61-2.24
	N + N (mg/L)	1.07	0.94-1.40
	TN (mg/L)	2.99	2.55-3.64
	TSS (mg/L)	11.25	4.00-21.00
	Turbidity (NTU)	11.00	6.10-15.90

A summary of water chemistry at the inlet to the impoundment, for 2014, 2015, and 2016, can be found in Table 14. The highest and lowest average TP and OP concentrations were recorded in 2014 and 2016, respectively. All forms of nitrogen analyzed had higher average concentrations in 2015 than in 2014 or 2016. In 2016, average concentrations for all analyzed parameters were lower than in the previous two sampling years.

Table 14. NOI inlet pollutant concentration averages and ranges for 2014, 2015 and 2016.

2014, 2015, and 2016 North Ottawa Inlet Water Chemistry			
Year	**Parameter**	**Average Concentration**	**Range**
2014	TP (mg/L)	0.46	0.31-0.64
	OP (mg/L)	0.34	0.28-0.40
	Kjeldahl N (mg/L)	1.73	1.26-1.94
	N + N (mg/L)	3.43	1.16-5.12
	TN (mg/L)	5.16	2.91-6.90
	TSS (mg/L)	69.40	9.00-161.00
	Turbidity (NTU)	36.10	9.60-120.40
2015	TP (mg/L)	0.43	0.21-0.74
	OP (mg/L)	0.23	0.004-0.35
	Kjeldahl N (mg/L)	2.04	1.28-2.90
	N + N (mg/L)	4.39	0.52-10.10
	TN (mg/L)	6.44	2.88-12.01
	TSS (mg/L)	135.12	14.00-378.00
	TSVS (mg/L)	21.06	4.00-58.00

2014, 2015, and 2016 North Ottawa Inlet Water Chemistry			
Year	**Parameter**	**Average Concentration**	**Range**
	Turbidity (NTU)	89.82	12.80-262.00
2016	TP (mg/L)	0.27	0.05-0.51
	OP (mg/L)	0.16	<0.003-0.36
	Kjeldahl N (mg/L)	1.35	0.58-1.94
	N + N (mg/L)	2.14	<0.03-9.17
	TN (mg/L)	3.49	0.87-10.84
	TSS (mg/L)	29.70	2.83-126.00
	TSVS (mg/L)	6.41	2.00-17.00
	Turbidity (NTU)	25.47	6.61-83.40

Outlet water chemistry data for 2015 and 2016 is summarized in Table 15. Similar to the average inlet concentrations, the 2016 monitoring year had the lowest average concentrations of all water quality parameters, with the exception of OP.

Table 15. NOI outlet pollutant concentration averages and ranges for 2015 and 2016.

2015 and 2016 North Ottawa Outlet Water Chemistry			
Year	**Parameter**	**Average Concentration**	**Range**
2015	TP (mg/L)	0.23	0.17-0.44
	OP (mg/L)	0.02	0.004-0.32
	Kjeldahl N (mg/L)	2.59	1.34-3.42
	N + N (mg/L)	0.24	<0.03-2.40
	TN (mg/L)	2.83	2.22-3.86
	TSS (mg/L)	28.00	18.00-74.00
	TSVS (mg/L)	15.23	10.00-26.00
	Turbidity (NTU)	19.97	12.80-40.50
2016	TP (mg/L)	0.22	0.07-0.487
	OP (mg/L)	0.09	0.002-0.428
	Kjeldahl N (mg/L)	1.83	0.57-2.85
	N + N (mg/L)	0.07	<0.03-0.47
	TN (mg/L)	1.88	0.002-0.428
	TSS (mg/L)	16.36	4.00-61.00

2015 and 2016 North Ottawa Outlet Water Chemistry			
	TSVS (mg/L)	6.93	2.00-21.00
	Turbidity (NTU)	14.18	3.59-43.50

4.3.2. Concentration and load reductions

The percent reduction in pollutant concentrations from the inlet to the outlet of the NOI is expressed in Table 16. Average TP concentrations decreased by 38%. A 70% reduction in average concentration was observed for TN. TSS saw a concentration decrease of 84% from inlet to outlet.

Table 16. Pollutant concentration reductions from the NOI inlet to outlet in 2014.

C Cell Concentration Reduction From Inlet to Outlet (mg L^{-1})		
2014	TP	38%
	TN	70%
	TSS	84%

The nutrient budget built for the impoundment in 2015 and 2016 allowed for the calculation of pollutant load reductions. Results are expressed in terms of percent reduction and mass of pollutant stored (lbs) for TP, TN, and TSS, in 2015 and 2016 (Table 17). Load reductions are separated into two categories, the C Cell and the A/B Cell system. The reason two nutrient budgets were calculated is because the A and B cells shared water throughout the operational season, and the C cell was isolated, as explained in the methods section. In 2016, load reductions achieved by the C cell were higher for TSS, lower for TP, and the same for TN as in 2015. The highest percent load reductions were achieved for TP and TN in the A/B Cell system in 2016. However, the high percent reduction in the A/B

cells does not equate to the highest mass capture of these pollutants. The percent and mass reduction both depend on the volume of water received by each cell (Table 18) and the corresponding water chemistry. Regarding pollutant mass capture, the best performance was achieved by the C cell in 2015, for all three parameters.

Table 17. Pollutant load reductions achieved by the C cell in 2015 and 2016, and the A/B Cell system in 2016, expressed as a percent and mass reduction.

C Cell Load Reduction			
Year	**Parameter**	**Percent**	**Pounds (lbs)**
2015	TP	31%	1,641
	TN	51%	31,479
	TSS	37%	522,454
2016	TP	27%	157
	TN	51%	3,212
	TSS	57%	2,6306
A/B Cell Load Reduction			
Year	**Parameter**	**Percent**	**Pounds (lbs)**
2016	TP	66%	852
	TN	73%	14,976
	TSS	42%	41,126

Table 18. Total annual inflow to the NOI in 2016.

Year	Impoundment Inflows (m^3 of Water)
2016	3.602×10^6

A visual representation of TP load reduction achieved by the A/B cells in 2016 can be seen in Figure 17. The left vertical axis corresponds to acre-feet storage of water in the cell system, which rises over the course of the year as runoff is allowed into the

impoundment, and then drops during drawdown in late October. The right vertical axis corresponds to TP (lbs), which rises as more water enters in the impoundment, but does not all exit the impoundment when the water is released. The difference between the initial and final mass of phosphorus in the impoundment is the mass stored, corresponding to a 66% load reduction. Analogous plots of water and mass pollutant storage for TP, TSS, and TN in the C and A/B cells in 2016 can be found in Appendix I.

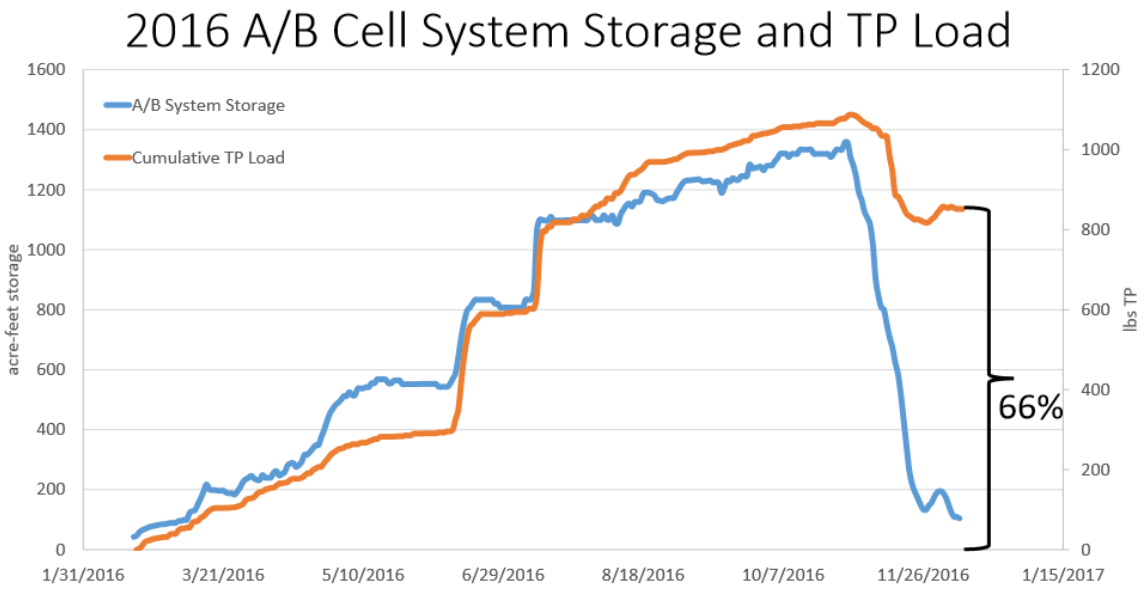

Figure 17. Graph of water storage and TP load in the A/B Cell System across the 2016 season.

The results of the slow-draw down model show a theoretical load reduction of 85%, 84%, and 83%, for TP, TN, and TSS respectively (Table 19). These results are higher by approximately 20%, 10%, and 40%, for TP, TN, and TSS, respectively, than the reductions achieved in 2016 with a quick draw-down of impoundment water.

Table 19. Modeled pollutant load reductions in the A/B Cell system in 2016, under a theoretical slow draw-down scenario.

North Ottawa A/B Cell System 2016 Load Reductions *Slow draw down scenario*			
TP Load Reduction	1,090 lbs	TP % Load Reduction	85%*
TN Load Reduction	17,079 lbs	TN % Load Reduction	84%*
TSS Load Reduction	81,606 lbs	TSS % Load Reduction	83%*

4.4. DISCUSSION

During its years of operation, the NOI captured pollutants and reduced nutrient loads to downstream waters (Vieths et al. 2017). A similar study conducted in the upper Midwestern region found between ~50-65% retention of TP load in two constructed wetland ponds, and ~60% concentration reduction between influent and effluent TP (Nairn and Mitsch 2000). These load reductions are slightly higher than those observed for the NOI C cell in 2015 and 2016, but slightly lower than the TP load reduction in the A/B cells in 2016. The observed TP concentration reduction for NOI was lower than that observed by Nairn and Mitsch (2000).

It is important to note that the reported input P loads to the impoundment are based only on inflow concentrations of the pollutant. An additional source of P to the impoundment, which is not accounted for this the nutrient budget, is atmospheric deposition. Sediment and detritus that is blown into the impoundment by wind, for example, will be an additional source of P to the impoundment water. A more detailed

budget that includes atmospheric, or dry, deposition of P may show that the P capture rates are even higher than those observed in this nutrient reduction calculation.

Load reductions of N achieved by the NOI are relatively high compared to similar systems. One recent study examining the nitrate reduction efficiency of constructed wetlands in an agricultural watershed observed a 40-90% efficiency range (Tournebize, Chaumont, and Mander 2017). Another study, conducted in an agricultural region in the upper Midwest, found a nitrate retention efficiency of 44% and 47% in 2014 and 2015, respectively (Schilling et al. 2017). In comparison, the NOI impoundment performs on the higher end of these N removal efficiency ranges, with an average of 51-73% load reduction across all cells and years of operation. It is important to note that retention results expressed as percentages must be interpreted with the context of water volume and pollutant mass (Nairn and Mitsch 2000). A 10% decrease from 10 mg is much smaller than a 10% decrease from 10 kg, for example.

The nutrient reductions achieved in the past three years have natural variability due to several factors. Climate has a great effect on load reductions, because flow rates are dependent on precipitation frequency and intensity, and concentrations of P and N are correlated to flow rates. In the three years of the impoundment's operation, there has been a droughty year, a wet year, and an intermediate year. Several additional years of monitoring will help to better characterize the water treatment performance of the impoundment. Management of the impoundment has also varied in the past three years, in terms of vegetation and crops planted, water storage and movement, and impoundment construction. These factors may have significant impacts on nutrient processes (Vieths et al. 2017).

Movement and storage of pollutants in the NOI will also vary across the lifespan of the impoundment. For example, harvesting and removing cattails growing in the impoundment is scheduled for upcoming years, and the removal of biomass may reduce the internal loading of nutrients to the water, as well as affect soil characteristics in the impoundment. Phosphorus storage is dependent on the availability of sorption sites in impoundment soils, and these may become saturated over time, reducing the nutrient storage potential of the site. However, periodic flooding and draining of the impoundment may reverse or slow soil-P saturation rate. Analysis of water quality and load capture based on flooding frequency, and timing, will be key.

The monitoring and nutrient budget data will be used to advise management of the impoundment to maximize water quality benefits. Management strategies will include plans for drawdown timing and speed, water retention time for settling of sediments, and optimizing vegetation for nutrient reduction. Continued sampling and water quality monitoring and analysis will allow for better characterization and prediction of pollutant behavior between inlet and outlet, under different conditions, in future years (Vieths et al. 2017). In-field verification of the stage-to-storage curves and mathematically derived weir equations will be necessary to fine-tune water budget calculations. There are plans to take detailed cross-sections in the inlet and outlet channel of the NOI. A flow tracker will be used to record flow (cfs) for these sites on days representing high, medium, and low flow conditions. Paired with staff gauge readings for water stage in the channels, this information will be used as an additional way to verify and constrain water and nutrient loads into and out of the impoundment. Ultimately, this research describes the water quality

treatment potential of the NOI and aims to advise best practices to achieve maximum water quality benefits for downstream waters.

Glossary of Terms

- A/B - the combination of the A and B cells
- BdSWD - Boise De Sioux Watershed District
- DNR - Department of Natural Resources
- Ce - expected C_i; mg L^{-1} PO_4-P
- C_{EPC0} - final, or equilibrium, concentration at EPC_0; mg L^{-1} PO_4-P
- C_f - final, or equilibrium, concentration; mg L^{-1} PO_4-P
- C_i - initial concentrations; mg L^{-1} PO_4-P
- Ct - measured C_i; mg L^{-1} PO_4-P
- DOC - dissolved organic carbon
- DI - deionized
- EPC - equilibrium P concentration at any C_f; mg L^{-1} PO_4-P
- EPC_0 -equilibrium P concentration at zero-sorption; mg L^{-1} PO_4-P. The EPC_0 is the x-intercept on a buffer diagram, representing the C_f at which there is no sorption, or S=0
- ET - evapotranspiration
- K - linear adsorption coefficient; L kg^{-1}
- K_f - adsorption value, representing the amount of P adsorbed; mg L^{-1}
- n - empirical constant; unitless
- N - nitrogen
- NOI - North Ottawa Impoundment
- P - phosphorus
- PO_4^{3-} - phosphate
- RAL - University of Minnesota Research Analytical Laboratory
- Re - expected C_f; mg L^{-1} PO_4-P
- RRBC - Red River Basin Commission
- Rt - measured C_f; mg L^{-1} PO_4-P
- S - mass of sorbed P for a given C_f; mg P kg^{-1} soil.
- S_{max} - maximum sorption capacity of the soil; mg kg^{-1}
- SSE - sum of squared error
- MWQL - University of Minnesota Water Quality Lab
- WQT - water quality treatment land use designation, describing the A4 and B4 cells

References

1. Anderson, J., Bell, J., Cooper, T., & Grigal, D. (2001). *Soils and landscapes of Minnesota.* Retrieved from https://www.extension.umn.edu/agriculture/soils/soil-properties/soils-and-landscapes-of-minnesota/
2. Barrow, N. J. (1983). A mechanistic model for describing the sorption and desorption of phosphate by soil. *J. Soil Sci, 34, 733-750.* doi: 10.1111/j.1365-2389.1983.tb01068.x
3. Barrow, N.J. 2008. The description of sorption curves. *European Journal of Soil Science, 59, 900–910.* doi: 10.1111/j.1365-2389.2008.01041.x
4. Bolster, C.H. (2016). *Microsoft Excel Spreadsheets for Fitting Sorption Data*. Retrieved from https://www.ars.usda.gov/midwest-area/bowling-green-ky/food-animal-environmental-systems-research/people/carl-bolster/sorption-isotherm-spreadsheet/
5. Bolster, C. H., & Homberger, G. M. (2007). On the Use of Linearized Langmuir Equations. *Soil Sci. Soc. Am. J, 71, 1796–1806*. doi:10.2136/sssaj2006.0304
6. Bowden, J. W., Posner, A. M., & Quirk, J.P. (1977). Ionic adsorption on variable charge mineral surfaces. Theoretical charge development and titration curves. *Austr. J. Soil Res, 15, 12 l-l 36*. https://doi.org/10.1071/SR9770121
7. Carignan R., & Vaithiyanathan P. (1999). Phosphorus availability in the Parana lakes (Argentina): influence of pH and phosphate buffering by fluvial sediments. *Limnol Ocea- nogr, 44, 1540–1548*. doi: 10.4319/lo.1999.44.6.1540
8. CENR (2003). An Assessment of Coastal Hypoxia and Eutrophication in U.S. Coastal Waters. *National Science and Technology Council Committee on Environment and Natural Resources, Washington*. Retrieved from http://www.nccos.noaa.gov/publications/hypoxia.pdf.
9. Chang-Ying F., Fang T., & Sheng Deng N. (2006) The research of phosphorus of Xiangxi River nearby Three Gorges, China. *Environ Geol, 49, 923–928.* doi:10.1007/s00254-005-0124-x
10. Chapra, S.C., & Canale, R.P. (1991). Long-Term Phenomenological Model of Phosphorus and Oxygen for Stratified Lakes. *Water Research, 25(6), 707-715.* http://dx.doi.org/10.1016/0043-1354(91)90046-S
11. Conidi, D., & Parker, W. J. (2015). The effect of solids residence time on phosphorus adsorption to hydrous ferric oxide floc. *Water Research, 84, 323–332.* http://doi.org/10.1016/j.watres.2015.07.046
12. Cummins, J. F., & Grigal, D. F. (1981). Soils and land surfaces of Minnesota 1980. *Soil Series, No 110 (Mischellaneous Publication 11).* Retrieved from http://www.mngeo.state.mn.us/pdf/Cummins&Grigal%20soils.pdf
13. Detenbeck, N. E., & Brezonik, P. L. (1991). Phosphorus sorption by sediments from a soft-water seepage lake. 1. An evaluation of kinetic and equilibrium models. *Environ. Sci. Technol, 25, 395-403*. doi: 10.1021/es00015a003

14. Dupas, R., Gruau, G., Gu, S., Humbert, G., Jaffrézic, A., & Gascuel-Odoux, C. (2015). Groundwater control of biogeochemical processes causing P release from riparian wetlands. *Water Resources, 84, 307-314.* https://doi.org/10.1016/j.watres.2015.07.048
15. Fang, F., Brezonik, P L., Mulla, D J., & Hatch, L K. (2002). Estimating Runoff Phosphorus Losses from Calcareous Soils in the Minnesota River Basin. *Journal of Environmental Quality, 31, 1918–1929.* doi: 10.2134/jeq2002.1918
16. FAO Corporate Document Repository (2012). FAO Penman-Monteith equation in *Natural Resources Management and Environment Department* (chapter 2). Retrieved from http://www.fao.org/docrep/X0490E/x0490e06.htm
17. Freundlich, H.M. (1906) Over the Adsorption in Solution. Journal of Physical Chemistry A, 57, 385-470.
18. Froelich, P. N. (1988). Kinetic control of dissolved phosphate in natural rivers and estuaries: A primer on the phosphate buffer mechanism. *Limnology and Oceanography, 33(July), 649–668.* Retrieved from http://www.jstor.org/stable/2837216
19. Gabriel, O., Balla, D., Kalettka, T., & Maassen, S. (2008). Sink or source? -The effect of hydrology on P release in the cultivated riverine wetland Spreewald (Germany). *Water Science and Technology 2008, 58(9), 1813-22*. doi: 10.2166/wst.2008.564.
20. Grundtner, A. (2013). *Role of Bank Materials as Potential Source and Carrier of Phosphorus.* Retrieved from ProQuest Digital Dissertations. (AAT 1536171)
21. Hach. (2014). Molybdovanadate Method 8114: 0.3 to 45.0 mg/L PO_4^{3-}. Phosphorus, Reactive (Orthophosphate), 9th Ed. Retrieved from: https://www.hach.com/asset-get.download.jsa?id=7639983832.
22. Harmsen, E. (2001/2002). *Penman Monteith Calculation*. Retrieved from http://academic.uprm.edu/abe/backup2/*.../PENMAN-MONTEITH%20CALCULATION.xls*
23. Hartikainen, H., Rasa, K., & Withers, P. J. a. (2010). Phosphorus exchange properties of European soils and sediments derived from them. *European Journal of Soil Science, 61(6), 1033–1042*. http://doi.org/10.1111/j.1365-2389.2010.01295.x
24. Healy R.W., & Scanlon, B.R. (2010). *Estimating groundwater recharge: Water-budget methods*. New York: Cambridge University Press, pp. 15-42.
25. Hodges, S.C. (2000). Methods of Phosphorus Analysis for Soils, Sediments, Residuals, and Waters. *Southern Cooperative Series Bulletin (Vol. 408*). http://doi.org/citeulike-article-id:7529961
26. Horowitz A.J., & Sandstrom M.W. (1998). Chapter A3, cleaning procedures 3.2., TWRI Book 9. Cleaning of equipment for water sampling (p15-30). U.S. Geological Survey.
27. Huett, D., Morris, S., Smith, G., & Hunt, N. (2005). Nitrogen and P removal from plant nursery runoff in vegetated and unvegetated subsurface flow wetlands. *Water Research, 39 (19), 3259-3272*. https://doi.org/10.1016/j.watres.2005.05.038
28. Huser B.J., Futter M., Lee J.T., & Perniel M. (2016) In-lake measures for phosphorus control: The most feasible and cost-effective solution for long-term management of

water quality in urban lakes. *Water Research. 97, 142-152*. doi: 10.1016/j.watres.2015.07.036
29. James, W. F., & Barko, J. W. (2005) Biologically labile and refractory phosphorus loads from the agriculturally-managed Upper Eau Galle River watershed, Wisconsin. *Lake Res Manage, 21, 165–173*. http://dx.doi.org/10.1080/07438140509354426
30. James, W. F., & Barko, J. W. (2004). Diffusive fluxes and equilibrium processes in relation to phosphorus dynamics in the Upper Mississippi River. River Research and Applications. *River Res. Applic, 20, 473–484*. http://doi.org/10.1002/rra.761
31. James, W. F., Barko, J. W., & Eakin, H. L. (2002). Labile and Refractory Forms of Phosphorus in Runoff of the Redwood River Basin, Minnesota. Journal of Freshwater Ecology, 17(2), 297–304. http://doi.org/10.1080/02705060.2002.9663898
32. James, W. F., Eakin, H. L., & Barko, J. W. (2004). *Phosphorus Loading and Compositional Watershed*. Retrieved from http://www.dtic.mil/docs/citations/ADA427500
33. James, W. F., & Larson, C. E. (2008). Phosphorus dynamics and loading in the turbid Minnesota River (USA): controls and recycling potential. *Biogeochemistry, 90, 75–92*. http://doi.org/10.1007/s10533-008-9232-5
34. Kadlec, R. H., Services, W. M., & Drive, W. (1999). The limits of phosphorus removal in wetlands. *Wetlands Ecology and Management, 7, 165-175*. Retrieved from https://link.springer.com/article/10.1023/A:1008415401082
35. Klotz, R. L. (1985) Factors controlling phosphorus limitation in stream sediments. *Limnol Oceanogr, 30, 543–553*. doi: 10.4319/lo.1985.30.3.0543
36. Koski-Vahala, J., & Hartikainen, H. (2001). Assessment of the risk of phosphorus loading due to resuspended sediment. *J Environ Qual 2001. May-Jun 30(3), 960-6*. Retrieved from https://www.ncbi.nlm.nih.gov/pubmed/11401287
37. LacCore, National Lacustrine Core Facility (2013). *Loss-on-Ignition Standard Operating Procedure*. Retrieved from http://lrc.geo.umn.edu/laccore/assets/pdf/sops/loi.pdf
38. Langmuir, I. (1918). The adsorption of gases on plane surfaces of glass, mica and platinum. *J. Am. Chem. Soc., 40, 1361-1403*. doi: 10.1021/ja02242a004
39. Larsen, D.P., Schults, D.W., & Malueg, K.W. (1981). Summer internal phosphorus supplies in Shagawa Lake, Minnesota. *Limnology. Oceanography, 26(4), 740-753*. Retrieved from onlinelibrary.wiley.com/doi/10.4319/lo.1981.26.4.0740/pdf
40. LMNO Engineering, Research, and Software, Ltd (2014). *Discharge, Head, and Design Calculations, Equations and Installation Guidelines: Rectangular Weir Calculator***.** Retrieved from https://www.lmnoeng.com/Weirs/RectangularWeir.php
41. Lucci, G. M., McDowell, R. W., & Condron, L. M. (2010). Evaluation of base solutions to determine equilibrium phosphorus concentrations (EPC0) in stream sediments. *International Agrophysics, 24, 57–163.* Retrieved from http://www.old.international-agrophysics.org/artykuly/international_agrophysics/IntAgr_2010_24_2_157.pdf

42. Mayer, L. M., Gloss, S. P. (1980). Buffering of silica and phosphate in a turbid river. *Limnol Oceanogr, 25, 12–25.* Retrieved from http://onlinelibrary.wiley.com/doi/10.4319/lo.1980.25.1.0012/pdf
43. Meyer, J.L. (1979). The role of sediments and bryophytes in phosphorus dynamics in a headwater stream ecosystem. *Limnol Oceanogr, 24, 365–375*. doi: 10.4319/lo.1979.24.2.0365
44. Mitsch, W.J., Cronk, J.K., Wu, X., Nairn, R.W., and Hey, D.L. (1995) Phosphorus Retention in Constructed Freshwater Riparian Marshes. Ecological Applications, Wiley. Vol. 5, No. 3. pp. 830-845
45. Nair, P. S., Logan, T. J., Sharpley, A. N., Sommers, L. E., Tabatabai, M. A., & Yuan, T. L. (1984). Interlaboratory Comparison of a Standardized Phosphorus Adsorption Procedure. *Journal of Environmental Quality, 13(4), 591-594*. Retrieved from https://dl.sciencesocieties.org/publications/jeq/pdfs/13/4/JEQ0130040591
46. Nairn, R. W., & Mitsch, W. J. (2000). Phosphorus removal in created wetland ponds receiving river overflow. *Ecological Engineering, 14, 107–126.* https://doi.org/10.1016/S0925-8574(99)00023-3
47. Ostlund, A. (2017) *North Ottawa Nutrient Capture and Biomass Harvesting* [PowerPoint slides].
48. Reddy, K., Kadlec, R., Flaig, E., and Gale, P. (1999). P Retention in Streams and Wetlands: A Review. Critical Reviews in Environmental Science and Technology, 28(1), 83-146.
49. Richardson, C. J. (1985). Mechanisms controlling P retention in freshwater wetlands. Science, 228(4706), 1424-1427.
50. Roeschlein, J. (2014). Cass County Flood Risk Reduction: North Ottawa Impoundment Project. Boise De Sioux Watershed District. Powerpoint.
51. Schlesinger, W. H., & Bernhardt, E. (2013) Biogeochemistry: An Analysis of Global Change. 3rd ed. San Diego, CA: Academic Press.
52. Schilling, K. E., Kult, K., Wilke, K., Streeter, M., & Vogelgesang, J. (2017). Nitrate reduction in a reconstructed floodplain oxbow fed by tile drainage. *Ecological Engineering, 102, 98–107*. http://doi.org/10.1016/j.ecoleng.2017.02.006
53. SFU Soil Science Lab (2011). *Direct Estimation of Organic Matter by Loss on Ignition: Methods Compiled by Robertson, S.* Accessed at https://www.sfu.ca/soils/lab_documents/Estimation_Of_Organic_Matter_By_LOI.pdf.
54. Tellinghuisen, J., & Bolster, C. H. (2010). Least-squares analysis of phosphorus soil sorption data with weighting from variance function estimation: A statistical case for the freundlich isotherm. *Environmental Science and Technology, 44(13), 5029–5034*. http://doi.org/10.1021/es100535b
55. Tian, J.-R., & Zhou, P.-J. (2008). Phosphorus fractions and adsorption characteristics of floodplain sediments in the lower reaches of the Hanjiang river, China. *Environmental Monitoring and Assessment, 137, 233–241*. doi: 10.1007/s10661-007-9743-x

56. Tournebize, J., Chaumont, C., & Mander, Ü. (2017). Implications for constructed wetlands to mitigate nitrate and pesticide pollution in agricultural drained watersheds. *Ecological Engineering, 103, 415–425*. http://doi.org/10.1016/j.ecoleng.2016.02.014
57. USEPA (2017) PhosVer 3® (Ascorbic Acid) Method 8048: 0.02 to 2.50 mg/L PO_4^{3-}. Phosphorus, Reactive (Orthophosphate), 10th Ed. USEPA, Hach.
58. *UW Extension Ag Weather (2010).* Estimated ET for Wisconsin and Minnesota. *Accessed at http://agwx.soils.wisc.edu/uwex_agwx/sun_water/et_wimn*
59. Vieths, T., Guzner, M., & Magner, J. (2017). North Ottawa Impoundment Water Quality Summary: Report Prepared for LCCMR.
60. Wang, N., & Mitsch, W. (n.d.). A detailed ecosystem model of P dynamics in created riparian wetlands. *Ecological Modelling, 126, 101-130*. doi: 10.1016/S0304-3800(00)00260-X
61. Wang, Q., & Li, Y. (2010). Phosphorus adsorption and desorption behavior on sediments of different origins. *Journal of Soils and Sediments, 10(6), 1159–1173*. http://doi.org/10.1007/s11368-010-0211-9
62. Wang, X., Zhang, L., & Zhang, H. (2012). Phosphorus adsorption characteristics at the sediment – water interface and relationship with sediment properties in FUSHI reservoir, China. Environmental Earth Sciences, 67, 15–22. http://doi.org/10.1007/s12665-011-1476-z
63. Wauchope R. D., & McDowell L. L. (1984). Adsorption of phosphate, arsenate, methanocarsonate and cacodylate by lake and stream sediments. Comparisons with soils. *J Environ Qual, 13, 499–504*. Retrieved from https://dl.sciencesocieties.org/publications/jeq/pdfs/13/3/JEQ0130030499
64. Weber, W. J. J., & DiGiano, F.A. (1996) Process Dynamics in Environmental Systems. Toronto, ON: John Wiley & Sons, Inc.
65. Zhang, L., Du, Y., Du, C., Xu, M., & Loáiciga, H. A. (2016). The adsorption / desorption of phosphorus in freshwater sediments from buffer zones: the effects of sediment concentration and pH. http://doi.org/10.1007/s10661-015-5018-0
66. Zhou AM, Tang HX, Wang DS. Phosphorus adsorption on natural sediments: modeling and effects of pH and sediment composition. Water Res 2005; 39:1245–54.
67. Zhou, A. M., Tang, H. X., & Wang, D. S. Phosphorus adsorption on natural sediments: modeling and effects of pH and sediment composition. *Water Res 2005; 39, 1245–54*. https://doi.org/10.1016/j.watres.2005.01.026

Appendix A. Soil profiles for NOI soil pits.

Profile No.	Pit No.	Coordinates	Horizon	Depth (cm)	Class	Hue	Value	Chroma
1			O	7				
			A	13+				
2			O	6	SiL	10YR	2	1
			A	20+	SiCL	10YR	2	1
			O	8	SiL	10YR	2	1
			A	20+	SiCL	10YR	2	1
3	C1-1	N 45.97858° W 096.26447°	O	7	SiC	10YR	2	1
			A	19+	C	2.5Y	4	3
4	Ca-b		O	7	SiL	2.5Y	2.5	1
			A	20+	SiL	2.5Y	2.5	1
5	C1-3(Ca/c)	N 45.98174° W 096.26440°	O	8	SiCL	10YR	2	1
			A	18+	SiL	10YR	2	1
6	Ca-d		O	9	SiL	2.5Y	2.5	1
			A	20	SiCL	2.5Y	2.5	1
			B	40	L	2.5Y	2	3
			B	60	L	2.5Y	2	4
			C	90	CL	2.5Y	2	4
7	Ca/e	N 45.98482° W 096.26453°	O	13	L	10YR	3	1
			A	26+	SiCL	10YR	2	1
8	Ca/f		O	7	SiCL	10YR	2	1
			A	20+	SiCL	10YR	2	1
9	C1-6(Ca/f)	N 45.98641° W 096.26456°	O	5	SiL	10YR	2	1
			A	19+	SiCL	2.5Y	3	1
10	Ca/g	N 45.98790° W 096.26464°	O	7	SiCL	10YR	2	1
			A	16+	SiCL	10YR	2	1
11	C1-8(Ca/h)	N 45.98965° W 096.26439°	O	10	SiL	10YR	2	1
			A	20+	SiCL	10YR	2	1
12	Ca/i	N 45.98999° W 096.26237°	O	5	SiL	10YR	2	1
			A	20+	SiCL	10YR	3	2
13	C1-10(Ca/j)	N 45.98810° W 096.26233°	O	14	L	10YR	2	1
			A	29+	SiL	10YR	2	1
14	Ca/k	N 45.98646° W 096.26297°	O	4	SiL	10YR	2	1
			A	20+	SiCL	10YR	3	1

Profile No.	Pit No.	Coordinates	Horizon	Depth (cm)	Class	Hue	Value	Chroma
15	C1-12(Ca/l)	N 45.98462° W 096.26360°	O	8	SiCL	2.5Y	2.5	1
			A	25+	SiC	2.5Y	3	1
16	Ca/m	N 45.98256° W 096.26328°	O	6	SiL	10YR	3	1
			A	20+	SiCL	10YR	4	2
17	C1-14(Ca/n)	N 45.98079° W 096.26334°	O	10	SiL	10YR	2	1
			A	23+	SiCL	10YR	2	1
18	C1-15(Ca/o)		O	5	SiCL	10YR	2	1
			A	15+	SiCL	10YR	3	1
19	Ca/p		O	9	SiL	10YR	2	1
			A	20+	SiL	10YR	2	1
20	C1-17(Ca/q)	N 45.98071° W 096.25767°	O	10	L	10YR	2	1
			A	20+	SiCL	10YR	2	1
21	Ca/r		O	10	SiL	10YR	3	1
			A	25+	SiCL	10YR	2	1
22	Ca/s	N 45.98417° W 096.25707°	O	8	SiL	2.5Y	3	1
			A	23+	SiL	2.5Y	2.5	1
23	Ca/t		O	10	SiL	10YR	2	1
			A	20+	SiCL	10YR	2	1
24	C1-21(Ca/u)	N 45.98796° W 096.25710°	O	9	SiL	2.5Y	2.5	1
			A	18+	SiCL	10YR	2	1
25	Ca/v		O	7	SiL	10YR	2	1
			A		SiCL	10YR	2	1
26	C1-23(Ca/w)	N 45.99048° W 096.25922°	O	9	SiL	2.5Y	2.5	1
			A	18+	SiL	10YR	2	1
27	Ca/x		O	11	L	10YR	2	1
			A	20+	SiCL	10YR	2	1
28	C1-25(Ca/y)	N 45.98764° W 096.26042°	O	10	SiL	2.5Y	2.5	1
			A	19+	SiCL	10YR	2	1
29	Ca/z	N 45.98628° W 096.25983°	O	11	SiL	10YR	2	1
			A	20+	SiCL	10YR	2	1
30	C1-27(Ca-aa)	N 45.98457°	O	10	SiL	10YR	2	1

Profile No.	Pit No.	Coordinates	Horizon	Depth (cm)	Class	Hue	Value	Chroma
		W 096.26043°	A	20+	SiCL	10YR	2	1
31	Ca/ab	N 45.98318° W 096.26055°	O	9	SiL	10YR	2	1
			A		SiCL	10YR	2	1
32	C1-29(Ca/ac)		O	10	SiCL	10YR	2	1
			A	18+	SiCL	10YR	2	1
33	Ca/ad	N 45.97966° W 096.26049°	O	10	SiL			
			A	33	SiCL			
			B	55	SiCL			
			B	80	L			
			C	100+	C			
34	Ca/ah	N 45.98324° W 096.26411°	O	6	SiCL	10YR	2	1
			A	19	SiCL	10YR	2	1
			B1	38	CL	2.5Y	6	2
			B2	78+	CL	2.5Y	5	2
35	Ca/af	N 45.98987° W 096.25696°	O	10	SiL	10YR	2	1
			A	20	SiCL	10YR	2	1
			B	90+	SiCL	10YR	5	1
36	C1-33(Ca/g)	N 45.99065° W 096.26323°	O	7	SiL	10YR	2	1
			A	12	SiCL	10YR	2	1
			B1	36	SiCL	2.5Y	6	3
			B2	63+	CL	2.5Y	6	2
37	C1-31(Ca/ae)	N 45.98175° W 096.25790°	O	8	SiL	10YR	2	1
			A	33	SiCL	10YR	2	1
			B1	56	SiCL	10YR	5	1
			B2	78	L	2.5Y	6	3
			C	90+	SL	2.5Y	5	4
38	Cb/a	N 45.98323° W 096.26438°	O	7	SiCL	10YR	2	1
			A	34	SiC	10YR	2	1
			B	65+	C	10YR	5	1
39	C2-2(Cb/b)	N 45.97612° W 096.26471°	O	8	SiC	10YR	2	1
			A	18+	C	10YR	5	2
40	Cb/c		O	7	SiL	10YR	2	1
			A	15+	SiCL	10YR	2	1
41		N 45.97311° W 096.26463°	O	7	SiCL	10YR	2	1
			A	15+	SiCL	10YR	2	1

Profile No.	Pit No.	Coordinates	Horizon	Depth (cm)	Class	Hue	Value	Chroma
42	C2-5(Cb/e)		O	9	SiL	10YR	2	1
			A	22+	SiC	10YR	2	1
43	C2-7(Cb/g)		O	9	SiCL	10YR	2	1
			A	20+	SiC	10YR	2	1
44	C2-8(Cb/h)		O	8	SiL	10YR	2	1
			A	19+	SiCL	2.5Y	2.5	1
45	Cb/i	N 45.96499° W 096.26166°	O	6	SiL	10YR	2	1
			A	42	SiCL	10YR	2	1
			B	76+	CL	10YR	5	3
46	Cb/j		O	5	SiL	10YR	2	1
			A	20+	SiCL	10YR	2	1
47	Cb/l		O	11	SiCL			
			A	55	SiCL			
			B	70+	CL			
48		N 45.97092° W 096.26099°	O	9	SiL	10YR	2	1
			A	20+	SiCL	10YR	2	1
49	Cb/h		O	7	SiCL	10YR	2	1
			A	20+	SiCL	10YR	2	1
50	C2-15(Cb/o)		O	7	SiL	10YR	2	1
			A	19+	SiCL	10YR	2	1
51	C2-15(Cb/o)		O	9		10YR	2	1
			A	17		10YR	2	1
52	C2-16(Cb/p)	N 45.97673° W 096.26062°	O	7	SiL	10YR	2	1
			A	38	SiCL			
			B	69+	SCL	10YR	5	3
53	C2-16(Cb/p)	N 45.97673° W 096.26062°	O	9	SiL	10YR	2	1
			A	23+	SiCL	10YR	2	1
54	Cb/q		O	8	SiL	10YR	2	1
			A	20+	SiCL	10YR	2	1
55	Cb/r		O	9	SiCL	10YR	2	1
			A	20+	SiCL	10YR	2	1
56	Cb/u		O	7	SiCL	10YR	2	1
			A	20+	SiCL	10YR	2	1
57	Cb/v		O	7	SiCL	10YR	2	1
			A	17+	SiCL	10YR	2	1
58	Cb/v		O	8	SiL	10YR	2	1
			A	17+	SiCL	10YR	2	1

Profile No.	Pit No.	Coordinates	Horizon	Depth (cm)	Class	Hue	Value	Chroma
59	Cb/w		O	2	SiL	10YR	2	1
			A	10	SiCL	10YR	2	1
60	Cb/x	N 45.96521° W 096.25658°	O	7	SiL	10YR	2	1
			A	41	SiCL	10YR	2	1
			B	68+	L	2.5Y	6	3
61	Cb/y		O	9	SiL	10YR	2	1
			A	18+	SiCL	10YR	2	1
62	Cb/z		O	7	SiL	10YR	2	1
			A	18+	SiCL	10YR	2	1
63	Cb/aa		O	9	SiL	10YR	2	1
			A	20+	SiCL	10YR	2	1
64	Cb/ab		O	7	SiL	10YR	2	1
			A	20+	SiCL	10YR	2	1

Appendix B. Coordinates of soil sampling points.

Site	Latitude	Longitude
A-1 Site 7	45.98935	-96.2395
A-1 Site 8	45.98923	-96.24336
A-2 Site 5	45.98232	-96.23929
A-2 Site 6	45.98214	-96.24366
A-3 Site 3	45.97495	-96.23903
A-3 Site 4	45.97492	-96.24362
A-4 Site 1	45.96749	-96.24366
A-4 Site 2	45.96743	-96.2392
B-1 Site 15	45.98912	-96.24825
B-1 Site 16	45.98915	-96.25366
B-2 Site 13	45.98196	-96.24866
B-2 Site 14	45.98187	-96.25366
B-3 Site 11	45.97459	-96.24843
B-3 Site 12	45.97462	-96.25358
B-4 Site 10	45.96782	-96.25349
B-4 Site 9	45.96785	-96.24851
C-1	45.96427	-96.26096
C-10	45.98077	-96.26405
C-11	45.98551	-96.26109
C-12	45.99061	-96.26418
C-13	45.99065	-96.25793
C-2	45.96415	-96.26478
C-3	45.97098	-96.26495
C-4	45.97746	-96.26512
C-5	45.96463	-96.25675
C-6	45.96609	-96.25894
C-7	45.9711	-96.26109
C-9	45.9808	-96.25894
Exterior	45.96332	-96.26473

Appendix C. Results for C_i, C_f, and S, before adjustments.

Site	Observed Vegetation Type	Cell Use Designation	C_i (mg L^{-1} PO_4-P)	C_f (mg L^{-1} PO_4-P)	S (mg kg^{-1} PO_4-P)
Exterior	Exterior	Exterior	0.13	0.27	-9.14
Exterior	Exterior	Exterior	0.29	0.36	-4.54
Exterior	Exterior	Exterior	0.54	0.43	7.51
Exterior	Exterior	Exterior	0.79	0.64	10.05
Exterior	Exterior	Exterior	1.04	1.16	-8.08
Exterior	Exterior	Exterior	1.59	1.75	-10.95
Exterior	Exterior	Exterior	2.04	2.16	-8.04
Exterior	Exterior	Exterior	2.58	2.26	21.48
A-1 Site 7	Corn	Cropped	0.16	0.34	-12.03
A-1 Site 7	Corn	Cropped	0.31	0.39	-5.50
A-1 Site 7	Corn	Cropped	0.56	0.51	3.48
A-1 Site 7	Corn	Cropped	0.81	0.63	12.29
A-1 Site 7	Corn	Cropped	1.08	1.14	-3.92
A-1 Site 7	Corn	Cropped	1.59	1.44	9.96
A-1 Site 7	Corn	Cropped	2.05	1.72	22.17
A-1 Site 7	Corn	Cropped	2.60	2.00	39.98
A-1 Site 8	Corn	Cropped	0.16	0.30	-9.54
A-1 Site 8	Corn	Cropped	0.31	0.29	1.56
A-1 Site 8	Corn	Cropped	0.56	0.38	12.23
A-1 Site 8	Corn	Cropped	0.81	0.49	21.06
A-1 Site 8	Corn	Cropped	1.08	0.92	10.34
A-1 Site 8	Corn	Cropped	1.59	1.27	21.38
A-1 Site 8	Corn	Cropped	2.05	2.05	0.10
A-1 Site 8	Corn	Cropped	2.60	1.79	54.19
A-2 Site 5	Submerged	Flooded	0.13	0.37	-16.32
A-2 Site 5	Submerged	Flooded	0.16	0.40	-16.22
A-2 Site 5	Submerged	Flooded	0.29	0.45	-10.62
A-2 Site 5	Submerged	Flooded	0.31	0.42	-7.46
A-2 Site 5	Submerged	Flooded	0.54	0.58	-2.45
A-2 Site 5	Submerged	Flooded	0.56	0.47	5.78
A-2 Site 5	Submerged	Flooded	0.79	1.17	-25.47
A-2 Site 5	Submerged	Flooded	0.81	0.60	13.82
A-2 Site 5	Submerged	Flooded	1.04	1.41	-24.76
A-2 Site 5	Submerged	Flooded	1.08	1.06	1.21
A-2 Site 5	Submerged	Flooded	1.59	1.35	15.68
A-2 Site 5	Submerged	Flooded	1.59	1.92	-22.02

Site	Observed Vegetation Type	Cell Use Designation	C_i (mg L^{-1} PO_4-P)	C_f (mg L^{-1} PO_4-P)	S (mg kg^{-1} PO_4-P)
A-2 Site 5	Submerged	Flooded	2.04	2.27	-15.22
A-2 Site 5	Submerged	Flooded	2.05	1.60	29.72
A-2 Site 5	Submerged	Flooded	2.58	2.40	12.27
A-2 Site 5	Submerged	Flooded	2.60	1.95	43.51
A-2 Site 6	Submerged	Flooded	0.16	0.30	-9.60
A-2 Site 6	Submerged	Flooded	0.31	0.36	-3.66
A-2 Site 6	Submerged	Flooded	0.56	0.46	6.85
A-2 Site 6	Submerged	Flooded	0.81	0.54	17.80
A-2 Site 6	Submerged	Flooded	1.08	1.00	5.08
A-2 Site 6	Submerged	Flooded	1.59	1.25	22.41
A-2 Site 6	Submerged	Flooded	2.05	1.55	33.01
A-2 Site 6	Submerged	Flooded	2.60	1.95	43.32
A-3 Site 3	Wheat	Cropped	0.16	0.24	-5.48
A-3 Site 3	Wheat	Cropped	0.31	0.28	2.18
A-3 Site 3	Wheat	Cropped	0.56	0.33	15.12
A-3 Site 3	Wheat	Cropped	0.81	0.47	22.44
A-3 Site 3	Wheat	Cropped	1.08	0.87	13.85
A-3 Site 3	Wheat	Cropped	1.59	1.12	31.21
A-3 Site 3	Wheat	Cropped	2.05	1.84	13.73
A-3 Site 3	Wheat	Cropped	2.60	1.69	60.39
A-3 Site 4	Wheat	Cropped	0.16	0.23	-4.51
A-3 Site 4	Wheat	Cropped	0.31	0.24	4.59
A-3 Site 4	Wheat	Cropped	0.56	0.32	15.86
A-3 Site 4	Wheat	Cropped	0.81	0.44	24.60
A-3 Site 4	Wheat	Cropped	1.08	0.85	15.29
A-3 Site 4	Wheat	Cropped	1.59	1.12	31.21
A-3 Site 4	Wheat	Cropped	2.05	1.39	43.78
A-3 Site 4	Wheat	Cropped	2.60	1.75	56.93
A-4 Site 1	Natives	Water Quality	0.16	0.12	2.70
A-4 Site 1	Natives	Water Quality	0.31	0.15	10.73
A-4 Site 1	Natives	Water Quality	0.56	0.15	27.02
A-4 Site 1	Natives	Water Quality	0.81	0.21	40.28
A-4 Site 1	Natives	Water Quality	1.08	0.35	48.69
A-4 Site 1	Natives	Water Quality	1.59	0.68	60.69
A-4 Site 1	Natives	Water Quality	2.05	0.89	77.31
A-4 Site 1	Natives	Water Quality	2.60	1.18	94.91
A-4 Site 2	Flooded, Natives	Water Quality	0.16	0.18	-1.54

Site	Observed Vegetation Type	Cell Use Designation	C_i (mg L^{-1} PO_4-P)	C_f (mg L^{-1} PO_4-P)	S (mg kg^{-1} PO_4-P)
A-4 Site 2	Flooded, Natives	Water Quality	0.31	0.21	6.99
A-4 Site 2	Flooded, Natives	Water Quality	0.56	0.27	19.50
A-4 Site 2	Flooded, Natives	Water Quality	0.81	0.36	30.23
A-4 Site 2	Flooded, Natives	Water Quality	1.08	0.65	28.68
A-4 Site 2	Flooded, Natives	Water Quality	1.59	1.08	34.26
A-4 Site 2	Flooded, Natives	Water Quality	2.05	1.22	55.10
A-4 Site 2	Flooded, Natives	Water Quality	2.60	1.64	63.79
A-4 Site 2	Flooded, Natives	Water Quality	0.16	0.23	-4.97
A-4 Site 2	Flooded, Natives	Water Quality	0.31	0.26	3.47
A-4 Site 2	Flooded, Natives	Water Quality	0.56	0.29	18.26
A-4 Site 2	Flooded, Natives	Water Quality	0.81	0.37	29.02
A-4 Site 2	Flooded, Natives	Water Quality	1.08	0.88	13.35
A-4 Site 2	Flooded, Natives	Water Quality	1.59	1.08	34.17
A-4 Site 2	Flooded, Natives	Water Quality	2.05	1.29	50.66
A-4 Site 2	Flooded, Natives	Water Quality	2.60	1.58	68.10
B-1 Site 15	Soybean	Cropped	0.16	0.21	-3.08
B-1 Site 15	Soybean	Cropped	0.31	0.21	6.35
B-1 Site 15	Soybean	Cropped	0.56	0.29	18.14
B-1 Site 15	Soybean	Cropped	0.81	0.40	27.51
B-1 Site 15	Soybean	Cropped	1.08	0.85	15.36
B-1 Site 15	Soybean	Cropped	1.59	0.97	41.13
B-1 Site 15	Soybean	Cropped	2.05	1.25	53.36
B-1 Site 15	Soybean	Cropped	2.60	1.58	68.04
B-1 Site 16	Soybean	Cropped	0.16	0.17	-0.45
B-1 Site 16	Soybean	Cropped	0.31	0.20	7.60
B-1 Site 16	Soybean	Cropped	0.56	0.29	17.99
B-1 Site 16	Soybean	Cropped	0.81	0.32	32.43
B-1 Site 16	Soybean	Cropped	1.08	0.49	39.64
B-1 Site 16	Soybean	Cropped	1.59	0.72	57.98
B-1 Site 16	Soybean	Cropped	2.05	0.93	74.50
B-1 Site 16	Soybean	Cropped	2.60	1.34	83.92
B-2 Site 13	Natives, Millet	Natives	0.16	0.30	-9.42
B-2 Site 13	Natives, Millet	Natives	0.31	0.34	-1.68
B-2 Site 13	Natives, Millet	Natives	0.56	0.43	8.88
B-2 Site 13	Natives, Millet	Natives	0.81	0.54	17.70
B-2 Site 13	Natives, Millet	Natives	1.08	1.12	-2.93
B-2 Site 13	Natives, Millet	Natives	1.59	1.40	12.45

Site	Observed Vegetation Type	Cell Use Designation	C_i (mg L^{-1} PO_4-P)	C_f (mg L^{-1} PO_4-P)	S (mg kg^{-1} PO_4-P)
B-2 Site 13	Natives, Millet	Natives	2.05	1.66	26.14
B-2 Site 13	Natives, Millet	Natives	2.60	2.04	37.02
B-3	Corn	Cropped	0.16	1.00	-55.69
B-3	Corn	Cropped	0.31	0.17	9.60
B-3	Corn	Cropped	0.56	0.21	23.56
B-3	Corn	Cropped	0.81	0.29	34.36
B-3	Corn	Cropped	1.08	0.71	24.84
B-3	Corn	Cropped	1.59	0.97	41.45
B-3	Corn	Cropped	2.05	1.46	39.52
B-3	Corn	Cropped	2.60	1.52	71.96
B-3 Site 11	Corn	Cropped	0.16	0.34	-11.67
B-3 Site 11	Corn	Cropped	0.31	0.34	-1.91
B-3 Site 11	Corn	Cropped	0.56	0.45	7.30
B-3 Site 11	Corn	Cropped	0.81	0.57	16.20
B-3 Site 11	Corn	Cropped	1.08	1.03	3.38
B-3 Site 11	Corn	Cropped	1.59	1.28	20.82
B-3 Site 11	Corn	Cropped	2.05	2.00	3.58
B-3 Site 11	Corn	Cropped	2.60	2.00	39.73
B-4 Site 10	Shallowly Flooded	Water Quality	0.16	0.21	-3.28
B-4 Site 10	Shallowly Flooded	Water Quality	0.31	0.25	3.88
B-4 Site 10	Shallowly Flooded	Water Quality	0.56	0.29	18.12
B-4 Site 10	Shallowly Flooded	Water Quality	0.81	0.41	26.77
B-4 Site 10	Shallowly Flooded	Water Quality	1.08	0.79	19.63
B-4 Site 10	Shallowly Flooded	Water Quality	1.59	0.99	39.70
B-4 Site 10	Shallowly Flooded	Water Quality	2.05	1.26	52.67
B-4 Site 10	Shallowly Flooded	Water Quality	2.60	1.62	65.26
B-4 Site 9	Shallowly Flooded	Water Quality	0.16	0.21	-3.26
B-4 Site 9	Shallowly Flooded	Water Quality	0.31	0.18	8.88
B-4 Site 9	Shallowly Flooded	Water Quality	0.56	0.24	21.54
B-4 Site 9	Shallowly Flooded	Water Quality	0.81	0.35	30.84
B-4 Site 9	Shallowly Flooded	Water Quality	1.08	0.74	22.77
B-4 Site 9	Shallowly Flooded	Water Quality	1.59	1.03	37.09
B-4 Site 9	Shallowly Flooded	Water Quality	2.05	1.34	47.59
B-4 Site 9	Shallowly Flooded	Water Quality	2.60	1.67	61.83
C-1	Cattail	Floodwater	0.16	0.38	-14.67
C-1	Cattail	Floodwater	0.31	0.46	-9.67
C-1	Cattail	Floodwater	0.56	0.51	3.64

Site	Observed Vegetation Type	Cell Use Designation	C_i (mg L^{-1} PO_4-P)	C_f (mg L^{-1} PO_4-P)	S (mg kg^{-1} PO_4-P)
C-1	Cattail	Floodwater	0.81	0.57	15.93
C-1	Cattail	Floodwater	1.08	1.04	2.63
C-1	Cattail	Floodwater	1.59	1.34	16.39
C-1	Cattail	Floodwater	2.05	1.58	31.08
C-1	Cattail	Floodwater	2.60	1.96	42.83
C-10	Natives	Floodwater	0.16	0.18	-1.38
C-10	Natives	Floodwater	0.31	0.19	8.20
C-10	Natives	Floodwater	0.56	0.29	17.89
C-10	Natives	Floodwater	0.81	0.38	28.78
C-10	Natives	Floodwater	1.08	0.78	20.13
C-10	Natives	Floodwater	1.59	1.10	32.49
C-10	Natives	Floodwater	2.05	1.30	49.88
C-10	Natives	Floodwater	2.60	1.61	65.86
C-11	Cattail	Floodwater	0.16	0.19	-1.89
C-11	Cattail	Floodwater	0.31	0.21	6.44
C-11	Cattail	Floodwater	0.56	0.29	18.19
C-11	Cattail	Floodwater	0.81	0.36	29.68
C-11	Cattail	Floodwater	1.08	0.69	26.16
C-11	Cattail	Floodwater	1.59	0.93	43.98
C-11	Cattail	Floodwater	2.05	1.14	60.88
C-11	Cattail	Floodwater	2.60	1.41	79.14
C-12	Natives	Floodwater	0.13	0.21	-5.27
C-12	Natives	Floodwater	0.29	0.27	1.43
C-12	Natives	Floodwater	0.54	0.36	11.79
C-12	Natives	Floodwater	0.79	0.48	20.53
C-12	Natives	Floodwater	1.04	0.94	6.43
C-12	Natives	Floodwater	1.59	1.30	19.35
C-12	Natives	Floodwater	2.04	1.64	26.61
C-12	Natives	Floodwater	2.58	1.80	51.72
C-13	Natives	Floodwater	0.13	0.32	-12.74
C-13	Natives	Floodwater	0.29	0.36	-4.72
C-13	Natives	Floodwater	0.54	0.46	5.64
C-13	Natives	Floodwater	0.79	0.58	13.73
C-13	Natives	Floodwater	1.04	1.13	-5.80
C-13	Natives	Floodwater	1.59	1.64	-3.57
C-13	Natives	Floodwater	2.04	1.97	4.97
C-13	Natives	Floodwater	2.58	2.02	37.43

Site	Observed Vegetation Type	Cell Use Designation	C_i (mg L^{-1} PO_4-P)	C_f (mg L^{-1} PO_4-P)	S (mg kg^{-1} PO_4-P)
C-2	Natives	Floodwater	0.16	0.24	-5.28
C-2	Natives	Floodwater	0.31	0.28	2.15
C-2	Natives	Floodwater	0.56	0.38	11.78
C-2	Natives	Floodwater	0.81	0.48	21.96
C-2	Natives	Floodwater	1.08	0.89	12.76
C-2	Natives	Floodwater	1.59	1.17	27.92
C-2	Natives	Floodwater	2.60	1.71	59.15
C-2	Natives	Floodwater	0.16	0.53	-24.67
C-2	Natives	Floodwater	0.31	0.60	-19.04
C-2	Natives	Floodwater	0.56	0.68	-7.96
C-2	Natives	Floodwater	0.81	0.83	-1.25
C-2	Natives	Floodwater	1.08	1.04	2.42
C-2	Natives	Floodwater	1.59	1.42	11.20
C-2	Natives	Floodwater	2.05	2.13	-5.48
C-2	Natives	Floodwater	2.60	2.02	38.96
C-3	Cattail	Floodwater	0.16	0.41	-16.84
C-3	Cattail	Floodwater	0.31	0.40	-6.30
C-3	Cattail	Floodwater	0.56	0.45	7.05
C-3	Cattail	Floodwater	0.81	0.55	17.22
C-3	Cattail	Floodwater	1.08	0.98	6.70
C-3	Cattail	Floodwater	1.59	1.30	19.05
C-3	Cattail	Floodwater	2.05	1.61	29.66
C-3	Cattail	Floodwater	2.60	1.97	42.04
C-4	Natives	Floodwater	0.16	0.30	-9.61
C-4	Natives	Floodwater	0.31	0.38	-4.43
C-4	Natives	Floodwater	0.56	0.42	9.03
C-4	Natives	Floodwater	0.81	0.49	21.35
C-4	Natives	Floodwater	1.08	0.89	12.90
C-4	Natives	Floodwater	1.59	1.17	28.03
C-4	Natives	Floodwater	2.05	1.82	15.27
C-4	Natives	Floodwater	2.60	1.68	61.30
C-5	Natives	Floodwater	0.16	0.30	-9.20
C-5	Natives	Floodwater	0.31	0.32	-0.39
C-5	Natives	Floodwater	0.56	0.41	10.21
C-5	Natives	Floodwater	0.81	0.59	14.75
C-5	Natives	Floodwater	1.08	0.92	10.51
C-5	Natives	Floodwater	1.59	1.24	23.62

Site	Observed Vegetation Type	Cell Use Designation	C_i (mg L^{-1} PO_4-P)	C_f (mg L^{-1} PO_4-P)	S (mg kg^{-1} PO_4-P)
C-5	Natives	Floodwater	2.05	1.92	8.35
C-5	Natives	Floodwater	2.60	1.86	49.42
C-5	Natives	Floodwater	0.13	0.35	-14.80
C-5	Natives	Floodwater	0.29	0.33	-2.44
C-5	Natives	Floodwater	0.54	0.40	9.22
C-5	Natives	Floodwater	0.79	0.52	17.93
C-5	Natives	Floodwater	1.04	0.95	5.96
C-5	Natives	Floodwater	1.59	1.36	15.45
C-5	Natives	Floodwater	2.04	1.69	23.32
C-5	Natives	Floodwater	2.58	1.82	50.50
C-6	Cattail	Floodwater	0.16	0.28	-8.22
C-6	Cattail	Floodwater	0.31	0.56	-16.73
C-6	Cattail	Floodwater	0.56	0.71	-9.77
C-6	Cattail	Floodwater	0.81	0.72	6.19
C-6	Cattail	Floodwater	1.08	1.25	-11.33
C-6	Cattail	Floodwater	1.59	1.53	3.93
C-6	Cattail	Floodwater	2.05	1.84	14.11
C-6	Cattail	Floodwater	2.60	2.14	30.49
C-7	Cattail	Floodwater	0.16	0.54	-25.07
C-7	Cattail	Floodwater	0.31	0.64	-22.22
C-7	Cattail	Floodwater	0.56	0.75	-12.40
C-7	Cattail	Floodwater	0.81	0.87	-4.19
C-7	Cattail	Floodwater	1.08	1.46	-25.21
C-7	Cattail	Floodwater	1.59	1.71	-7.78
C-7	Cattail	Floodwater	2.05	2.08	-2.15
C-7	Cattail	Floodwater	2.60	2.55	3.01
C-8	Natives	Floodwater	0.16	0.36	-13.25
C-8	Natives	Floodwater	0.31	0.38	-4.98
C-8	Natives	Floodwater	0.56	0.48	5.51
C-8	Natives	Floodwater	0.81	0.60	14.32
C-8	Natives	Floodwater	1.08	0.93	10.15
C-8	Natives	Floodwater	1.59	1.28	20.38
C-8	Natives	Floodwater	2.05	1.82	15.31
C-8	Natives	Floodwater	2.60	1.88	48.21
C-9	Submerged	Floodwater	0.13	0.04	6.21
C-9	Submerged	Floodwater	0.29	0.12	11.06
C-9	Submerged	Floodwater	0.54	0.14	26.38

Site	Observed Vegetation Type	Cell Use Designation	C_i (mg L^{-1} PO_4-P)	C_f (mg L^{-1} PO_4-P)	S (mg kg^{-1} PO_4-P)
C-9	Submerged	Floodwater	0.79	0.22	37.78
C-9	Submerged	Floodwater	1.04	0.69	23.39
C-9	Submerged	Floodwater	1.59	1.06	35.31
C-9	Submerged	Floodwater	2.04	1.38	44.30
C-9	Submerged	Floodwater	2.58	1.42	77.39
C-Inlet	Submerged	Floodwater	0.16	0.29	-8.45
C-Inlet	Submerged	Floodwater	0.31	0.32	-0.44
C-Inlet	Submerged	Floodwater	0.56	0.41	10.19
C-Inlet	Submerged	Floodwater	0.81	0.48	21.88
C-Inlet	Submerged	Floodwater	1.08	0.86	14.78
C-Inlet	Submerged	Floodwater	1.59	1.18	27.13
C-Inlet	Submerged	Floodwater	2.05	1.53	34.97
C-Inlet	Submerged	Floodwater	2.60	1.88	48.02

Appendix D. Results for C_f and S, including adjustments for DOC.

Site	Ci (mg L^{-1} PO_4-P)	DOC Color Reading (mg L^{-1} PO_4-P)	Cf (mg L^{-1} PO_4-P)	S (mg kg^{-1} PO_4-P)
A-1 Site 7	0.16	0.29	0.33	-11.15
A-1 Site 7	0.31	0.35	0.38	-4.93
A-1 Site 7	0.56	0.47	0.50	3.83
A-1 Site 7	0.81	0.59	0.62	12.56
A-1 Site 7	1.08	0.72	0.76	21.19
A-1 Site 7	1.59	1.02	1.07	34.72
A-1 Site 7	2.05	1.33	1.36	46.13
A-1 Site 7	2.60	1.58	1.64	64.33
A-1 Site 8	0.16	0.22	0.28	-7.92
A-1 Site 8	0.31	0.24	0.28	2.10
A-1 Site 8	0.56	0.34	0.37	12.49
A-1 Site 8	0.81	0.46	0.49	21.23
A-1 Site 8	1.08	0.47	0.50	38.44
A-1 Site 8	1.59	0.81	0.85	49.01
A-1 Site 8	2.05	1.61	1.65	26.81
A-1 Site 8	2.60	1.33	1.38	81.29
A-2 Site 5	0.13	0.35	0.37	-15.73
A-2 Site 5	0.16	0.35	0.38	-14.53
A-2 Site 5	0.29	0.42	0.44	-10.05
A-2 Site 5	0.31	0.38	0.41	-6.35
A-2 Site 5	0.54	0.55	0.57	-2.05
A-2 Site 5	0.56	0.44	0.46	6.47
A-2 Site 5	0.79	1.13	1.16	-24.96
A-2 Site 5	0.81	0.57	0.59	14.37
A-2 Site 5	1.04	0.77	0.79	16.68
A-2 Site 5	1.08	0.4	0.42	44.04
A-2 Site 5	1.59	0.69	0.72	58.07
A-2 Site 5	1.59	1.23	1.28	20.42
A-2 Site 5	2.04	1.63	1.66	25.64
A-2 Site 5	2.05	0.97	0.99	70.78
A-2 Site 5	2.58	1.73	1.78	53.65
A-2 Site 5	2.60	1.28	1.32	85.29
A-2 Site 6	0.16	0.25	0.28	-7.75
A-2 Site 6	0.31	0.32	0.35	-2.44
A-2 Site 6	0.56	0.42	0.45	7.60
A-2 Site 6	0.81	0.51	0.54	18.33
A-2 Site 6	1.08	0.28	0.30	52.32
A-2 Site 6	1.59	0.53	0.55	69.05
A-2 Site 6	2.05	0.86	0.88	78.17
A-2 Site 6	2.60	1.22	1.26	89.26
A-3 Site 3	0.16	0.17	0.22	-3.77

Site	Ci (mg L^{-1} PO_4-P)	DOC Color Reading (mg L^{-1} PO_4-P)	Cf (mg L^{-1} PO_4-P)	S (mg kg^{-1} PO_4-P)
A-3 Site 3	0.31	0.23	0.27	2.84
A-3 Site 3	0.56	0.3	0.33	15.39
A-3 Site 3	0.81	0.44	0.47	22.64
A-3 Site 3	1.08	0.37	0.40	45.57
A-3 Site 3	1.59	0.62	0.65	62.37
A-3 Site 3	2.05	1.36	1.39	43.86
A-3 Site 3	2.60	1.19	1.24	90.97
A-3 Site 4	0.16	0.16	0.21	-3.20
A-3 Site 4	0.31	0.2	0.23	5.05
A-3 Site 4	0.56	0.29	0.32	16.07
A-3 Site 4	0.81	0.41	0.44	24.74
A-3 Site 4	1.08	0.46	0.49	39.10
A-3 Site 4	1.59	0.73	0.77	54.60
A-3 Site 4	2.05	1.03	1.05	66.37
A-3 Site 4	2.60	1.35	1.40	79.87
A-4 Site 1	0.16	0.1	0.51	-23.38
A-4 Site 1	0.31	0.13	0.18	8.84
A-4 Site 1	0.56	0.14	0.16	26.65
A-4 Site 1	0.81	0.19	0.21	40.19
A-4 Site 1	1.08	0.18	0.20	58.95
A-4 Site 1	1.59	0.49	0.52	71.26
A-4 Site 1	2.05	0.72	0.74	87.41
A-4 Site 1	2.60	0.97	1.01	105.99
A-4 Site 2	0.16	0.13	0.20	-2.42
A-4 Site 2	0.31	0.17	0.21	6.79
A-4 Site 2	0.56	0.24	0.27	19.48
A-4 Site 2	0.81	0.33	0.36	30.28
A-4 Site 2	1.08	0.23	0.25	55.46
A-4 Site 2	1.59	0.64	0.68	60.80
A-4 Site 2	2.05	0.82	0.84	80.65
A-4 Site 2	2.60	1.2	1.25	90.16
A-4 Site 2	0.16	0.18	0.23	-4.97
A-4 Site 2	0.31	0.22	0.26	3.47
A-4 Site 2	0.56	0.26	0.29	18.26
A-4 Site 2	0.81	0.35	0.37	29.02
A-4 Site 2	1.08	0.41	0.44	42.68
A-4 Site 2	1.59	0.61	0.64	63.04
A-4 Site 2	2.05	0.85	0.87	78.65
A-4 Site 2	2.60	1.11	1.15	96.49
B-1 Site 15	0.16	0.15	0.20	-2.56
B-1 Site 15	0.31	0.18	0.21	6.53
B-1 Site 15	0.56	0.26	0.29	18.23

Site	Ci (mg L^{-1} PO_4-P)	DOC Color Reading (mg L^{-1} PO_4-P)	Cf (mg L^{-1} PO_4-P)	S (mg kg^{-1} PO_4-P)
B-1 Site 15	0.81	0.37	0.40	27.56
B-1 Site 15	1.08	0.65	0.70	25.48
B-1 Site 15	1.59	0.78	0.82	51.05
B-1 Site 15	2.05	1.08	1.11	62.94
B-1 Site 15	2.60	1.38	1.43	77.78
B-1 Site 16	0.16	0.11	0.16	0.04
B-1 Site 16	0.31	0.16	0.19	7.74
B-1 Site 16	0.56	0.26	0.29	18.05
B-1 Site 16	0.81	0.3	0.32	32.47
B-1 Site 16	1.08	0.35	0.38	46.86
B-1 Site 16	1.59	0.58	0.61	65.06
B-1 Site 16	2.05	0.81	0.83	81.34
B-1 Site 16	2.60	1.19	1.24	90.87
B-2 Site 13	0.16	0.24	0.28	-8.13
B-2 Site 13	0.31	0.29	0.33	-1.02
B-2 Site 13	0.56	0.39	0.42	9.24
B-2 Site 13	0.81	0.51	0.54	17.95
B-2 Site 13	1.08	0.62	0.66	28.01
B-2 Site 13	1.59	0.9	0.95	42.90
B-2 Site 13	2.05	1.19	1.22	55.57
B-2 Site 13	2.60	1.54	1.60	66.92
B-3 Site 10	0.16	0.1	0.38	-14.66
B-3 Site 10	0.31	0.12	0.16	9.87
B-3 Site 10	0.56	0.18	0.21	23.62
B-3 Site 10	0.81	0.27	0.29	34.39
B-3 Site 10	1.08	0.24	0.26	54.61
B-3 Site 10	1.59	0.5	0.53	70.56
B-3 Site 10	2.05	1.01	1.04	67.58
B-3 Site 10	2.60	1.05	1.09	100.44
B-3 Site 11	0.16	0.26	0.32	-10.45
B-3 Site 11	0.31	0.29	0.33	-1.40
B-3 Site 11	0.56	0.41	0.45	7.57
B-3 Site 11	0.81	0.53	0.56	16.37
B-3 Site 11	1.08	0.62	0.66	27.85
B-3 Site 11	1.59	0.87	0.92	44.88
B-3 Site 11	2.05	1.61	1.65	26.87
B-3 Site 11	2.60	1.59	1.65	63.37
B-4 Site 10	0.16	0.15	0.19	-1.96
B-4 Site 10	0.31	0.21	0.24	4.45
B-4 Site 10	0.56	0.26	0.28	18.34
B-4 Site 10	0.81	0.38	0.41	26.94
B-4 Site 10	1.08	0.38	0.41	44.87

Site	Ci (mg L^{-1} PO_4-P)	DOC Color Reading (mg L^{-1} PO_4-P)	Cf (mg L^{-1} PO_4-P)	S (mg kg^{-1} PO_4-P)
B-4 Site 10	1.59	0.59	0.62	64.49
B-4 Site 10	2.05	0.88	0.90	76.62
B-4 Site 10	2.60	1.21	1.26	89.60
B-4 Site 9	0.16	0.12	0.24	-5.50
B-4 Site 9	0.31	0.14	0.18	8.71
B-4 Site 9	0.56	0.21	0.24	21.55
B-4 Site 9	0.81	0.32	0.35	30.91
B-4 Site 9	1.08	0.41	0.44	42.44
B-4 Site 9	1.59	0.7	0.74	56.51
B-4 Site 9	2.05	1.03	1.06	66.31
B-4 Site 9	2.60	1.33	1.38	81.13
C-1	0.16	0.33	0.36	-13.18
C-1	0.31	0.41	0.44	-8.56
C-1	0.56	0.47	0.50	4.32
C-1	0.81	0.54	0.56	16.42
C-1	1.08	0.42	0.44	42.61
C-1	1.59	0.72	0.75	55.96
C-1	2.05	0.99	1.01	69.41
C-1	2.60	1.33	1.37	81.82
C-10	0.16	0.11	0.15	0.41
C-10	0.31	0.15	0.18	8.67
C-10	0.56	0.26	0.29	18.11
C-10	0.81	0.35	0.38	28.92
C-10	1.08	0.32	0.34	49.04
C-10	1.59	0.64	0.68	60.86
C-10	2.05	0.87	0.89	77.25
C-10	2.60	1.15	1.20	93.66
C-11	0.16	0.14	0.19	-1.74
C-11	0.31	0.18	0.21	6.50
C-11	0.56	0.26	0.29	18.21
C-11	0.81	0.34	0.36	29.70
C-11	1.08	0.6	0.64	29.04
C-11	1.59	0.84	0.89	46.81
C-11	2.05	1.07	1.10	63.62
C-11	2.60	1.32	1.37	81.93
C-12	0.13	0.18	0.20	-4.78
C-12	0.29	0.24	0.26	1.73
C-12	0.54	0.34	0.36	11.94
C-12	0.79	0.46	0.48	20.64
C-12	1.04	0.59	0.61	28.63
C-12	1.59	0.91	0.96	42.02
C-12	2.04	1.29	1.31	48.40

Site	Ci (mg L^{-1} PO_4-P)	DOC Color Reading (mg L^{-1} PO_4-P)	Cf (mg L^{-1} PO_4-P)	S (mg kg^{-1} PO_4-P)
C-12	2.58	1.43	1.47	73.79
C-13	0.13	0.29	0.31	-11.99
C-13	0.29	0.33	0.35	-4.17
C-13	0.54	0.43	0.45	5.96
C-13	0.79	0.56	0.58	13.96
C-13	1.04	0.56	0.58	30.88
C-13	1.59	1.03	1.08	33.97
C-13	2.04	1.4	1.42	41.07
C-13	2.58	1.43	1.47	73.98
C-2	0.16	0.19	0.22	-3.87
C-2	0.31	0.24	0.27	2.94
C-2	0.56	0.35	0.38	12.26
C-2	0.81	0.45	0.48	22.29
C-2	1.08	0.33	0.35	48.65
C-2	1.59	0.61	0.64	63.31
C-2	2.60	1.15	1.19	93.93
C-2	0.16	0.48	0.50	-22.75
C-2	0.31	0.55	0.57	-17.46
C-2	0.56	0.64	0.66	-6.79
C-2	0.81	0.79	0.81	-0.24
C-2	1.08	0.22	0.23	56.81
C-2	1.59	0.59	0.61	65.38
C-2	2.05	1.32	1.34	47.32
C-2	2.60	1.18	1.21	92.57
C-3	0.16	0.35	0.39	-15.04
C-3	0.31	0.36	0.39	-5.28
C-3	0.56	0.42	0.45	7.64
C-3	0.81	0.52	0.55	17.66
C-3	1.08	0.37	0.39	46.01
C-3	1.59	0.69	0.72	57.92
C-3	2.05	1.02	1.04	67.30
C-3	2.60	1.35	1.40	80.32
C-4	0.16	0.25	0.28	-8.31
C-4	0.31	0.33	0.36	-3.60
C-4	0.56	0.39	0.42	9.46
C-4	0.81	0.46	0.49	21.63
C-4	1.08	0.39	0.41	44.44
C-4	1.59	0.67	0.70	59.14
C-4	2.05	1.34	1.37	45.42
C-4	2.60	1.18	1.22	91.89
C-5	0.16	0.23	0.28	-8.21
C-5	0.31	0.27	0.31	0.03

Site	Ci (mg L^{-1} PO_4-P)	DOC Color Reading (mg L^{-1} PO_4-P)	Cf (mg L^{-1} PO_4-P)	S (mg kg^{-1} PO_4-P)
C-5	0.56	0.37	0.40	10.42
C-5	0.81	0.55	0.59	14.92
C-5	1.08	0.57	0.61	31.38
C-5	1.59	0.88	0.93	44.15
C-5	2.05	1.59	1.63	28.21
C-5	2.60	1.5	1.56	69.57
C-5	0.13	0.32	0.34	-14.27
C-5	0.29	0.3	0.32	-2.12
C-5	0.54	0.38	0.40	9.40
C-5	0.79	0.5	0.52	18.06
C-5	1.04	0.61	0.63	27.41
C-5	1.59	0.98	1.03	37.40
C-5	2.04	1.35	1.37	44.43
C-5	2.58	1.46	1.50	71.88
C-6	0.16	0.25	0.27	-7.17
C-6	0.31	0.51	0.54	-15.37
C-6	0.56	0.66	0.69	-8.78
C-6	0.81	0.68	0.71	6.86
C-6	1.08	0.52	0.54	35.75
C-6	1.59	0.8	0.83	50.54
C-6	2.05	1.14	1.16	59.29
C-6	2.60	1.41	1.45	76.44
C-7	0.16	0.48	0.51	-23.39
C-7	0.31	0.59	0.62	-20.85
C-7	0.56	0.7	0.73	-11.43
C-7	0.81	0.83	0.86	-3.43
C-7	1.08	0.67	0.70	25.38
C-7	1.59	0.92	0.96	42.30
C-7	2.05	1.33	1.35	46.43
C-7	2.60	1.76	1.81	52.48
C-8	0.16	0.3	0.34	-12.19
C-8	0.31	0.34	0.38	-4.38
C-8	0.56	0.44	0.47	5.85
C-8	0.81	0.56	0.59	14.57
C-8	1.08	0.52	0.55	35.23
C-8	1.59	0.87	0.91	45.13
C-8	2.05	1.43	1.46	39.28
C-8	2.60	1.46	1.51	72.55
C-9	0.13	0.11	0.73	-40.28
C-9	0.29	0.09	0.11	11.79
C-9	0.54	0.13	0.14	26.48
C-9	0.79	0.21	0.22	37.81

Site	Ci (mg L^{-1} PO_4-P)	DOC Color Reading (mg L^{-1} PO_4-P)	Cf (mg L^{-1} PO_4-P)	S (mg kg^{-1} PO_4-P)
C-9	1.04	0.21	0.22	54.71
C-9	1.59	0.55	0.59	66.99
C-9	2.04	0.9	0.92	74.74
C-9	2.58	0.93	0.96	107.94
C-Inlet	0.16	0.22	0.26	-6.96
C-Inlet	0.31	0.27	0.31	0.25
C-Inlet	0.56	0.37	0.40	10.54
C-Inlet	0.81	0.45	0.48	22.10
C-Inlet	1.08	0.39	0.42	44.26
C-Inlet	1.59	0.71	0.75	56.16
C-Inlet	2.05	1.08	1.10	63.03
C-Inlet	2.60	1.4	1.45	76.54
Exterior	0.13	0.23	0.25	-8.24
Exterior	0.29	0.32	0.35	-3.93
Exterior	0.54	0.4	0.42	7.79
Exterior	0.79	0.61	0.64	10.27
Exterior	1.04	0.52	0.54	33.50
Exterior	1.59	1.06	1.12	31.58
Exterior	2.04	1.52	1.55	32.82
Exterior	2.58	1.59	1.64	62.85

Appendix E. Buffer diagrams.

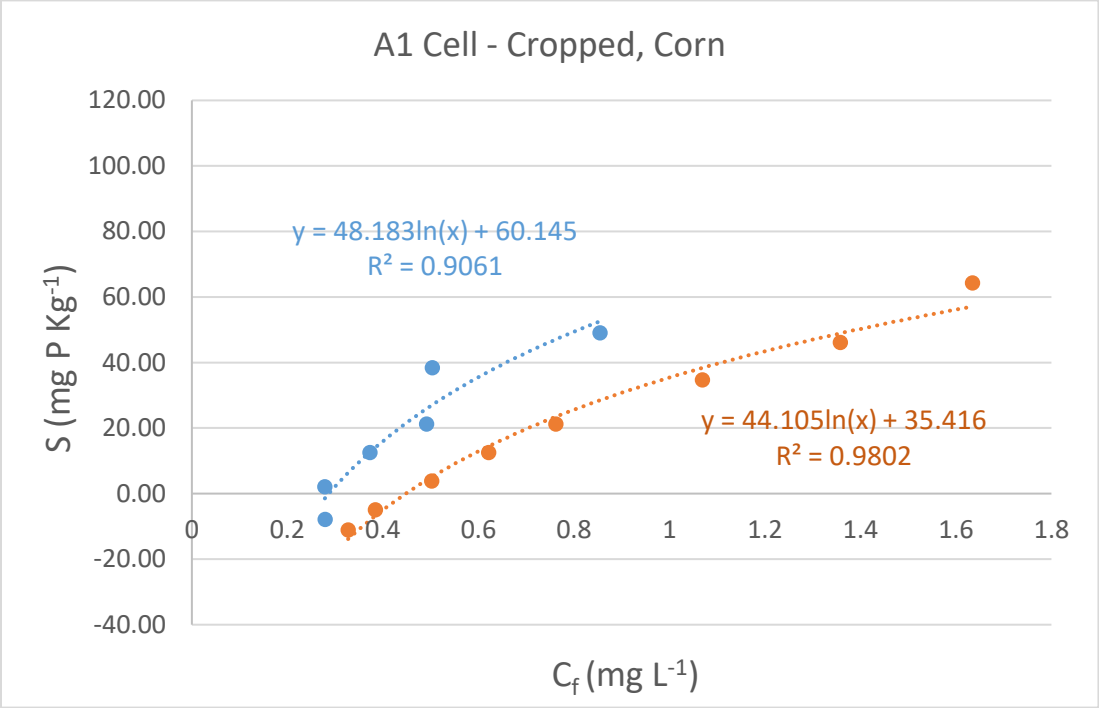

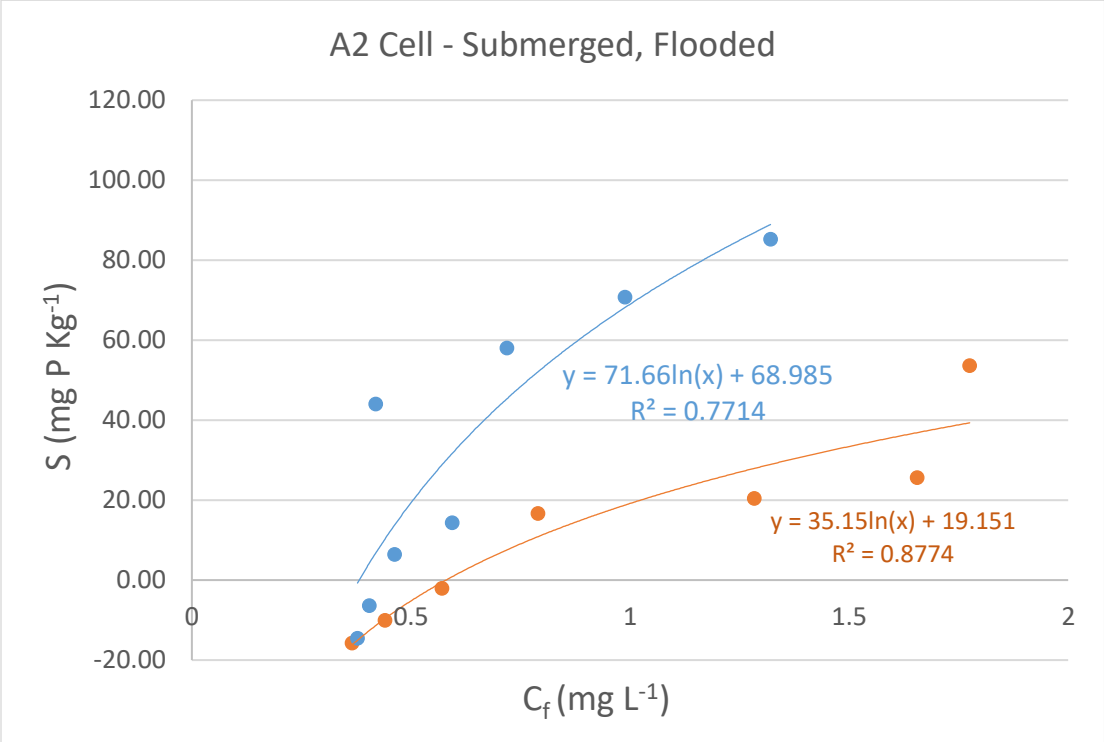

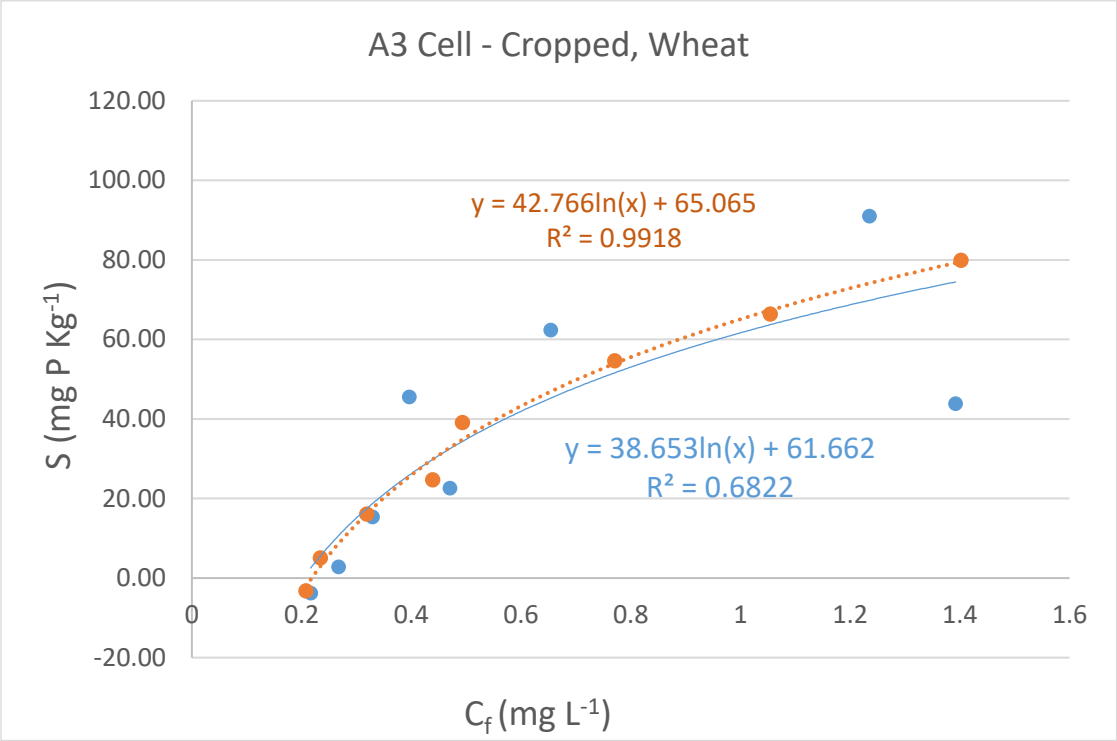
A3 Cell - Cropped, Wheat
y = 42.766ln(x) + 65.065
R² = 0.9918
y = 38.653ln(x) + 61.662
R² = 0.6822
S (mg P Kg-1)
Cf (mg L-1)
120.00
100.00
80.00
60.00
40.00
20.00
0.00
-20.00
0
0.2
0.4
0.6
0.8
1
1.2
1.4
1.6

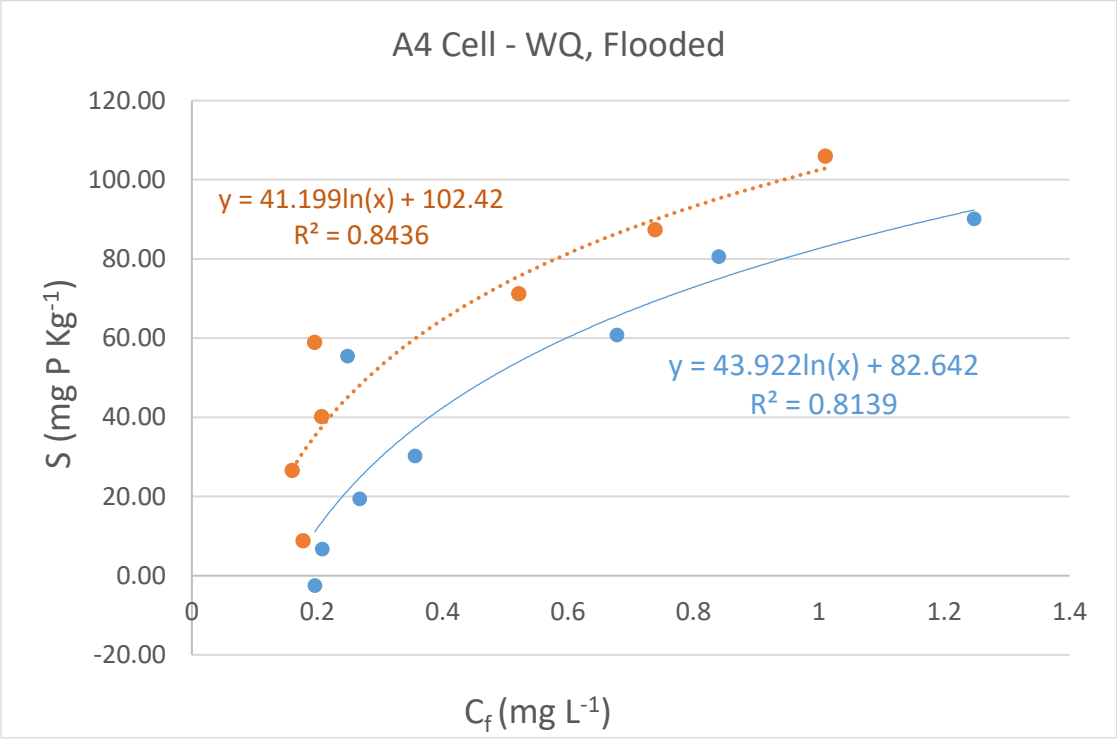
A4 Cell - WQ, Flooded
y = 41.199ln(x) + 102.42
R² = 0.8436
y = 43.922ln(x) + 82.642
R² = 0.8139
S (mg P Kg-1)
Cf (mg L-1)
120.00
100.00
80.00
60.00
40.00
20.00
0.00
-20.00
0
0.2
0.4
0.6
0.8
1
1.2
1.4

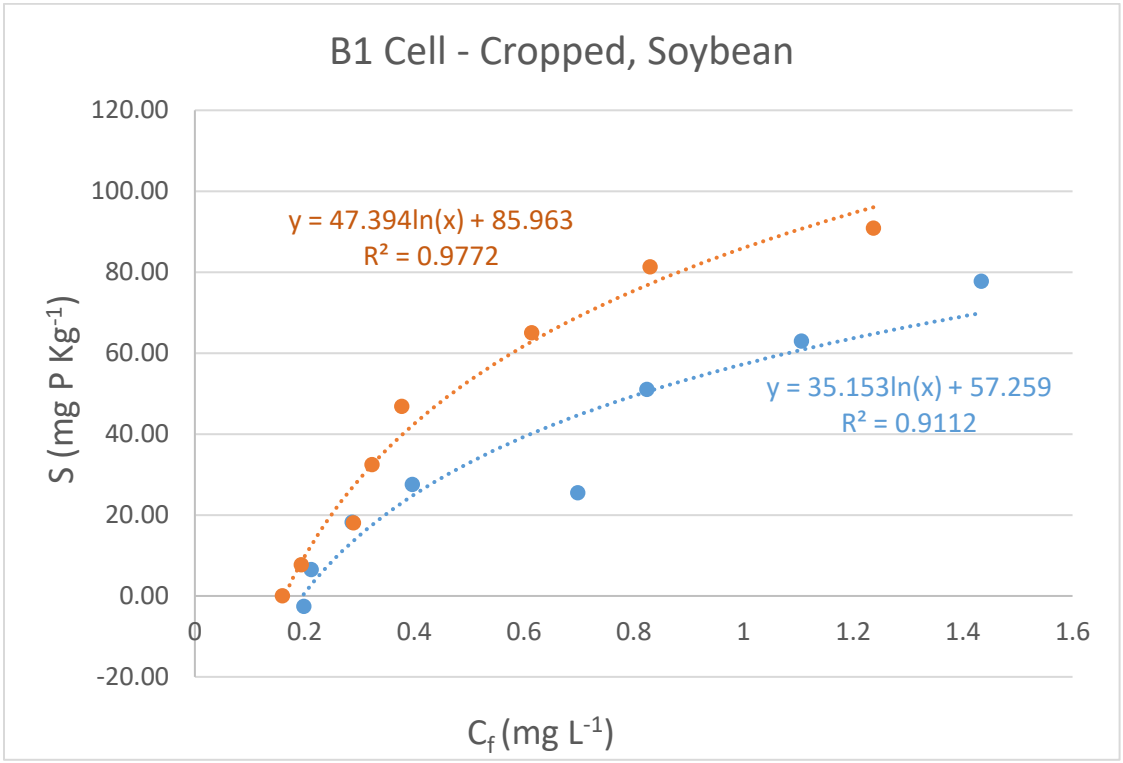
B1 Cell - Cropped, Soybean
120.00
100.00
80.00
60.00
40.00
20.00
0.00
-20.00
0
0.2
0.4
0.6
0.8
1
1.2
1.4
1.6
S (mg P Kg-1)
Cf (mg L-1)
y = 47.394ln(x) + 85.963
R² = 0.9772
y = 35.153ln(x) + 57.259
R² = 0.9112

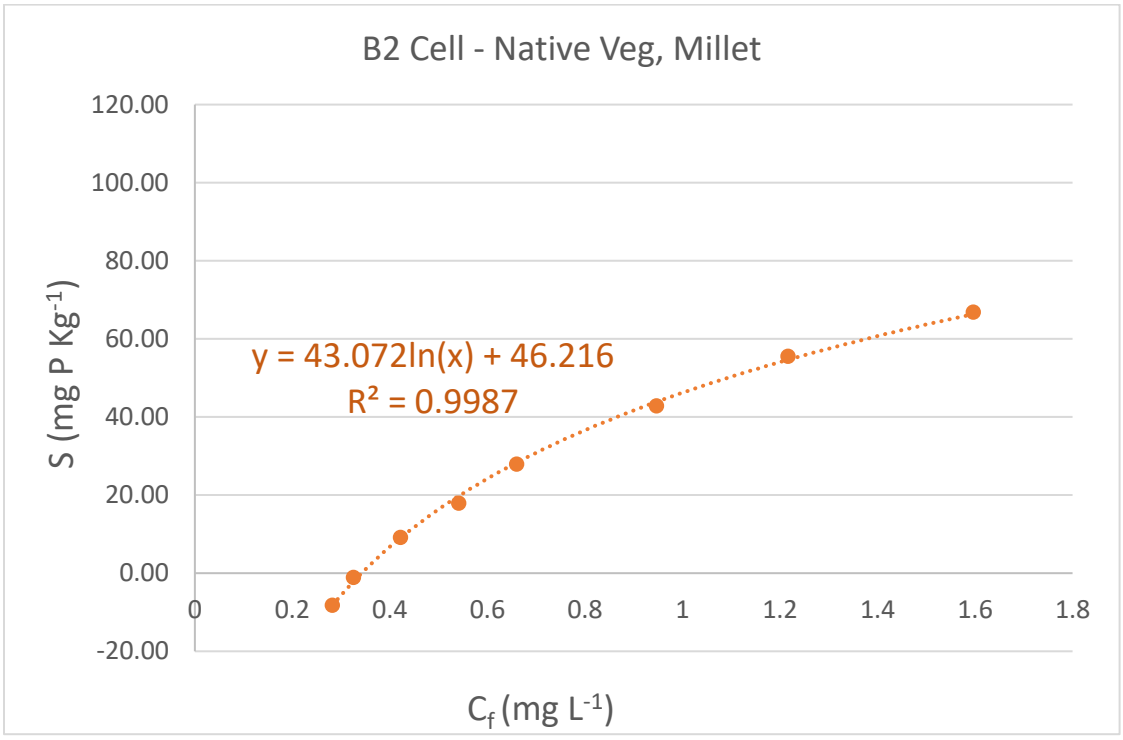
B2 Cell - Native Veg, Millet
120.00
100.00
80.00
60.00
40.00
20.00
0.00
-20.00
0
0.2
0.4
0.6
0.8
1
1.2
1.4
1.6
1.8
S (mg P Kg-1)
Cf (mg L-1)
y = 43.072ln(x) + 46.216
R² = 0.9987

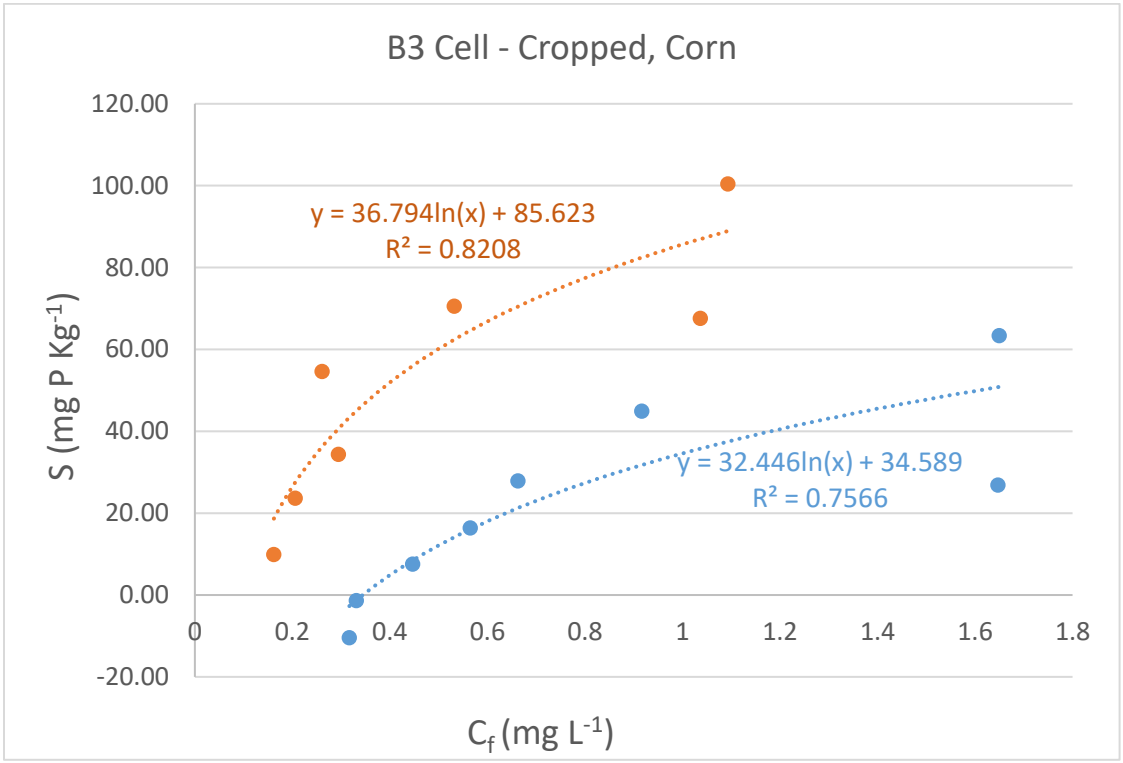
B3 Cell - Cropped, Corn
120.00
100.00
80.00
60.00
40.00
20.00
0.00
-20.00
0
0.2
0.4
0.6
0.8
1
1.2
1.4
1.6
1.8
S (mg P Kg-1)
Cf (mg L-1)
y = 36.794ln(x) + 85.623
R² = 0.8208
y = 32.446ln(x) + 34.589
R² = 0.7566

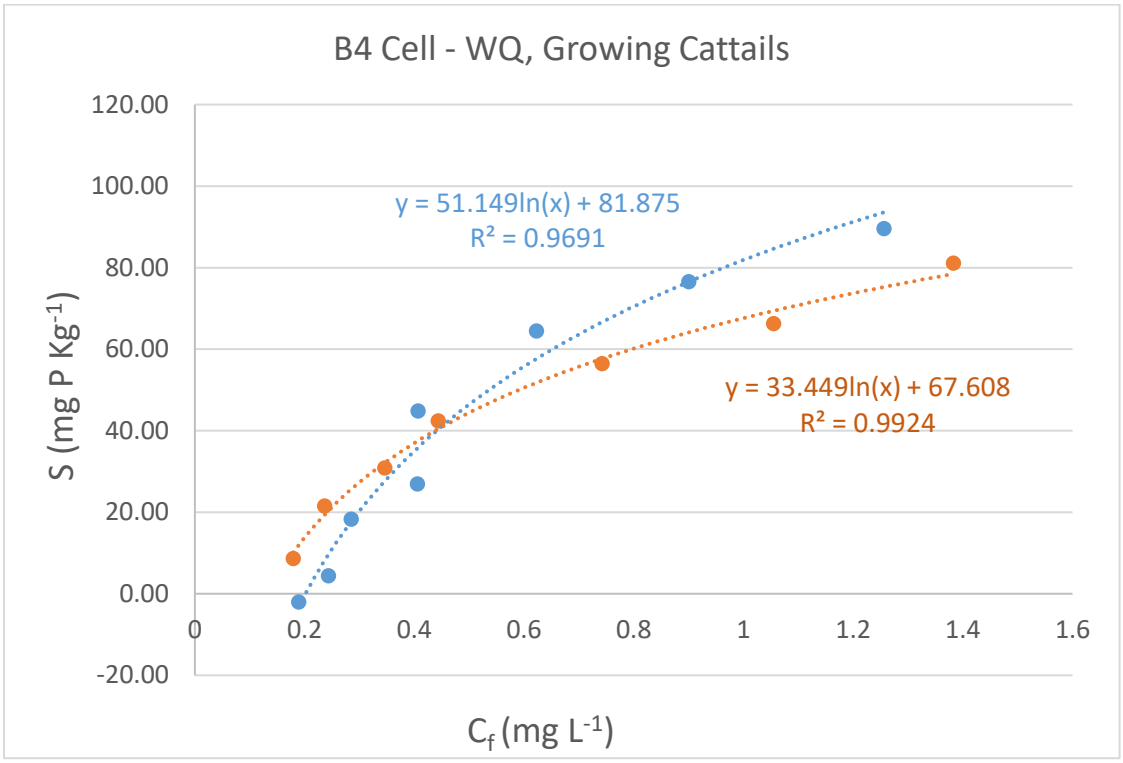
B4 Cell - WQ, Growing Cattails
120.00
100.00
80.00
60.00
40.00
20.00
0.00
-20.00
0
0.2
0.4
0.6
0.8
1
1.2
1.4
1.6
S (mg P Kg-1)
Cf (mg L-1)
y = 51.149ln(x) + 81.875
R² = 0.9691
y = 33.449ln(x) + 67.608
R² = 0.9924

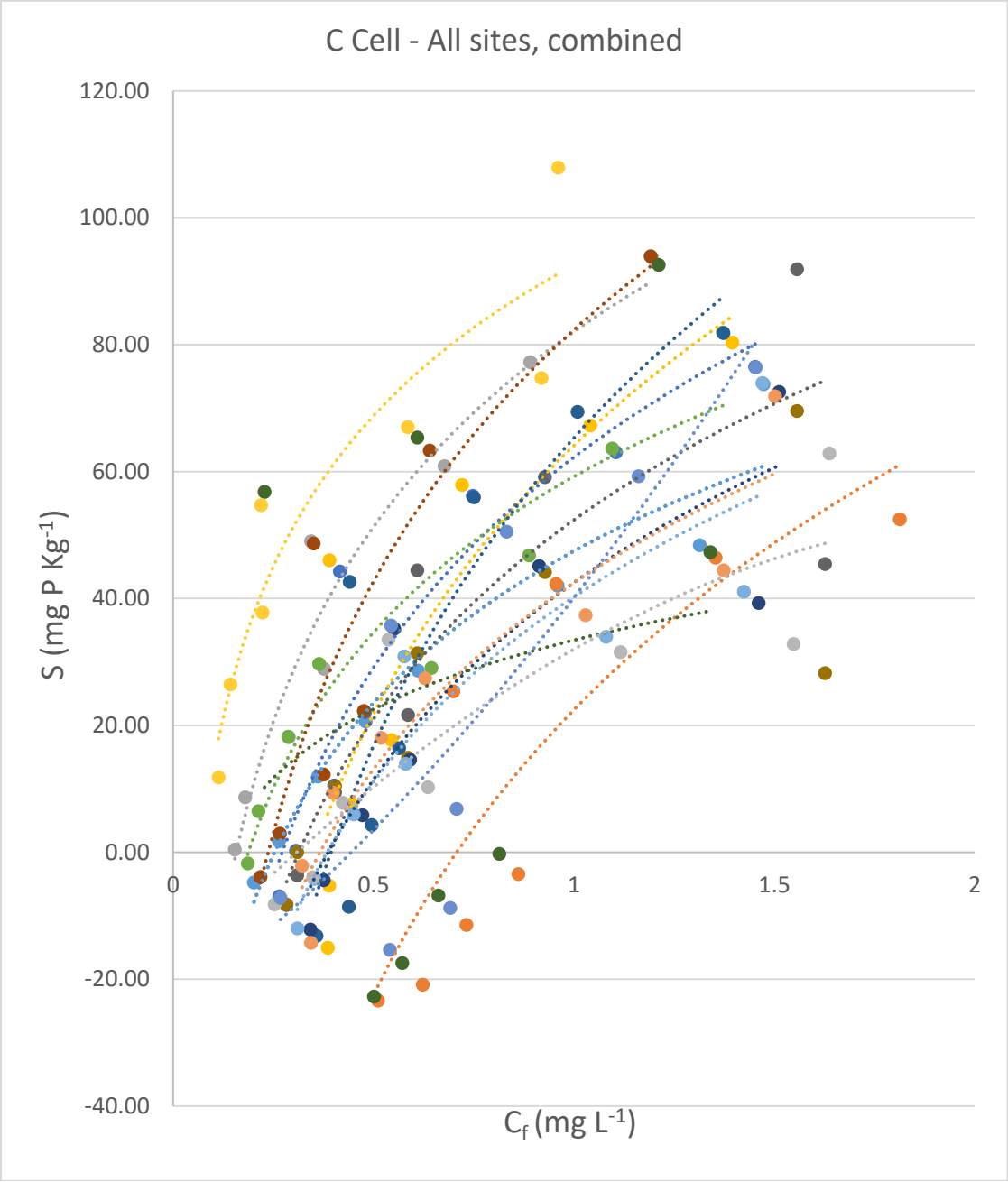
C Cell - All sites, combined
120.00
100.00
80.00
60.00
40.00
20.00
0.00
-20.00
-40.00
S (mg P Kg-1)
0
0.5
1
1.5
2
Cf (mg L-1)

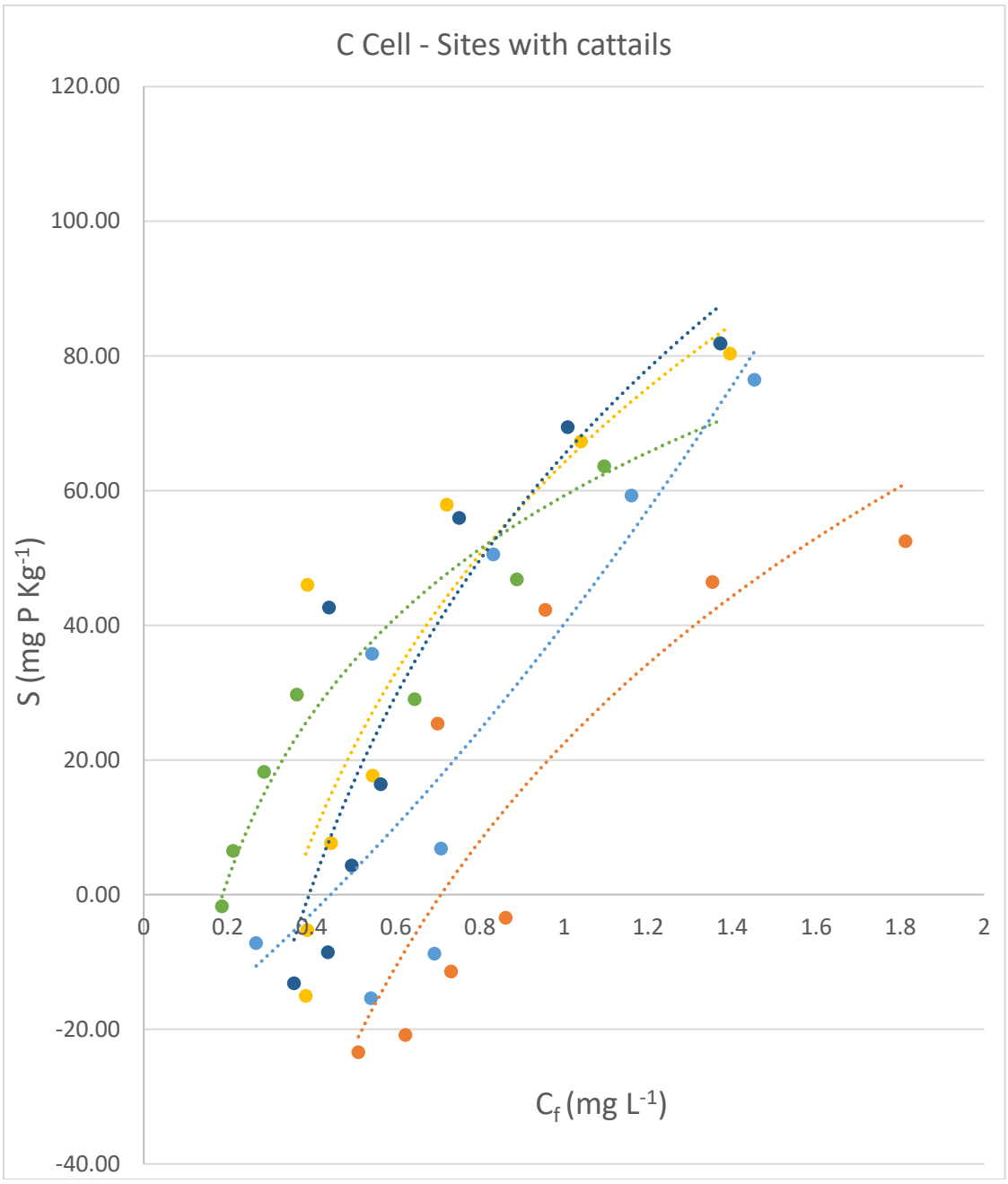
C Cell - Sites with cattails
120.00
100.00
80.00
60.00
40.00
20.00
0.00
-20.00
-40.00
S (mg P Kg-1)
0
0.2
0.4
0.6
0.8
1
1.2
1.4
1.6
1.8
2
Cf (mg L-1)

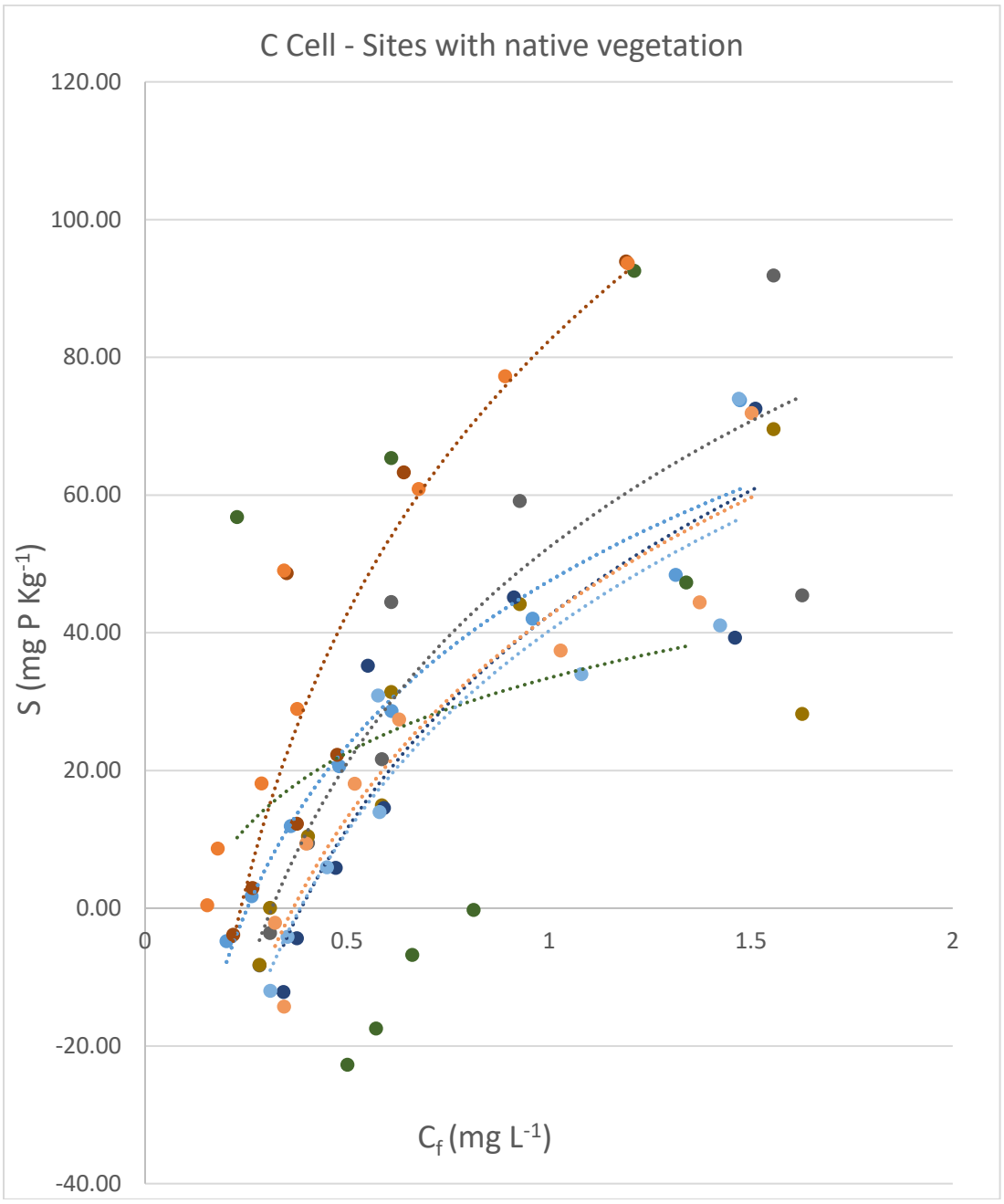
C Cell - Sites with native vegetation
120.00
100.00
80.00
60.00
40.00
20.00
0.00
-20.00
-40.00
S (mg P Kg-1)
0
0.5
1
1.5
2
Cf (mg L-1)

Appendix F. EPC_0 and K results.

Cell	Observed Vegetation Type	Cell Use Designation	K (L kg^{-1})	EPC0 (mg L^{-1})
A1	Corn	Cropped	115.99	0.30
A1	Corn	Cropped	78.84	0.46
A2	Submerged	Flooded	101.24	0.36
A2	Submerged	Flooded	125.58	0.46
A2	Submerged	Flooded	75.95	0.58
A3	Wheat	Cropped	114.07	0.21
A3	Wheat	Cropped	103.81	0.23
A4	Flooded, Natives	WQ	373.91	0.11
A4	Flooded, Natives	WQ	189.11	0.19
A4	Natives	WQ	232.71	0.24
B1	Soybean	Cropped	175.24	0.16
B1	Soybean	Cropped	138.58	0.18
B2	Natives, Millet	Natives	98.50	0.35
B3	Corn	Cropped	176.27	0.09
B3	Corn	Cropped	95.79	0.38
B4	Shallowly Flooded	WQ	135.79	0.19
B4	Shallowly Flooded	WQ	126.65	0.09
C	Cattail	Floodwater	148.23	0.47
C	Cattail	Floodwater	179.11	0.43
C	Cattail	Floodwater	97.23	0.71
C	Cattail	Floodwater	59.83	0.93
C	Cattail	Floodwater	169.77	0.18
C	Natives	Floodwater	98.39	0.25
C	Natives	Floodwater	154.07	0.36
C	Natives	Floodwater	68.12	0.33
C	Natives	Floodwater	102.66	0.44
C	Natives	Floodwater	117.87	0.13
C	Natives	Floodwater	91.68	0.25
C	Natives	Floodwater	92.56	0.41
C	Natives	Floodwater	73.80	0.80
C	Natives	Floodwater	134.91	0.38
C	Submerged	Floodwater	217.41	0.04
C	Submerged	Floodwater	131.03	0.31
Exterior	Exterior	Floodwater	49.44	0.39

Appendix G. Loss on ignition results.

Soil Sample #	Cell	Initial Soil Weight (g)	Final Soil Weight (g)	OM (g)	OM (%)
1	C	5.0033	4.3093	0.694	14%
2	C	4.997	4.3524	0.6446	13%
3	C	4.9987	4.51	0.4887	10%
4	C	5.0053	4.4601	0.5452	11%
5	C	5.0081	4.5542	0.4539	9%
6	C	5.0071	4.1771	0.83	17%
7	C	4.9996	4.0389	0.9607	19%
8	C	5.0085	4.503	0.5055	10%
9	C	4.9974	4.5257	0.4717	9%
10	C	5.0003	4.3909	0.6094	12%
11	C	5.0045	4.2768	0.7277	15%
12	C	4.9944	4.4795	0.5149	10%
13	C	5.0033	4.4598	0.5435	11%
14	Exterior	4.9996	4.4385	0.5611	11%
15	C	4.998	4.3655	0.6325	13%
15b	B4	4.9989	4.5501	0.4488	9%
18	B4	5.0007	4.444	0.5567	11%
19	B4	5.003	4.4235	0.5795	12%
20	B3	5.0078	4.5074	0.5004	10%
21	B3	5.0016	4.4391	0.5625	11%
23	B2	5.0039	4.3761	0.6278	13%
24	B1	5.0038	4.4885	0.5153	10%
25	B1	4.9964	4.5655	0.4309	9%
26	A1	4.9988	4.5455	0.4533	9%
27	A1	5.0048	4.5156	0.4892	10%
28	A2	5.0048	4.5673	0.4375	9%
29	A2	5.0022	4.5669	0.4353	9%
30	A3	4.9972	4.5837	0.4135	8%
31	A3	4.9957	4.4999	0.4958	10%
32	A4	5.0005	4.6779	0.3226	6%
33	A4	5.0005	4.6004	0.4001	8%
34	C	4.9982	4.0028	0.9954	20%
35	C	5.0098	4.5279	0.4819	10%
				Average:	11%

Appendix H. Parameter and statistics results for the Langmuir, Forced-Intercept Langmuir, Freundlich and Forced-Intercept Freundlich models, for each soil sample.

	Langmuir				Forced-Intercept Langmuir				
Cell	**K**	**S_{max}**	**SSE**	**E**	**Ci**	**K**	**S_{max}**	**SSE**	**E**
A1	0.00	12692.66	351.90	0.86	0.46	0.50	228.61	37.71	0.99
A1	0.75	100.76	2306.21	0.45	0.30	7.66	250.00	1922.87	0.54
A2	0.18	505.89	2933.28	0.46	0.36	1.54	250.00	6753.15	-0.24
A2	0.01	4435.71	1605.16	0.67	0.46	1.40	250.00	4429.30	0.09
A2	0.00	110776.19	390.33	0.54	0.58	0.50	162.85	415.01	0.51
A3	0.11	609.20	251.36	0.94	0.21	1.60	178.67	45.91	0.99
A3	0.65	147.18	2512.76	0.54	0.23	7.23	250.00	1923.83	0.65
A4	0.01	12846.42	505.71	0.93	0.24	2.47	250.00	114.32	0.98
A4	0.53	235.00	1291.25	0.78	0.19	6.06	250.00	1572.78	0.73
A4	1.08	200.48	1147.63	0.84	0.11	8.82	250.00	1194.96	0.83
B1	0.29	373.04	849.53	0.89	0.16	2.62	199.02	149.42	0.98
B1	0.01	10028.04	270.40	0.93	0.18	0.51	226.47	396.35	0.90
B2	0.00	10934.74	124.73	0.95	0.35	1.23	183.67	3.84	1.00
B3	1.19	155.08	1229.55	0.79	0.09	3.88	158.64	996.66	0.83
B3	0.38	123.23	990.40	0.51	0.38	6.77	250.00	812.50	0.60
B4	0.58	180.94	109.27	0.97	0.09	1.48	142.76	47.71	0.99
B4	0.18	510.46	711.27	0.88	0.19	2.33	209.59	233.69	0.96
B4	0.56	107.01	49.43	0.88	0.93	0.54	250.00	4030.45	-8.95
B4	0.12	779.99	685.59	0.91	0.13	1.22	202.92	406.48	0.95
C	0.00	19217.59	982.56	0.64	0.71	0.91	250.00	6103.02	-1.21
C	0.06	1144.89	1344.30	0.67	0.43	1.43	250.00	3783.30	0.07
C	0.08	725.85	1102.95	0.78	0.31	3.59	250.00	819.16	0.83
C	0.00	19067.46	204.41	0.95	0.18	0.50	238.35	403.78	0.90
C	0.00	24213.72	1408.73	0.69	0.47	1.42	250.00	3553.33	0.22
C	0.00	29096.28	1463.06	0.76	0.25	1.92	250.00	1278.32	0.79
C	0.54	164.79	2294.27	0.45	0.36	2.85	250.00	2912.02	0.31
C	0.23	186.55	1361.03	0.58	0.33	8.02	250.00	1056.08	0.68
C	0.01	3417.13	1006.48	0.64	0.44	3.46	250.00	1039.76	0.63
C	16.41	72.67	1040.07	0.09	0.80	2.54	0.00	18311.00	15.08
C	1.55	152.99	910.54	0.86	0.04	2.97	143.93	860.56	0.86
C	0.00	18863.18	285.78	0.92	0.25	0.62	186.56	227.90	0.94
C	0.00	13916.77	817.47	0.71	0.41	4.44	250.00	839.12	0.70
C	0.00	15545.26	319.16	0.87	0.38	2.04	183.14	421.56	0.83
Ext.	0.00	37595.74	781.11	0.61	0.39	7.29	250.00	956.43	0.52
	Avg:	**989.34**	**0.73**				**Avg:**	**2001.54**	**0.73**

	Freundlich				Forced-Intercept Freundlich			
Cell	**K**	**n**	**SSE**	**E**	**Kf**	**n**	**SSE**	**E**
A1	28.67	1.65	46.77	0.98	84.92	0.61	26.62	0.99
A1	41.10	0.65	2483.61	0.40	1959397.76	0.00	2421.35	0.42
A2	75.24	0.86	2919.13	0.47	212.59	0.44	6145.65	-0.12
A2	64.35	1.19	1516.27	0.69	993.63	0.09	3242.26	0.33
A2	14.76	1.86	321.34	0.62	19.96	1.65	382.16	0.55
A3	61.10	0.96	270.16	0.94	451.11	0.10	48.43	0.99
A3	56.47	0.71	2677.22	0.51	3308654.44	0.00	2354.72	0.57
A4	87.51	1.10	459.91	0.93	3227590.66	0.00	82.13	0.99
A4	80.85	0.76	1341.79	0.77	3570981.90	0.00	1748.17	0.70
A4	106.95	0.68	1182.60	0.83	2179979.35	0.00	1463.94	0.79
B1	83.88	0.90	967.52	0.88	140313.99	0.00	190.27	0.98
B1	54.61	1.02	269.08	0.93	100.91	0.49	364.54	0.91
B2	41.41	1.14	94.23	0.96	718.37	0.06	3.15	1.00
B3	84.40	0.64	1372.25	0.76	1077669.34	0.00	1050.24	0.82
B3	32.67	0.76	1024.07	0.50	1718445.30	0.00	1029.16	0.49
B4	65.37	0.74	161.73	0.96	133.43	0.29	52.95	0.99
B4	78.56	0.94	760.09	0.87	731890.84	0.00	263.02	0.96
B4	37.77	0.61	60.08	0.85	17.15	2.43	3420.43	-7.44
B4	82.93	0.97	708.27	0.91	164.56	0.35	404.63	0.95
C	48.44	1.24	922.01	0.67	48.20	2.13	4104.17	-0.49
C	60.73	0.97	1347.53	0.67	572559.76	0.00	3410.82	0.16
C	56.38	0.98	1116.67	0.77	3660485.72	0.00	997.78	0.80
C	57.05	1.06	195.63	0.95	99.83	0.53	357.79	0.91
C	60.33	1.17	1347.48	0.70	2085552.71	0.00	2578.10	0.43
C	79.54	1.14	1398.01	0.77	4110.72	0.01	1266.96	0.79
C	56.57	0.72	2371.01	0.44	3254296.94	0.00	3177.63	0.24
C	33.82	0.88	1400.10	0.57	1924159.97	0.00	1198.78	0.63
C	38.90	1.01	1006.38	0.64	2455788.49	0.00	1178.69	0.58
C	67.76	0.10	1059.97	0.07	0.00	0.00	18311.00	15.08
C	95.85	0.62	948.39	0.85	174.67	0.24	849.86	0.87
C	42.45	1.19	234.38	0.93	101.81	0.43	210.52	0.94
C	35.00	1.33	732.15	0.74	682484.45	0.00	842.02	0.70
C	37.86	1.22	270.59	0.89	558280.34	0.00	405.23	0.83
Ext.	30.17	1.00	781.04	0.61	791635.79	0.00	976.55	0.51
		Avg:	**993.16**	**0.74**		**Avg:**	**1898.81**	**0.73**

Appendix I. Plots of water and mass pollutant storage for TP, TSS, and TN, in the C and A/B cells in 2016, showing percent pollutant load reduction.

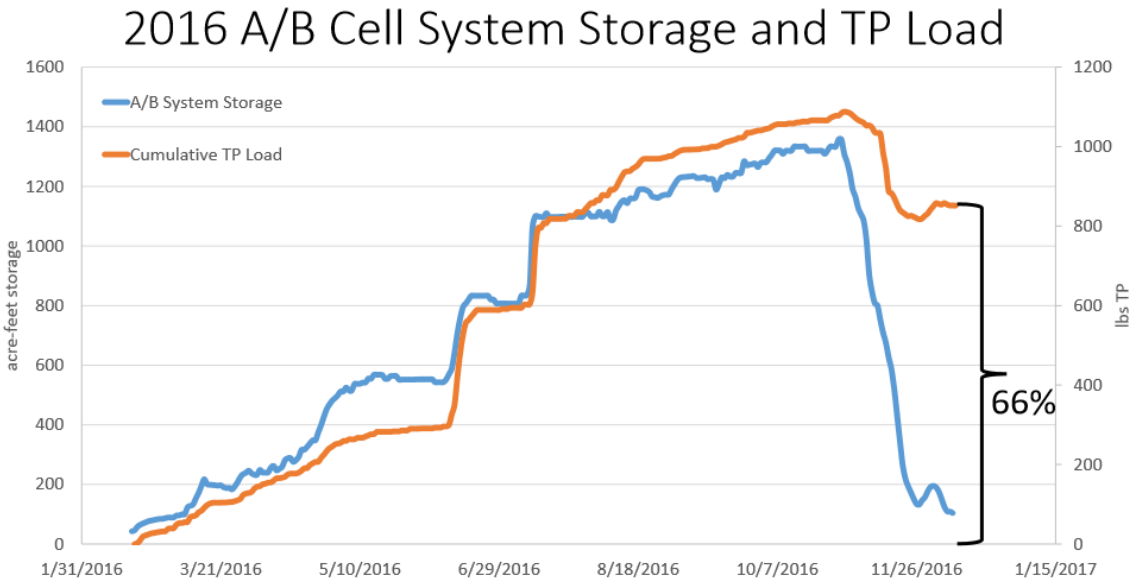

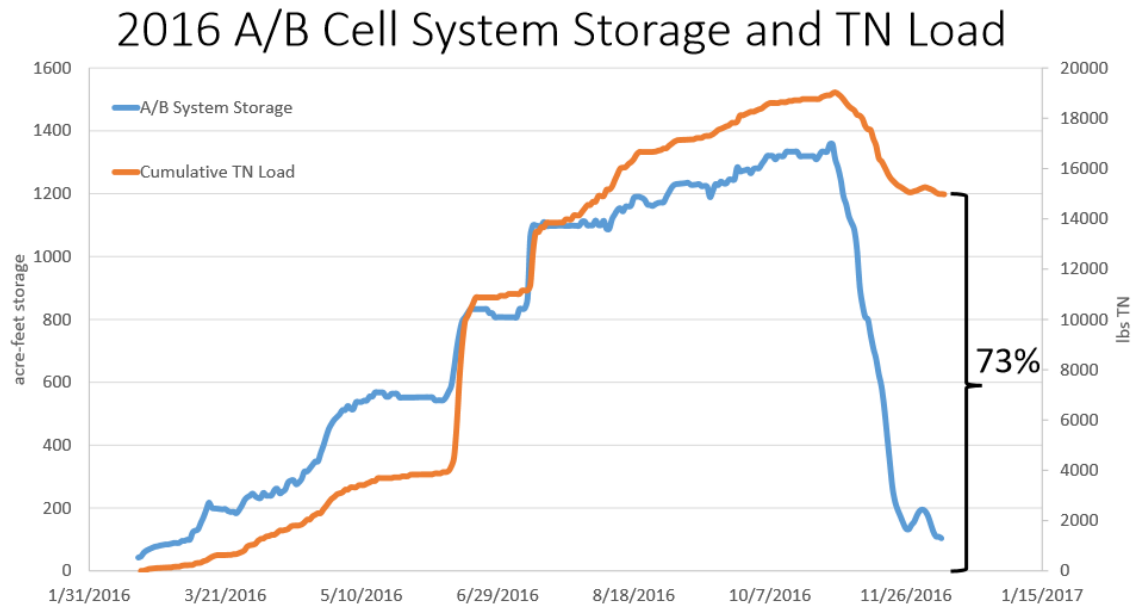

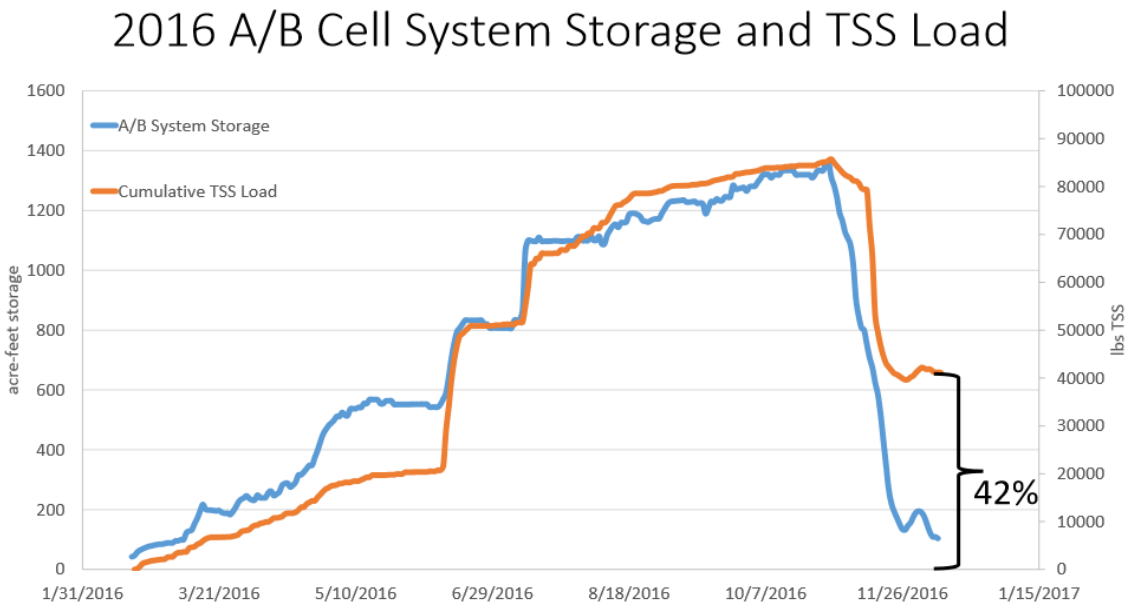
2016 A/B Cell System Storage and TSS Load
A/B System Storage
Cumulative TSS Load
acre-feet storage
lbs TSS
42%
1600
1400
1200
1000
800
600
400
200
0
100000
90000
80000
70000
60000
50000
40000
30000
20000
10000
0
1/31/2016
3/21/2016
5/10/2016
6/29/2016
8/18/2016
10/7/2016
11/26/2016
1/15/2017

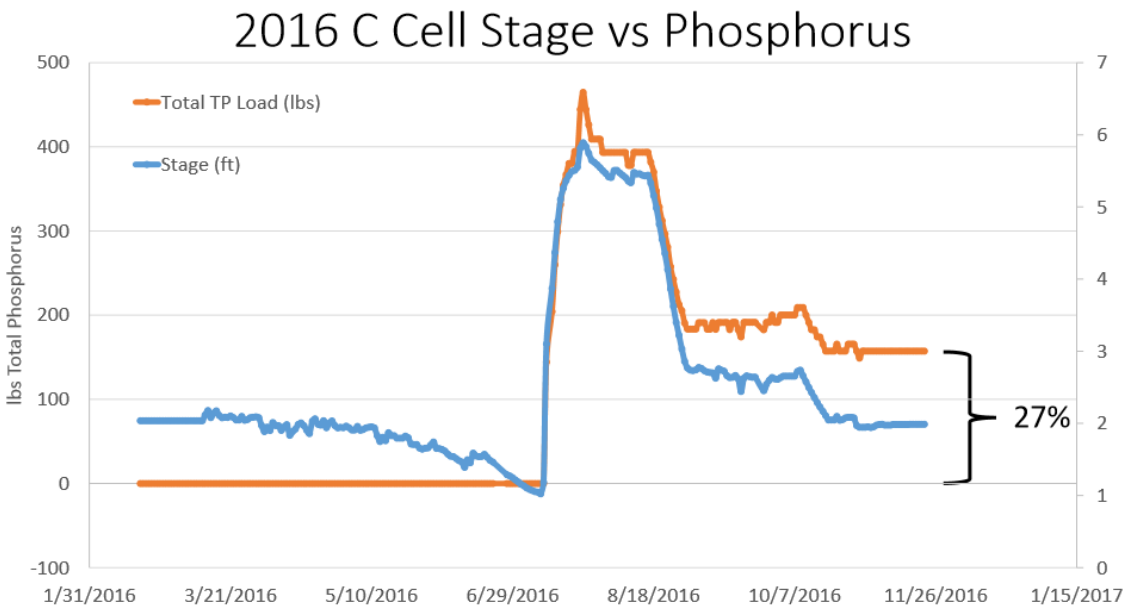
2016 C Cell Stage vs Phosphorus
Total TP Load (lbs)
Stage (ft)
lbs Total Phosphorus
27%
500
400
300
200
100
0
-100
7
6
5
4
3
2
1
0
1/31/2016
3/21/2016
5/10/2016
6/29/2016
8/18/2016
10/7/2016
11/26/2016
1/15/2017

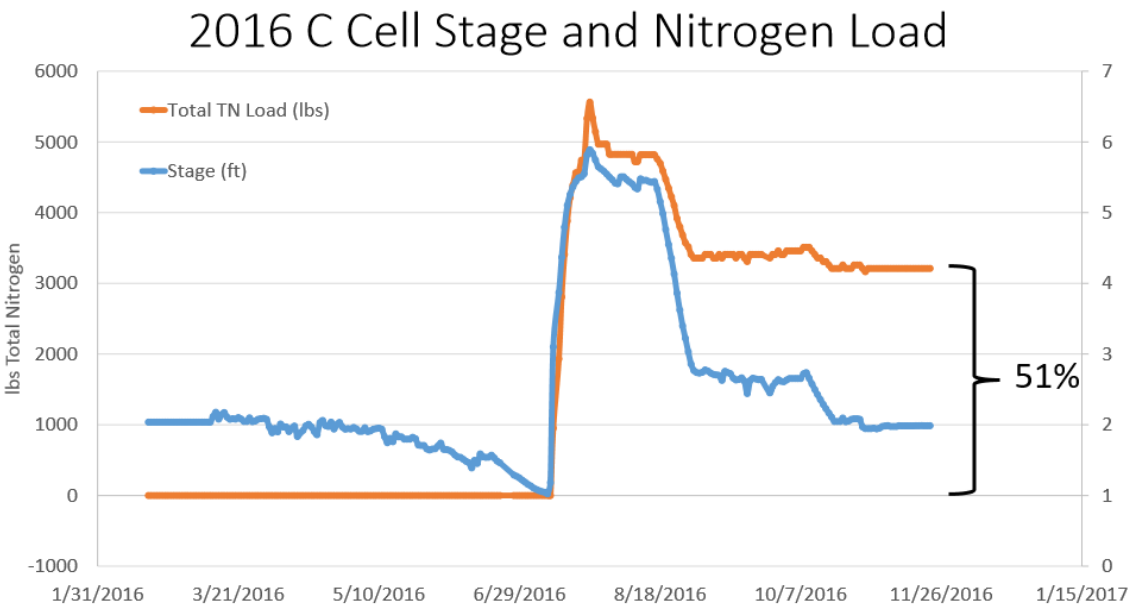
2016 C Cell Stage and Nitrogen Load
Total TN Load (lbs)
Stage (ft)
lbs Total Nitrogen
6000
5000
4000
3000
2000
1000
0
-1000
7
6
5
4
3
2
1
0
51%
1/31/2016
3/21/2016
5/10/2016
6/29/2016
8/18/2016
10/7/2016
11/26/2016
1/15/2017

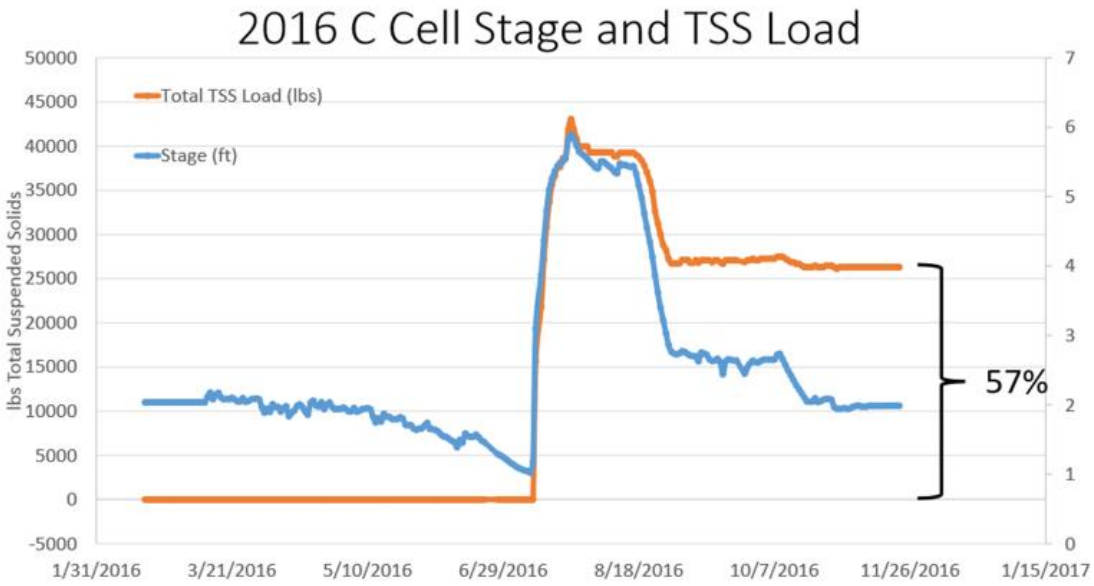
2016 C Cell Stage and TSS Load
Total TSS Load (lbs)
Stage (ft)
lbs Total Suspended Solids
50000
45000
40000
35000
30000
25000
20000
15000
10000
5000
0
-5000
7
6
5
4
3
2
1
0
57%
1/31/2016
3/21/2016
5/10/2016
6/29/2016
8/18/2016
10/7/2016
11/26/2016
1/15/2017

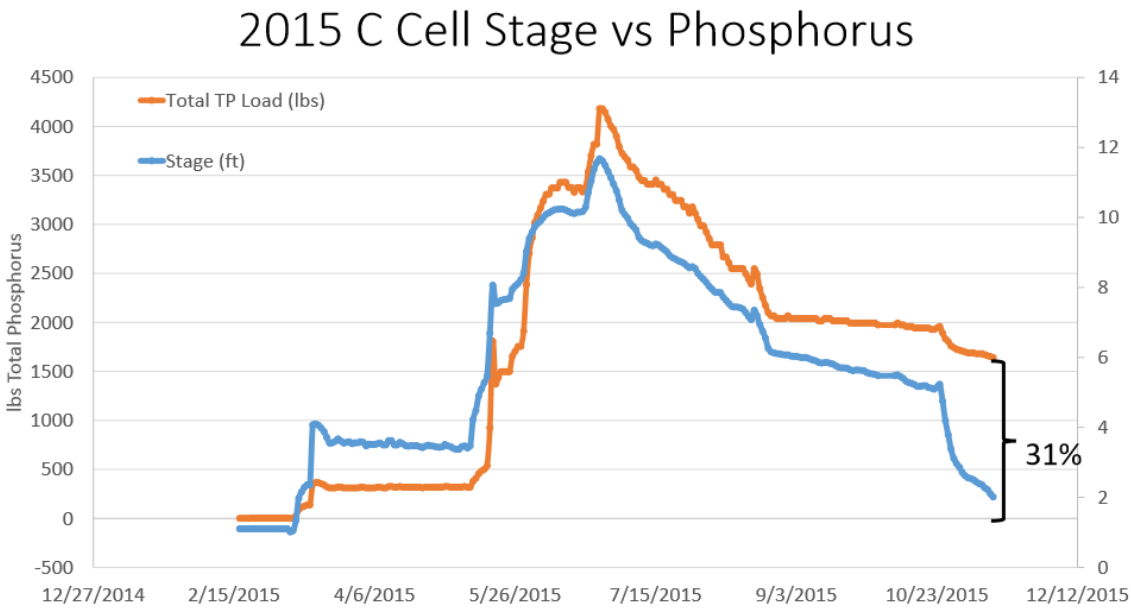
2015 C Cell Stage vs Phosphorus
Total TP Load (lbs)
Stage (ft)
lbs Total Phosphorus
4500
4000
3500
3000
2500
2000
1500
1000
500
0
-500
14
12
10
8
6
4
2
0
31%
12/27/2014
2/15/2015
4/6/2015
5/26/2015
7/15/2015
9/3/2015
10/23/2015
12/12/2015

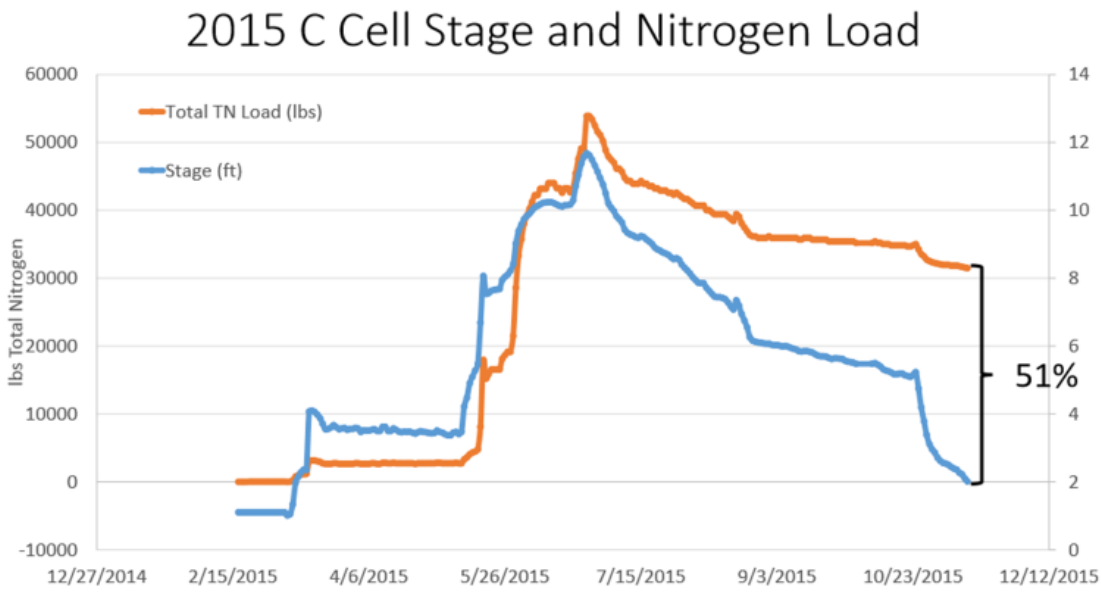
2015 C Cell Stage and Nitrogen Load
Total TN Load (lbs)
Stage (ft)
lbs Total Nitrogen
60000
50000
40000
30000
20000
10000
0
-10000
14
12
10
8
6
4
2
0
51%
12/27/2014
2/15/2015
4/6/2015
5/26/2015
7/15/2015
9/3/2015
10/23/2015
12/12/2015

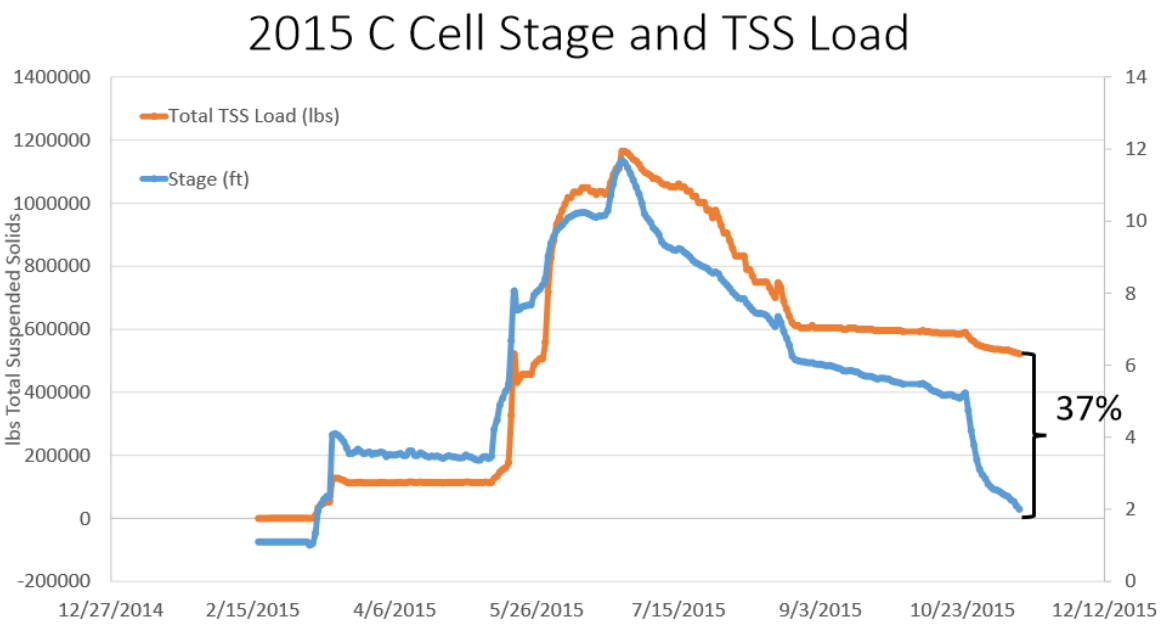
2015 C Cell Stage and TSS Load
Total TSS Load (lbs)
Stage (ft)
lbs Total Suspended Solids
1400000
1200000
1000000
800000
600000
400000
200000
0
-200000
14
12
10
8
6
4
2
0
37%
12/27/2014
2/15/2015
4/6/2015
5/26/2015
7/15/2015
9/3/2015
10/23/2015
12/12/2015